International Journal of Polymer Science

Formation and Photoluminescence of Fluorescent Polymers

Guest Editors: Jinying Yuan, Shanfeng Wang, Jun Shan, Jing Peng, LiuHe Wei, and Xurong Xu

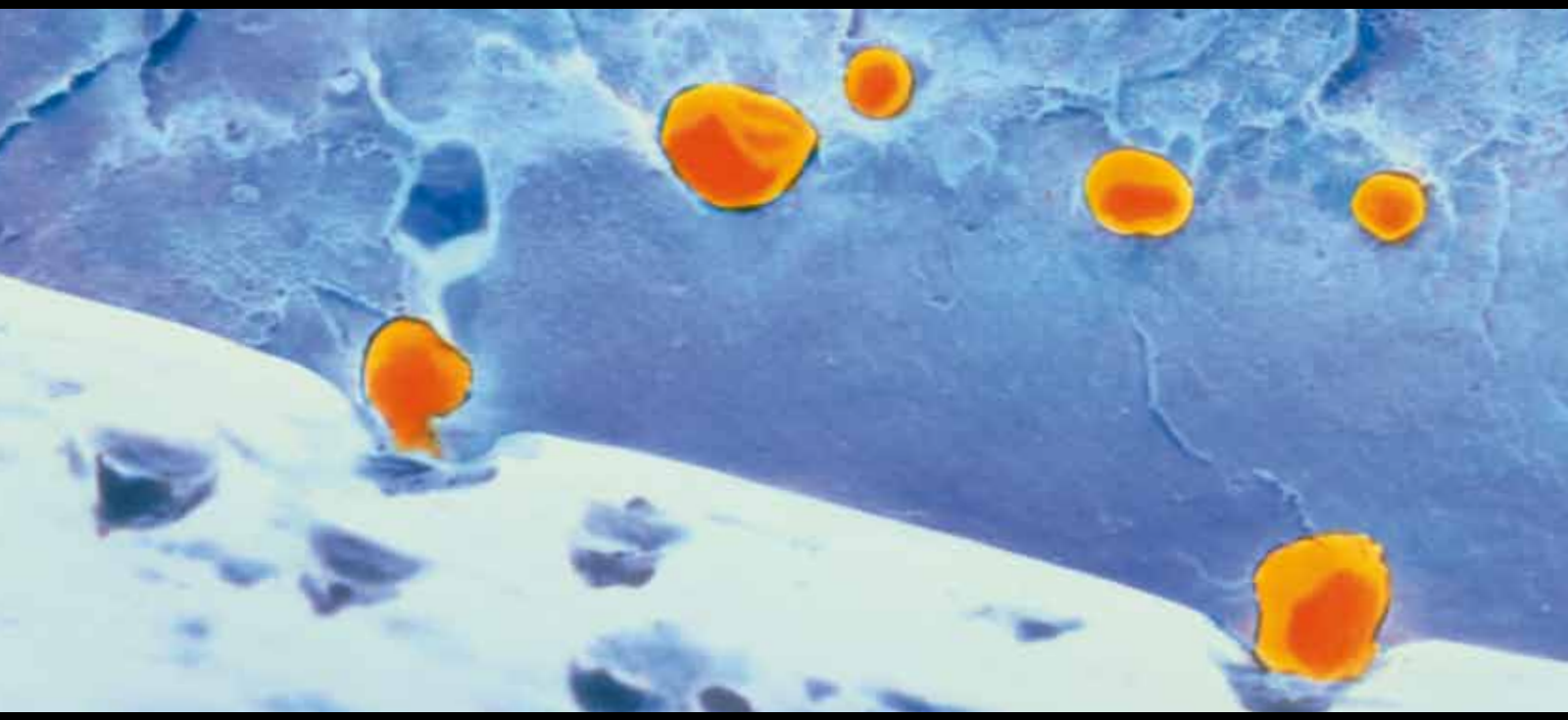

Formation and Photoluminescence of Fluorescent Polymers

International Journal of Polymer Science

Formation and Photoluminescence of Fluorescent Polymers

Guest Editors: Jinying Yuan, Shanfeng Wang, Jun Shan, Jing Peng, Liuhe Wei, and Xurong Xu

Editorial Board

Contents

Formation and Photoluminescence of Fluorescent Polymers, Jinying Yuan, Shanfeng Wang, Jun Shan, Jing Peng, Liuhe Wei, and Xurong Xu
Volume 2010, Article ID 526348, 2 pages

Synthesis and Characterization of Well-Defined Soluble Alq_3- and Znq_2-Functionalized Polymers via RAFT Copolymerization, Chengchao Wang, Wei Zhang, Nianchen Zhou, Yansheng Qiu, Zhengping Cheng, and Xiulin Zhu
Volume 2010, Article ID 340926, 7 pages

Synthesis and Characterization of New Photoluminescent Oxadiazole/Carbazole-Containing Polymers, Simona Concilio, Valeria Bugatti, Pio Iannelli, and Stefano Piotto Piotto
Volume 2010, Article ID 581056, 6 pages

New Type of Donor-Acceptor Through-Space Conjugated Polymer, Lin Lin, Yasuhiro Morisaki, and Yoshiki Chujo
Volume 2010, Article ID 908128, 9 pages

Photoluminescent Patterned Papers Resulting from Printings of Polymeric Nanoparticles Suspension, Pierre Sarrazin, Davide Beneventi, Aurore Denneulin, Olivier Stephan, and Didier Chaussy
Volume 2010, Article ID 612180, 8 pages

Prevention of H-Aggregates Formation in Cy5 Labeled Macromolecules, Jing Kang, Oliver Kaczmarek, Jürgen Liebscher, and Lars Dähne
Volume 2010, Article ID 264781, 7 pages

Polymersomes and Wormlike Micelles Made Fluorescent by Direct Modifications of Block Copolymer Amphiphiles, Karthikan Rajagopal, David A. Christian, Takamasa Harada, Aiwei Tian, and Dennis E. Discher
Volume 2010, Article ID 379286, 10 pages

Hindawi Publishing Corporation
International Journal of Polymer Science
Volume 2010, Article ID 526348, 2 pages
doi:10.1155/2010/526348

Editorial

Formation and Photoluminescence of Fluorescent Polymers

Jinying Yuan,[1] Shanfeng Wang,[2] Jun Shan,[3] Jing Peng,[4] Liuhe Wei,[5] and Xurong Xu[6]

[1] *Department of Chemistry, Tsinghua University, Beijing 100084, China*
[2] *Department of Materials Science and Engineering, The University of Tennessee, Knoxville, TN 37996, USA*
[3] *KCL (Oy Keskuslaboratorio-Centrallaboratorium Ab), Tekniikantie, P.O. Box 70, 02151 Espoo, Finland*
[4] *Department of Applied Chemistry, Peking University, Beijing 100871, China*
[5] *Department of Chemistry, Zhengzhou University, Zhengzhou 450001, China*
[6] *Departament of Chemistry, Zhejiang University, Hangzhou 310027, China*

Correspondence should be addressed to Jinying Yuan, yuanjy@mail.tsinghua.edu.cn

Received 14 July 2010; Accepted 14 July 2010

During the past several decades, there is an enormous demand for fluorescent materials, and research on fluorescent polymers has gathered great scientific attention because of their engrossing properties and important application in the fields of materials and life science. The latest research progress in fluorescent polymers is focused on the formation and photoluminescence of fluorescent polymers with new architecture. There are different methods to classify fluorescent polymers. For example, based on their solubility, fluorescent polymers can be divided into three types which are hydrophobic, hydrophilic and amphiphilic, individually. Various methods of design and synthesis of fluorescent polymers have also been developed. Fluorescent polymers can be synthesized by polymerization of fluorescent functional monomers, using fluorescent compounds as initiator, fluorescent compounds as chain transfer agents, chemical bonding between fluorescent groups and polymers, and polymerization of nonfluorescent functional monomer.

Fluorescent polymers are functional macromolecules with enormous important applications. Their emerging applications involve the fields of fluorescent probe, smart polymer machines, fluorescent chemosensor, fluorescent molecular thermometers, fluorescent imaging, drug delivery carriers, and so on. Polymers are convenient due to the fact that they are easily processable to small particles and thin films that can be deposited onto optical fibers and waveguides for sensor fabrication. Advanced strategies such as electrostatic layer-by-layer assembly and self-assembly of amphiphilic block copolymers containing chromophores have also been used for the formation of fluorescent systems.

The aim of this special issue is to bring forth the synergy between architecture and photoluminescence through new and significant contributions from active researchers in the field. All the papers in this issue are invited review or invited research papers by leading authorities and research groups in this field from universities, industry, and government laboratories.

The first paper of this special issue addresses the reversible addition-fragmentation chain transfer (RAFT) copolymerization of 2-((8-hydroxyquinolin-5-yl)methoxy)ethyl methacrylate (HQHEMA) with styrene (St) or methyl methacrylate (MMA) carried out in the presence of 2-cyanoprop-2-yl dithionaphthalenoate (CPDN). The soluble polymers having tris(8-hydroxyquinoline)aluminum (Alq_3) and bis(8-hydroxyquinoline) znic(II) (Znq_2) side chains were obtained via complexation of the polymers with aluminium isopropoxide or zinc acetate in the presence of monomeric 8-hydroxyquinoline, which had strong fluorescent emission at 520 nm. The second paper is on the synthesis and characterization of new photoluminescent oxadiazole/carbazole-containing polymers (POCs). The polymers exhibit a high thermal stability, high glass transition temperatures, and good solubility in common organic solvents, despite the extended aromatic portion in the main polymer chain, and are potential candidate materials for fabricating blue light-emitting devices. The third paper proposes the synthesis and properties of a

novel through-space conjugated polymer with a [2.2]paracyclophane skeleton. The obtained polymer possessed donor (fluorene) and acceptor (2,1,3-benzothiadiazole) segments that were alternately π-stacked in proximity via the [2.2]paracyclophane moieties.

The fourth paper presents the study on the printability of a copolyfluorene-fluorenone (PFFO) photoluminescent nanoparticle aqueous suspension on commercial tracing paper. This suspension was suited to inkjet or flexography printing techniques because it is composed of nanosized "pigments" (nanoparticles) and it showed suitable properties such as low viscosity and surface tension. The fifth paper describes that H-aggregates of cyanine dye Cy5 covalently linked to the polymer PAH have been observed and the behavior of the "H-aggregate band" at different solvent and synthesis conditions has been investigated. In order to reduce the undesired H-aggregates effect a different synthetic route in organic solvent has been developed yielding much higher label degrees and remarkable less H-aggregates on the polymer. The final paper of this special issue is more forward-looking. It addresses the technological applications of worm-like micelles and vesicles prepared from diblock copolymers. Although transmission electron microscopy has remained as the method of choice for assessing the morphologies, fluorescence microscopy has a number of advantages. When commercially available fluorophores are covalently attached to diblock copolymers, a number of their physicochemical characteristics can be investigated. This method becomes particularly useful for visualizing phase separation within polymer assemblies and assessing the dynamics of worm-like micelles in real time. Near-IR fluorophores can be covalently conjugated to polymers, and this opens the possibility for deep-tissue fluorescence imaging of polymer assemblies in drug delivery applications.

Jinying Yuan
Shanfeng Wang
Jun Shan
Jing Peng
Liuhe Wei
Xurong Xu

Hindawi Publishing Corporation
International Journal of Polymer Science
Volume 2010, Article ID 340926, 7 pages
doi:10.1155/2010/340926

Research Article

Synthesis and Characterization of Well-Defined Soluble Alq_3- and Znq_2-Functionalized Polymers via RAFT Copolymerization

Chengchao Wang, Wei Zhang, Nianchen Zhou, Yansheng Qiu, Zhengping Cheng, and Xiulin Zhu

Key Laboratory of Organic Synthesis of Jiangsu Province, College of Chemistry, Chemical Engineering and Materials Science, Soochow University, Suzhou 215123, China

Correspondence should be addressed to Xiulin Zhu, xlzhu@suda.edu.cn

Received 31 October 2009; Accepted 21 February 2010

Academic Editor: Jinying Yuan

The reversible addition-fragmentation chain transfer (RAFT) copolymerizations of 2-((8-hydroxyquinolin-5-yl)methoxy)ethyl methacrylate (HQHEMA) with styrene (St) or methyl methacrylate (MMA) were successfully carried out in the presence of 2-cyanoprop-2-yl dithionaphthalenoate (CPDN). The polymerization behaviors showed the typical living natures by the first-order polymerization kinetics, the linear dependence of molecular weights of the polymers on the monomer conversions with the relatively narrow molecular weight distributions (M_w/M_n), and the successful chain extension experiments. The soluble polymers having tris(8-hydroxyquinoline)aluminum (Alq_3) and bis(8-hydroxyquinoline) znic(II) (Znq_2) side chains were obtained via complexation of the polymers with aluminium isopropoxide or zinc acetate in the presence of monomeric 8-hydroxyquinoline, which had strong fluorescent emission at 520 nm. The obtained polymers were characterized by GPC, ^{1}H NMR, UV-vis, and fluorescent spectra.

1. Introduction

In recent years, organic electroluminescence (EL) display devices have attracted more intensive attention as a promising technology for flat panel display [1]. Many emitting materials, including low-weight molecules and polymers, have been designed and utilized in fabricating organic light emitting diodes (OLEDs) [2–5]. Among them, metal 8-hydroxyquinoline (Mq_n) chelates, especially for tris(8-hydroxyquinoline)aluminum (Alq_3), and bis(8-hydroxyquinoline) znic(II) (Znq_2) have been extensively investigated for their high stabilities, good emissions, and electron-transporting properties [6–8]. Compared with low-weight 8-hydroxyquinoline (Mq_n) chelate, the polymers containing Mq_n pendant groups combine the fluorescent property of Mq_n and the processability of the polymer [6, 7, 9]. Up to now, two types of Mq_n-containing polymers (main-chain type and side-chain type) have been reported. Yamamoto and Yamaquchi reported the synthesis of poly(quinolinol) [10] and poly(aryleneethynylene) [11] containing 8-quinolinol moieties. On the other hand, various side-chain type polymers including poly(arylene ether) [12], copolymers of 7-allyl-, or 7-(2-methylvinyl)-functionalized derivatives of 8-hydroquinoline with styrene [13], functionalized polystyrene [14], and copolymers of methacrylates having 8-hydroxyquinoline moieties were also successfully prepared [15]. Furthermore, Mq_n-containing polymers were obtained by the reaction of the above polymers with metal compounds in the presence of monomeric 8-hydroxyquinoline. Meyers and Weck, reported the synthesis of an Alq_3-functionalized polymer via ring-open metathesis polymerization of norbornene monomer containing Alq_3 unit [6]. Most recently, Liang et al. reported the formation of Al^{3+} complex micelles via self-assembly of diblock copolymers containing pendent 8-hydroxyquinoline units [16]. However, the molecular weights and molecular weight distributions of the obtained polymers containing Mq_n units were not well controlled in most cases.

The development of controlled/"living" radical polymerization (CRP) methods, such as atom transfer radical polymerization (ATRP) [17–19], nitroxide-mediated radical polymerization (NMRP) [20], reversible addition-fragmentation chain transfer (RAFT) [21] polymerization, and single-electron transfer mediated living radical polymerization (SET-LRP) [22] lead to unprecedented opportunities in design and synthesis of functional polymer materials. Among them, RAFT technique has been considered as one of the most advantageous techniques due to the mild reaction conditions, functional group compatibility, and versatility to monomers. Up to date, RAFT polymerization have been applied to a wide variety of monomers, including functionalized monomers, such as methyl methacrylate, styrene, methyl acrylate, acrylamide, 6-[4-(4-methoxyphenyl)phenoxy] hexyl methacrylate, and 3-[tris(trimethylsiloxy)silyl] propyl methacrylate [23]. However, the living radical polymerization of vinyl monomers containing 8-quinolinol moieties is rarely reported [16], although the common radical polymerization of vinyl monomers containing 8-quinolinol moieties have been successfully conducted [12–15].

From these points of view, we investigated the feasibility of preparation of 8-hydroxyquinoline-containing soluble polymers via RAFT technique. Furthermore, the well-defined side-chain Mq_n-containing (M = Al and Zn) polymers were also prepared via complexation of the polymers with aluminium isopropoxide and zinc acetate, respectively, and their optical properties were also investigated.

2. Experimental Part

2.1. Materials. Styrene (St) and methyl methacrylate (MMA) (chemically pure, Shanghai Chemical Reagent Co. Ltd) were purified by extracting with a 5% sodium hydroxide aqueous solution, followed by washing with water and dried with anhydrous magnesium sulfate overnight, finally distillated freshly before use. 2, 2′-Azobisisobutyronitrile (AIBN) (Shanghai Chemical Reagent Co. Ltd, China, 99%) was recrystallized two times from ethanol. 2-Hydroxyethyl methacrylate (HEMA) (Alfa Aesar, 98%), 8-hydroxyquinoline (Alfa Aesar, 98%), aluminium isopropoxide (Alfa Aesar, 98%), sodium acetate (analytical reagent, Shanghai Chemical Reagent Co. Ltd), and zinc acetate (analytical reagent, Shanghai Chemical Reagent Co. Ltd) were used as received. Carbon disulphide (analytical reagent, Shanghai Chemical Reagent Co. Ltd), 1-bromonaphthalene (Alfa Aesar, 98%), and tetrahydrofuran (analytical reagent, Shanghai Chemical Reagent Co. Ltd) were dried by 4 Å molecular sieve before use. 2-Cyanoprop-2-yl 1-dithionaphthalate (CPDN) [24] and 2-((8-hydroxyquinolin-5-yl)methoxy)ethyl methacrylate (HQHEMA) [25] (Scheme 1) were synthesized according to the references, respectively. Unless otherwise specified, all other chemicals were purchased from Shanghai Chemical Reagents Co. Ltd and used as received without further purification.

2.2. RAFT Copolymerization of HQHEMA with St or MMA. The typical procedures for the RAFT copolymerization are as follows: 2-((8-hydroxyquinolin-5-yl)methoxy)ethyl methacrylate (HQHEMA) (0.251 g, 0.873 mmol), styrene (St) (1 mL, 8.73 mmol), 2-cyanoprop-2-yl 1-dithionaphthalate (CPDN) (26.02 mg, 0.096 mmol) and 2, 2′-azobisisobutyronitrile (AIBN) (1.57 mg, 0.0096 mmol), ($[M]_0/[\text{CPDN}]_0/[\text{AIBN}]_0$ = 1000 : 10 : 1, M = (HQHEMA + St), $[\text{St}]_0/[\text{HQHEMA}]_0$ = 10 : 1) were added to a dry glass ampoule with a magnetic bar. The solution was bubbled with argon for approximately 10 minutes to eliminate the oxygen, and then the ampoule was flame-sealed under argon atmosphere and placed in the water bath at 70°C. At the designed time, the ampoule was opened, and the contents was diluted with about 2 mL THF, and precipitated into 250 mL methanol. The sample was obtained by filtration and dried to constant weight under vacuum. The conversion of the monomer was determined by gravimetry. The procedures of copolymerization of HQHEMA with MMA are similar to those described above.

2.3. Chain Extension Experiment with St or MA. The procedures of chain extension experiment are similar to those mentioned above except CPDN was substituted by poly(HQHEMA-*co*-St) or poly(HQHEMA-*co*-MMA) and the second monomer is St and methacrylate (MA), respectively.

2.4. Preparation of Alq_3-Polymer Complex. To a 20 mL THF solution containing poly(HQHEMA-*co*-St) ($M_{n(\text{GPC})}$ = 5400 g/mol, M_w/M_n = 1.17, (St unit)/(HQHEMA unit) = 7 : 1 based on the ^{1}H NMR spectrum) (4.32 g, 0.8 mmol) and 8-hydroxyquinoline (0.493 g, 3.4 mmol) was added dropwise a 10 mL THF solution of aluminium isopropoxide (0.265 g, 1.3 mmol). The reaction mixture was stirred at room temperature for 1 hour and at 50°C for another 17 hours. After being cooled to room temperature, the solution was poured into methanol. To remove any trace amounts of low molecular weight Alq_3, the reprecipitation was repeated several times until the methanol solution was not colored anymore to yield the product as a light yellow solid (3.66 g, 85%). The similar procedures were used to prepare Znq_2-polymer complex.

2.5. Characterization. ^{1}H NMR spectra of the polymers were recorded on an INOVA 400 MHz NMR instrument, using $CDCl_3$ as solvent and TMS as the internal standard. The molecular weight and molecular weight distribution of the polymer was determined with a Waters 1515 gel permeation chromatography (GPC) equipped with refractive index detector, using HR1, HR3, and HR4 column with molecular weight range 100–500,000 calibrated with poly(methyl methacrylate) standard sample. UV-vis absorption spectra were performed on a Shimadzu UV-240 recording spectrophotometer at room temperature in $CHCl_3$ solutions. The Fluorescence emission spectra were obtained on a PerkinElmer LS-50B Fluorescence spectrophotometer in $CHCl_3$ at room temperature. The metal ion concentrations were determined by VISTA-MPX CCD Simultaneous ICP-AES, and the operation conditions are listed: plasma flow rate: 15 L min^{-1}; carrier gas (Ar) flow rate: 1.5 L min^{-1}; incident power (kW): 1.2 kW; vaporization press: 240 kPa.

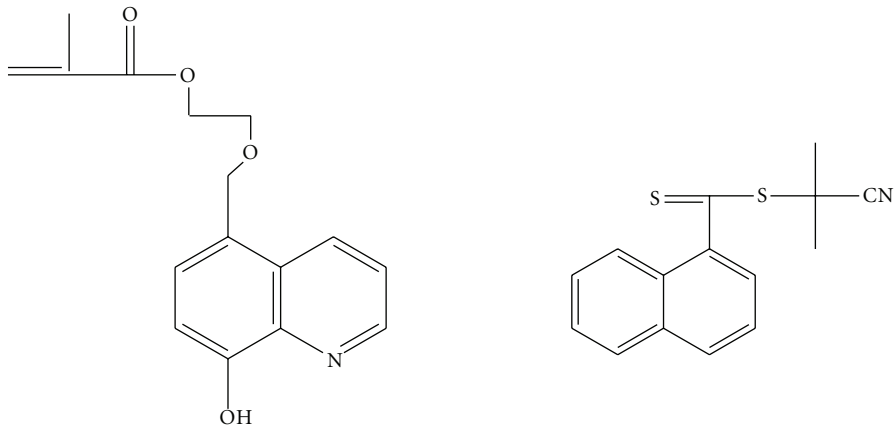

HQHEMA CPDN

Scheme 1: The chemical structures of 2-((8-hydroxyquinolin-5-yl)methoxy)ethyl methacrylate (HQHEMA) and 2-cyanoprop-2-yl 1-dithionaphthalate (CPDN).

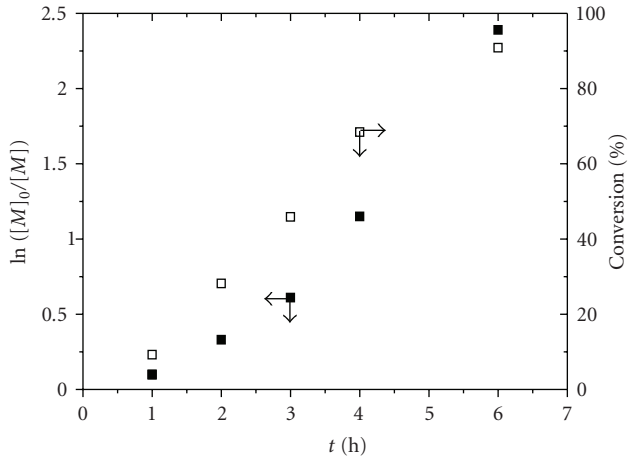

Figure 1: $\ln([M_0]/[M])$ and monomer conversion versus polymerization time. Kinetic plot of RAFT copolymerization of HQHEMA and MMA. Polymerization conditions: $[\text{Monomer}]_0/[\text{CPDN}]_0/[\text{AIBN}]_0 = 1000:10:1$, $[\text{Monomer}]_0 = [\text{MMA}]_0/[\text{HQHEMA}]_0 = 10:1$; $T = 70^\circ\text{C}$.

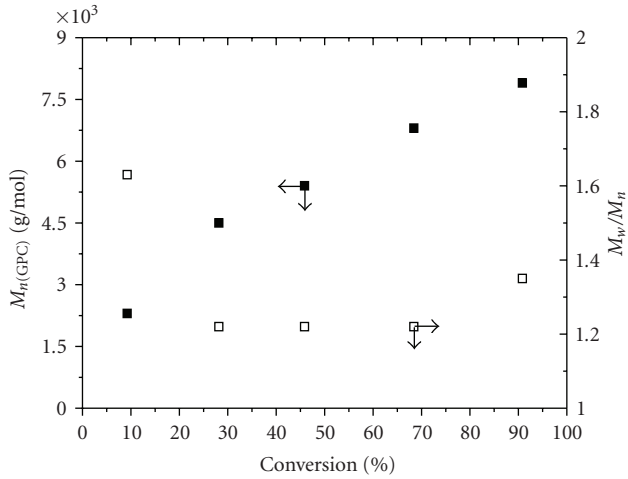

Figure 2: Dependence of molecule weights and molecule weight distributions on monomer conversions for RAFT copolymerization of HQHEMA and MMA. Polymerization conditions are the same as in Figure 1.

3. Results and Discussion

3.1. RAFT Copolymerization of HQHEMA and MMA. The monomer containing 8-hydroxyquinoline moiety, 2-((8-hydroxyquinolin-5-yl)methoxy)ethyl methacrylate (HQHEMA) was often used to prepare side-chain Mq_n-containing (M = Al or Zn) polymers. However, the Mq_n-containing PHQHEMA was also difficult to be dissolved in common organic solvents. Takayama et al. [9] increased the solubility of the polymer via introducing alkyl side chain in 7-position of 8-hydroxyquinoline unit. We aimed to increase the processability of Mq_n-containing polymer by copolymerization of HQHEMA with other vinyl monomers. Firstly, we conducted atom transfer radical copolymerization (ATRP) of HQHEMA with St or MMA, however, no polymer was obtained, which may be due to the coordination between 8-hydroxyquinoline and catalyst (CuBr/Ligand) used in ATRP and resulted in the catalyst ineffective [16]. RAFT copolymerizations of HQHEMA with MMA or St were successfully carried out in the presence of 2-cyanoprop-2-yl 1-dithionaphthalate (CPDN). The results are presented in Figures 1–4 and Tables 1 and 2, respectively. Figure 1 illustrates the kinetic plot for the copolymerization of HQHEMA and MMA. The linear relationship between $\ln([M]_0/[M])$ and the reaction time can be observed, which indicated that the polymerization was first-order with respect to the monomer, and the radical concentration remained constant throughout the polymerization process. Figure 2 presents the dependence of the molecular weight and molecular weight distribution (M_w/M_n) on the monomer conversion for the RAFT copolymerization of HQHEMA and MMA. The molecular

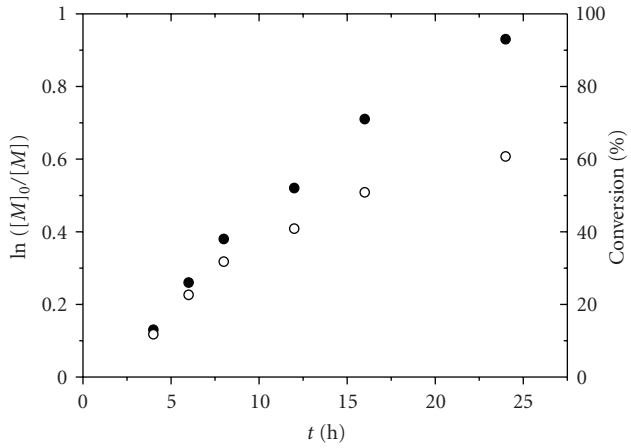

Figure 3: $\ln([M]_0/[M])$ and monomer conversion versus polymerization time. Kinetic plot of RAFT copolymerization of HQHEMA and St. Polymerization conditions: $[\text{Monomer}]_0/[\text{CPDN}]_0/[\text{AIBN}]_0 = 1000:10:1$, $[\text{Monomer}]_0 = [\text{St}]_0/[\text{HQHEMA}]_0 = 10:1$; $T = 70^\circ\text{C}$.

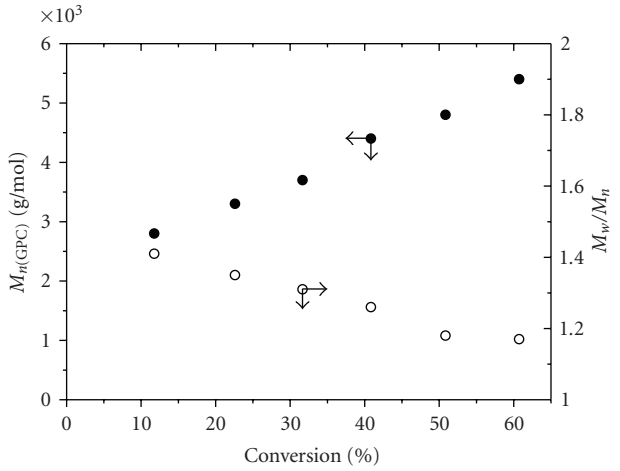

Figure 4: Dependence of molecule weights and molecule weight distributions on monomer conversions for RAFT copolymerization of HQHEMA and St. Polymerization condition are the same as in Figure 3.

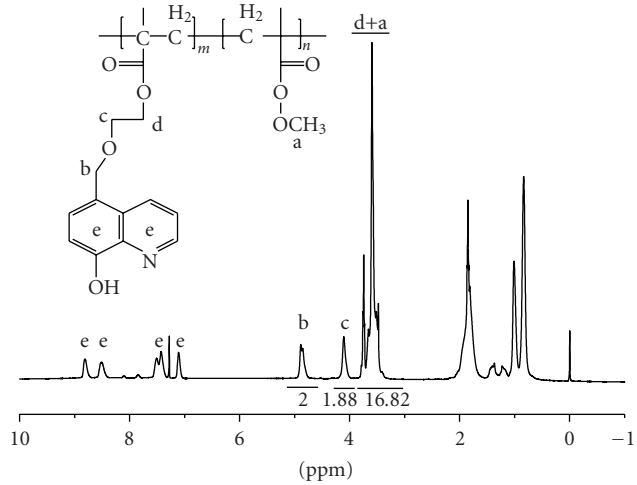

Figure 5: The ^{1}H NMR spectrum of random copolymer of HQHEMA and MMA (poly(HQHEMA-*co*-MMA)) in $CDCl_3$.

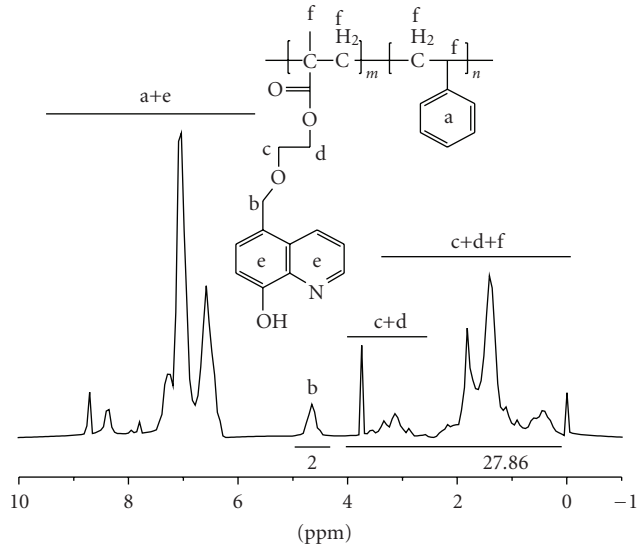

Figure 6: The ^{1}H NMR spectrum of random copolymer of HQHEMA and St (poly(HQHEMA-*co*-St)) in $CDCl_3$.

weight of poly(HQHEMA-*co*-MMA) measured by GPC ($M_{n(\text{GPC})}$) increased linearly with the monomer conversion while keeping the relatively narrow molecular weight distribution ($M_w/M_n \leq 1.63$). The influence of the molar ratio of $[\text{CPDN}]_0/[\text{AIBN}]_0$ on the polymerization was also investigated. As shown in Table 1, the polymerization rate obviously decreased with increasing the initial concentration of CPDN in the polymerization system, which was agreed well with the RAFT polymerization mechanism [26].

3.2. RAFT Copolymerization of HQHEMA and St. The copolymerization of HQHEMA and St mediated by CPDN was also conducted and the results are given in Figure 3, Figure 4, and Table 2. Figure 3 shows the kinetic plot of $\ln([M_0]/[M])$ versus polymerization time. The resulting slope indicates this copolymerization proceeded with approximately constant number of active species for the duration of the reaction. Figure 4 presents the molecular weight measured by GPC ($M_{n(\text{GPC})}$) and molecular weight distribution (M_w/M_n) of poly(HQHEMA-*co*-St) as a function of monomer conversion. Both the linear $M_{n(\text{GPC})}$ versus monomer conversion plot and the corresponding narrow molecular weight distribution imply the living nature of RAFT copolymerization. As expected, increasing the RAFT agent concentration (CPDN) decreased the polymerization rate as presented in Table 2 (entries 1–3).

3.3. Characterization of Copolymers and Chain Extension Experiment. The obtained copolymers were characterized by ^{1}H NMR spectra as shown in Figures 5 and 6. In Figure 5, the signal $\delta = 3.70$ ppm (a) was attributed to the methyl protons of the MMA units, and the signals $\delta =$

Table 1: RAFT copolymerization of HQHEMA and MMA with different CPDN concentrations.

$([MMA]_0 : [HQHEMA]_0) : [CPDN]_0 : [AIBN]_0$	t	T(°C)	Conversion(%)	$M_{n(GPC)}$g/mol	M_w/M_n
1000(10 : 1) : 10 : 1	3	70	45.9	5500	1.22
1000(10 : 1) : 5 : 1	3	70	72.0	11500	1.52
1000(10 : 1) : 3 : 1	3	70	99.1	19100	1.27

Table 2: RAFT copolymerization of St and HQHEMA with different CPDN concentrations.

$([St]_0 : [HQHEMA]_0) : [CPDN]_0 : [AIBN]_0$	t (h)	T (°C)	Conversion (%)	$M_{n(GPC)}$	M_w/M_n
1000(10 : 1) : 10 : 1	12	70	40.8	4400	1.26
1000(10 : 1) : 5 : 1	12	70	66.3	7800	1.20
1000(10 : 1) : 3 : 1	12	70	71.1	10100	1.18

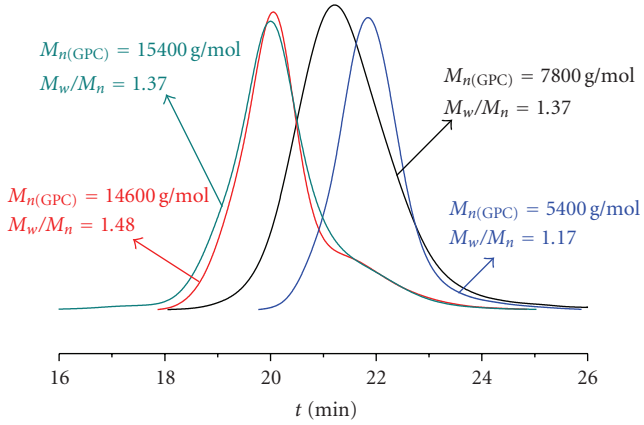

Figure 7: GPC curves of macro-RAFT agent (poly(HQHEMA-*co*-MMA) and poly(HQHEMA-*co*-St)) and polymers after chain-extension. Chain-extended experiment conditions: $[St]_0 : [\text{poly(HQHEMA-}co\text{-MMA)}]_0 : [AIBN]_0 = 500 : 5 : 1$, t = 24 hour, T = 70°C, conversion(%) = 68.6%; $[MA]_0 : [\text{poly(HQHEMA-}co\text{-St)}]_0 : [AIBN]_0 = 500 : 5 : 1$, t = 3 hour, T = 80°C, conversion(%) = 75.3%. Poly(HQHEMA-*co*-St) (-), poly(HQHEMA-*co*-MMA) (-), poly(HQHEMA-*co*-St)-*b*-PMA (-), poly(HQHEMA-*co*-MMA)- *b*-PS (-).

7.10 ppm (e), 7.44 ppm (e), 7.53 ppm (e), 8.54 ppm (e), and 8.83 ppm (3) demonstrate the existence of HQHEMA units, which confirmed that HQHEMA and MMA units were contained in the polymer chain. Based on Figure 5, we also can calculate that the ratio of HQHEMA unit to MMA unit is near 5 : 1 in the copolymer chain. In Figure 6, the signal δ = 6.40 − 7.10 ppm (b) of protons of phenyl ring and the signals δ = 7.53 ppm (e), 8.54 ppm (e), and 8.83 ppm (e) of protons of 8-hydroxyquinoline units indicate the polymer chain contains HQHEMA and St units. The near 7 : 1 ratio of HQHEMA to St unit is also calculated based on Figure 6. To further prove the "living" nature of RAFT polymerization, the obtained copolymers, poly(HQHEMA-*co*-MMA), and poly(HQHEMA-*co*-St) were both used as macro-RAFT agents to conduct chain extension reactions with St and MA as the second monomers, respectively. GPC curves for the block copolymers are shown in Figure 7. It can be seen from Figure 7 that the peaks shift to higher molecular weights from macro-RAFT agent to the chain-extended block copolymers. The molecular weights increased from 7800 g/mol (M_w/M_n = 1.37) to 15400 g/mol (M_w/M_n = 1.37, 68.6% conversion) with poly(HQHEMA-*co*-MMA) as the macro-RAFT agent and St as the second monomer, and from 5400 g/mol (M_w/M_n = 1.17) to 14600 g/mol (M_w/M_n = 1.48, 79.3% conversion) with poly(HQHEMA-*co*-St) as the macro-RAFT agent and MA as the second monomer. These results reveal that almost all the macro-RAFT agents participate in the block copolymerization of MA or St, and block copolymers poly(HQHEMA-*co*-MMA)-*b*-PS and poly(HQHEMA-*co*-St)-*b*-PMA) are formed in a controlled manner.

3.4. Synthesis of Alq_3 and Znq_2-Containing Copolymer. Formation of Alq_3-containing copolymers was performed in THF using poly(HQHEMA-*co*-St) (8-hydroxyquinoline unit/St unit = 1 : 7), 8-hydroxyquinoline and aluminium isopropoxide in a ratio of 8 : 8 : 3. The use of excess 8-hydroxyquinoline and aluminium isopropoxide was adopted in order to minimize the formation of interchain cross-linked complexes. The obtained polymer complex was soluble in several common organic solvents, such as chloroform ($CHCl_3$), tetrahydrofuran (THF), and N,N-dimethylformamide (DMF). The Formation of Znq_2-containing copolymers was also successfully obtained via the similar procedures. As shown in Figure 8, the color of the polymer complex (solid and $CHCl_3$ solution) turned from slightly red to yellow, which demonstrated the successful coordination reaction between metal ion (Al^{3+} and Zn^{2+}) and 8-hydroxyquinoline units. The metal (Al and Zn) ion concentrations of final samples were also determined by VISTA-MPX CCD Simultaneous ICP-AES, and the results are 6.5×10^{-6} mol/L for Al^{3+} and 9.5×10^{-6} mol/L for Zn^{2+}, respectively. The above results demonstrated that the metal ions (Al^{3+} and Zn^{2+}) molar ratios to 8-hydroxyquinoline unit are both close to 1 : 3 and 1 : 2, respectively, which demonstrated that almost all 8-hydroxyquinoline units in the copolymer chains were successfully complexed to form Alq_3 and Znq_2 in the side chain.

UV-vis and fluorescent spectra of the Alq_3- and Znq_2-containing copolymers were investigated as shown in Figures 9 and 10. In Figure 9, the Alq_3- and Znq_2-containing copolymers had the absorption in the range of 300 nm and 450 nm, which were the typical UV-vis absorption of

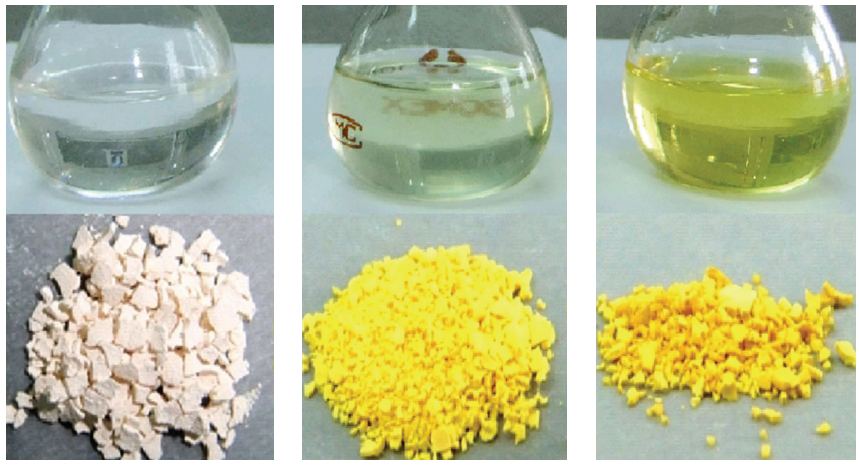

(a) (b) (c)

Figure 8: The images of poly(HQHEMA-*co*-St) and the corresponding Alq_3- and Znq_2-containing copolymers in solid and solution, respectively. (a) poly(HQHEMA-*co*-St); (b) Znq_2-containing poly(HQHEMA-*co*-St); (c) Alq_3-containing poly(HQHEMA-*co*-St). The concentration of 8-hydroxyquinoline moieties is 2.0×10^{-5} M for all the solutions.

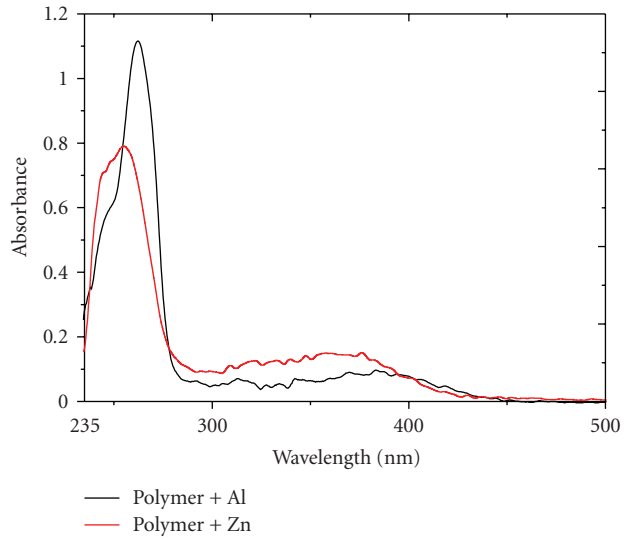

Figure 9: The UV-vis absorption spectra of Alq_3- and Znq_2-containing copolymers in $CHCl_3$. The concentration of 8-hydroxyquinoline moieties is 2.0×10^{-5} M.

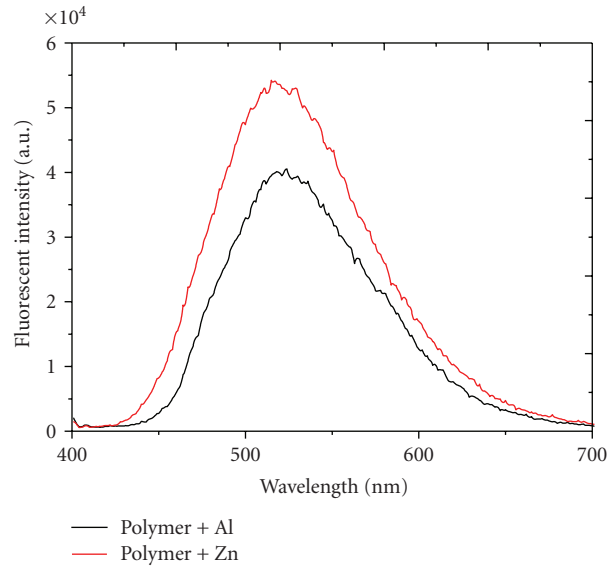

Figure 10: The fluorescence spectra of Alq_3- and Znq_2-containing copolymers in $CHCl_3$. The concentration of 8-hydroxyquinoline moieties is 2.0×10^{-5} M and excitation wavelength is 380 nm.

Alq_3- and Znq_2 complexs. Figure 10 presented the fluorescent spectra of Alq_3- and Znq_2-containing copolymers with an excitation wavelength of 380 nm. As expected, the Alq_3- and Znq_2-containing copolymers had strong emission at around 520 nm. These studies clearly show that the optical properties of Alq_3 and Znq_2 are preserved in the copolymers, respectively.

4. Conclusion

The well-defined poly(HQHEMA-*co*-MMA) and poly (HQHEMA-*co*-St) were successfully prepared via RAFT copolymerization of HQHEMA and MMA (or St) mediated by a typical RAFT agent (CPDN). The soluble copolymers having Alq_3 and Znq_2 side chains were obtained via complexation of the polymers with aluminium isopropoxide and zinc acetate in the presence of monomeric 8-hydroxyquinoline, respectively, which had typical UV-vis absorption in the range from 300 nm to 450 nm and strong fluorescent emission at 520 nm.

Acknowledgments

The financial support from the National Nature Science Foundation of China (nos. 20874069, 50803044, 20974071

and 20904036), the Specialized Research Fund for the Doctoral Program of Higher Education contract Grant (no. 200802850005). This work was also sponsored by Qing Lan Project, Program of Innovative Research Team and the Preresearch Project of Soochow University. C. Wang and W. Zhang contributed equally to this work.

References

[1] C. W. Tang and S. A. Vanslyke, "Organic electroluminescent diodes," *Applied Physics Letters*, vol. 51, no. 12, pp. 913–915, 1987.

[2] C. H. Chen, J. Shi, and C. W. Tang, "Recent developments in molecular organic electroluminescent materials," *Macromolecular Symposia*, vol. 125, pp. 1–48, 1997.

[3] Y. Hamada, T. Sano, H. Fujii, Y. Nishio, H. Takahashi, and K. Shibata, "White-light-emitting material for organic electroluminescent devices," *Japanese Journal of Applied Physics*, vol. 35, no. 10, pp. L1339–L1341, 1996.

[4] H. Tanaka, S. Tokito, Y. Taga, and A. Okada, "Novel metal-chelate emitting materials based on polycyclic aromatic ligands for electroluminescent devices," *Journal of Materials Chemistry*, vol. 8, no. 9, pp. 1999–2003, 1998.

[5] Y. Qiu, Y. Shao, D. Zhang, and X. Hong, "Preparation and characterization of high efficient blue-light emitting materials with a secondary ligand for organic electroluminescence," *Japanese Journal of Applied Physics*, vol. 39, no. 3, pp. 1151–1153, 2000.

[6] A. Meyers and M. Weck, "Design and synthesis of Alq_3-functionalized polymers," *Macromolecules*, vol. 36, no. 6, pp. 1766–1768, 2003.

[7] A. Meyers, C. South, and M. Weck, "Design, synthesis, characterization, and fluorescent studies of the first zinc-quinolate polymer," *Chemical Communications*, vol. 10, no. 10, pp. 1176–1177, 2004.

[8] B. J. Chen, W. Y. Lai, Z. Q. Gao, C. S. Lee, S. T. Lee, and W. A. Gambling, "Electron drift mobility and electroluminescent efficiency of tris(8-hydroxyquinolinolato) aluminum," *Applied Physics Letters*, vol. 75, no. 25, pp. 4010–4012, 1999.

[9] T. Takayama, M. Kitamura, Y. Kobayashi, Y. Arakawa, and K. Kudo, "Soluble polymer complexes having Alq_3-type pendent groups," *Macromolecular Rapid Communications*, vol. 25, no. 12, pp. 1171–1174, 2004.

[10] T. Yamamoto and I. Yamaguchi, "Enzymatic synthesis of poly(quinolinol) and its fluorescent aluminum complex," *Polymer Bulletin*, vol. 50, no. 1-2, pp. 55–60, 2003.

[11] T. Iijima, S.-I. Kuroda, and T. Yamamoto, "Main-chain-type 8-quinolinol polymers: synthesis, optical properties, and complex formation with metals," *Macromolecules*, vol. 41, no. 5, pp. 1654–1662, 2008.

[12] J. Lu, A. R. Hlil, Y. Meng, et al., "Synthesis and characterization of a novel Alq_3-containing polymer," *Journal of Polymer Science A*, vol. 38, no. 16, pp. 2887–2892, 2000.

[13] Y.-F. Duann, Y.-J. Liao, W. Guo, and S.-M. Chang, "The characteristic of photoluminescence of tris-(7-substituted-8-hydroxyquinoline) aluminum complexes and polymeric complexes," *Applied Organometallic Chemistry*, vol. 17, no. 12, pp. 952–957, 2003.

[14] X.-Y. Wang and M. Weck, "Poly(styrene)-supported Alq_3 and BPh_2q," *Macromolecules*, vol. 38, no. 17, pp. 7219–7224, 2005.

[15] Q. Mei, N. Du, and M. Lu, "Synthesis, characterization and thermal properties of metaloquinolate-containing polymers," *European Polymer Journal*, vol. 43, no. 6, pp. 2380–2386, 2007.

[16] S. Li, M. Lin, J. Lu, and H. Liang, "Synthesis, self-assembly, and formation of Al^{3+} complex micelles for diblock copolymer of 2-((8-hydroxyquinolin-5-yl)methoxy)ethyl methacrylate and styrene," *Macromolecules*, vol. 42, no. 4, pp. 1258–1263, 2009.

[17] M. Kamigaito, T. Ando, and M. Sawamoto, "Metal-catalyzed living radical polymerization," *Chemical Reviews*, vol. 101, no. 12, pp. 3689–3745, 2001.

[18] M. Kamigaito, T. Ando, and M. Sawamoto, "Metal-catalyzed living radical polymerization: discovery and developments," *Chemical Record*, vol. 4, no. 3, pp. 159–175, 2004.

[19] K. Matyjaszewski and J. Xia, "Atom transfer radical polymerization," *Chemical Reviews*, vol. 101, no. 9, pp. 2921–2990, 2001.

[20] C. J. Hawker, "Molecular weight control by a "living" free-radical polymerization process," *Journal of the American Chemical Society*, vol. 116, no. 24, pp. 11185–11186, 1994.

[21] J. Chiefari, Y. K. Chong, F. Ercole, et al., "Living free-radical polymerization by reversible addition—fragmentation chain transfer: the RAFT process," *Macromolecules*, vol. 31, no. 16, pp. 5559–5562, 1998.

[22] V. Percec, T. Guliashvili, J. S. Ladislaw, et al., "Ultrafast synthesis of ultrahigh molar mass polymers by metal-catalyzed living radical polymerization of acrylates, methacrylates, and vinyl chloride mediated by SET at 25°C," *Journal of the American Chemical Society*, vol. 128, no. 43, pp. 14156–14165, 2006.

[23] G. Moad, E. Rizzardo, and S. H. Thang, "Living radical polymerization by the RAFT process," *Australian Journal of Chemistry*, vol. 58, no. 6, pp. 379–410, 2005.

[24] J. Zhu, X. Zhu, Z. Cheng, F. Liu, and J. Lu, "Study on controlled free-radical polymerization in the presence of 2-cyanoprop-2-yl 1-dithionaphthalate (CPDN)," *Polymer*, vol. 43, no. 25, pp. 7037–7042, 2002.

[25] Q. Mei, N. Du, and M. Lu, "Synthesis and characterization of high molecular weight metaloquinolate-containing polymers," *Journal of Applied Polymer Science*, vol. 99, no. 4, pp. 1945–1952, 2006.

[26] W. Zhang, X. Zhu, D. Zhou, X. Wang, and J. Zhu, "Reversible addition-fragmentation chain transfer polymerization of 2-naphthyl acrylate with 2-cyanoprop-2-yl 1-dithionaphthalate as a chain-transfer agent," *Journal of Polymer Science A*, vol. 43, no. 12, pp. 2632–2642, 2005.

Hindawi Publishing Corporation
International Journal of Polymer Science
Volume 2010, Article ID 581056, 6 pages
doi:10.1155/2010/581056

Research Article

Synthesis and Characterization of New Photoluminescent Oxadiazole/Carbazole-Containing Polymers

Simona Concilio,[1] Valeria Bugatti,[1] Pio Iannelli,[2] and Stefano Piotto Piotto[2]

[1] *Department of Chemical and Food Engineering, University of Salerno, Via Ponte Don Melillo, 84084 Fisciano, Italy*
[2] *Department of Pharmaceutical Science, University of Salerno, Via Ponte Don Melillo, 84084 Fisciano, Italy*

Correspondence should be addressed to Simona Concilio, sconcilio@unisa.it

Received 5 November 2009; Accepted 14 March 2010

Academic Editor: Jinying Yuan

We report on the synthesis and the characterization of a new class of segmented polyethers POC containing the oxadiazole and carbazole units. The polymers exhibit a high thermal stability, high glass transition temperatures, and good solubility in common organic solvents, despite the extended aromatic portion in the main polymer chain. The synthetic procedures are simple, and no acid side-products are obtained. According to previous reports on oxadiazole/carbazole-containing materials, POCs show high photoluminescence activity in the blue region of the visible spectra. The good solubility in chlorinate solvents allows the preparation of films with homogeneous thickness by spin coating. Glass transition temperature in the range 115–125°C ensures good stability of film morphology at room temperature. The only exception is POC(6), which shows a poor solubility and higher T_g (170°C), due to its shorter aliphatic chain portion. For these features, polymers POC are potential candidate materials for fabricating blue light-emitting devices.

1. Introduction

Phosphorescent polymer light-emitting diodes (PLEDs) have attracted considerable attention for their convenient preparation from solution by spin coating or inkjet printing methods. In order to have a balanced carrier recombination in the emitting layer, the polymer should possess good carrier transport properties, as well as energy level matching with electrodes for effective charge injection [1–13].

To improve the electron transfer in PLEDs, researchers usually spin a p-type polymer on an n-type polymer with electron transport properties. But this kind of multilayer system may suffer difficulties in spinning a polymer solution on an organic film, which can easily dissolve. To deal with this issue, polymers containing both hole- and electron-transporting moieties have been prepared. Recently, polymers with either electron-withdrawing (such as oxadiazole, diphenylquinoline, etc.) or electron-donating groups (such as triphenylamine, carbazole, etc.) have been prepared [14–17].

Oxadiazole/carbazole derivatives having good solubility, high quality film formation, and a strong blue emission can play a very important role in organic/polymeric optoelectronic materials, and they can be used as single-layer materials for OLEDs.

In this work we report on the synthesis and characterization of a series of oxadiazole/carbazole-containing polymers (POCs), having the formula mentioned in Scheme 1, where n is 12 or 6 for the two homopolymers and 12 and 6 or 8 and 4 for the two copolymers. The synthetic procedures are based on the Williamson condensation reaction. All the polymers show high glass transition temperatures and good solubility in common organic solvents. According to previous reports on oxadiazole/carbazole-containing materials [18], POCs show high photoluminescence activity in the blue region of the visible spectrum. Compared to the low-molecular-weight compounds, the new polymers show higher thermal stability and the possibility to be processed in high-quality thin films by solution casting or spin coating.

2. Experimental

2.1. Materials. All reagents and solvents were purchased from Aldrich and Carlo Erba. *N,N*-dimethylacetamide

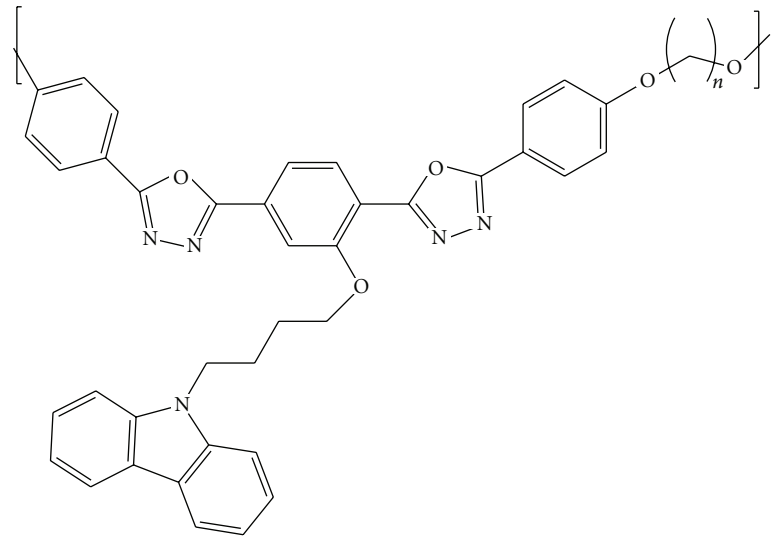

Scheme 1

(DMAc) and *N,N*-dimethylformamide (DMF) were refluxed on calcium hydride, distilled in vacuum, and stored on 4 Å molecular sieves. Other reagents were used without further purification. 2-(4-carbazol-9-yl-butoxy)-terephthalic acid dihydrazide was synthesized according to a previously reported procedure [18].

2.2. Synthesis of the Monomer

*2.2.1. Synthesis of Compound **1**.* To a suspension of compound 2-(4-carbazol-9-yl-butoxy)-terephthalic acid dihydrazide (0.00460 mol, 2.00 g) in dry DMAc (50 mL) at room temperature, the 4-acetoxybenzylchloride (0.0101 mol, 2 : 1 + 10%) was added and the reaction was left to take place overnight under stirring. The reaction mixture was then poured into cold water (600 mL) and the resulting solid product was filtered, washed twice with water, and dried under vacuum. m.p. = 256°C. The product was used in the subsequent intramolecular ring closure reaction. The proton resonance data are in agreement with the expected values.

*2.2.2. Synthesis of Compound **2**.* The freshly synthesized azide 1 (1.0 g) was poured in 80 mL of phosphorous oxychloride ($POCl_3$); the reaction was conducted at refluxing temperature for 5 hours. The mixture was then slowly dropped into ice water (600 mL), and a precipitate was collected. The crude product was then hydrolyzed with 500 mL of aqueous KOH (pH = 12–14), under stirring at 50°C. The clear solution was finally neutralized to pH = 7, and the final product (compound **2**, Scheme 2) was purified by crystallization from DMF/water to obtain pale yellow crystals, with m.p. = 350°C. The proton resonance data are in agreement with the expected values: ^{1}H NMR (DMSO): δ (ppm) = 8.16–8.07 (m, 3H), 7.98 (*d*, *J* = 8.4 Hz, 2H), 7.89–7.78 (m, 4H), 7.52 (*d*, *J* = 8.1 Hz, 2H), 7.30 (*t*, *J* = 7.5 Hz, 2H), 7.11 (*t*, *J* = 7.5 Hz, 2H), 6.98–6.93 (m, 4H), 4.44 (bt, 2H), 4.28 (bt, 2H), 2.03 (m, 2H), 1.88 (m, 2H).

2.3. General Procedure for the Syntheses of Polymers POC (Scheme 3). To a suspension of monomer **2** (0.000897 mol, 0.570 g), in dry DMF (12 mL) at 70°C, and potassium carbonate (0.00429 mol, 4 : 1 + 20%), the appropriate 1,n-dibromoalkane (0.000449 mol), in DMF solution, was added drop-wise, and the mixture was left to reflux overnight under stirring. The reaction mixture was then poured into water (200 mL) and the resulting solid product was filtered and washed twice with water. The crude polymer was then collected and dried under vacuum. It was easily soluble in Chloroform, DMF, and DMSO. The proton resonance data are in agreement with the expected values.

For example, for POC(12,6): ^{1}H NMR ($CDCl_3$): δ (ppm) = 8.12–7.98 (m, 6H), 7.74–7.67 (m, 2H), 7.36 (m, 5H), 7.22 (m, 2H), 7.01–6.90 (m, 4H), 4.40 (m, 2H), 4.22 (m, 2H), 4.02 (m, 4H), 2.22 (m, 2H), 1.98–1.82 (m, 6H), 1.62–1.32 (m, 10H). The spectrum is reported in Figure 1.

For the other polymers of the series, the spectra are similar, the difference is only in integration of the signals for the $-CH_2-$ aliphatic group in the interval (1.62–1.32) ppm.

2.4. Characterization. Thermal measurements were performed by a DSC-7 Perkin Elmer calorimeter under nitrogen flow at 10°C/min rate.

Thermogravimetric analysis was performed with a TA Instruments SDT 2960 apparatus, in air at 20°C/min.

X-ray diffraction spectra were recorded using a flat camera with a sample-to-film distance of 90.0 mm (uni-filtered Cu K_α radiation). The Fujifilm MS 2025 imaging plate and a Fuji Bio-imaging Analyzer System, mod. BAS-1800, were used for recording and digitizing the diffraction patterns.

^{1}H NMR spectra were recorded with a Brucker DRX/400 Spectrometer. Chemical shifts are reported relative to the residual solvent peak.

UV-Vis measurements were performed by a Perkin Elmer Lambda 800 Spectrophotometer and photoluminescence was recorded by a Jasco FP-750 Spectrofluorometer.

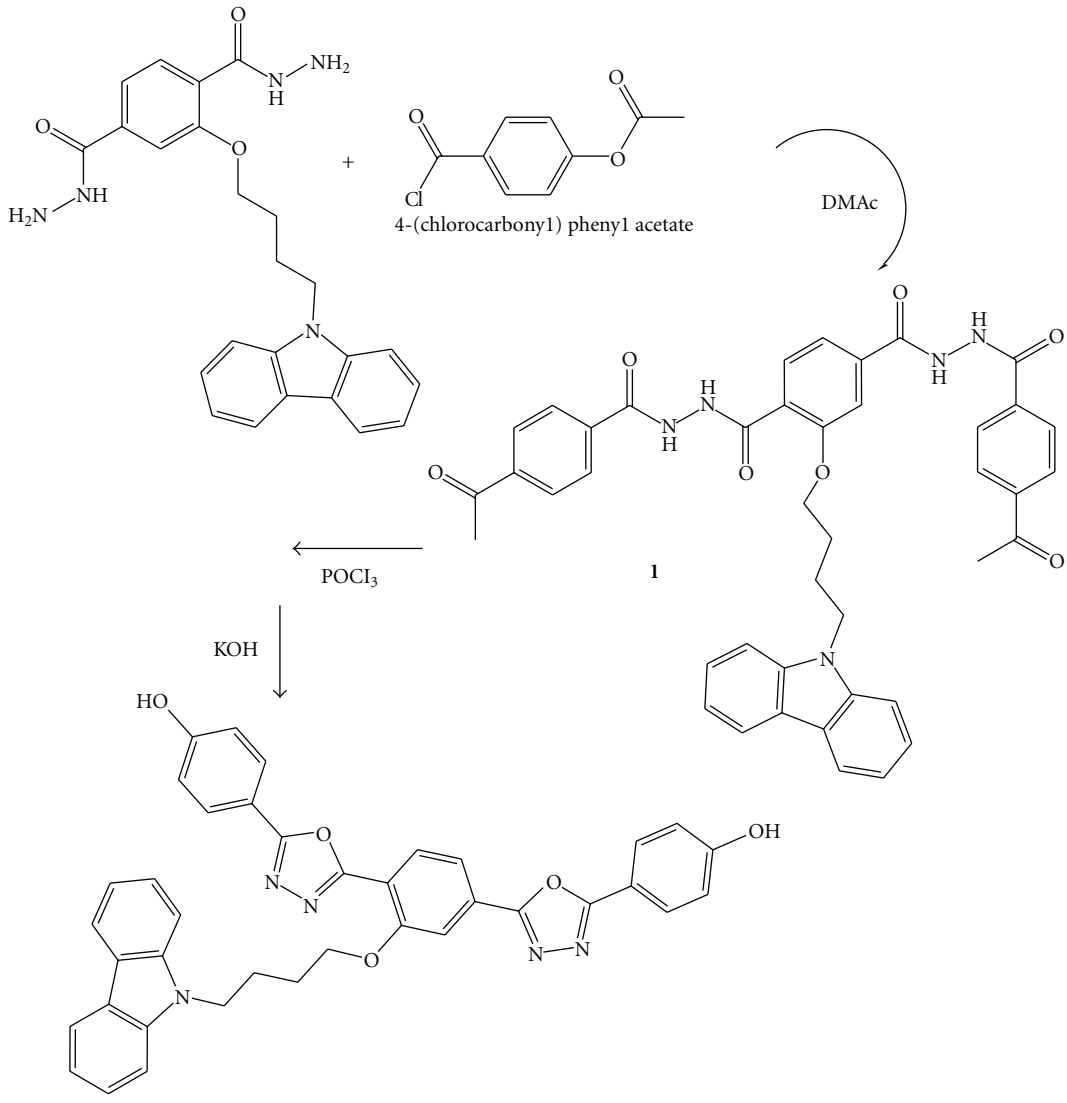

Scheme 2: Synthesis of the monomer.

3. Results and Discussion

3.1. Structural and Calorimetric Characterization. The structure of all polymers POC was confirmed by proton NMR analysis. The NMR spectrum of POC(12,6) in deuterated chloroform solution is reported in Figure 1 as a representative example.

Thermodynamic data of POC are listed in Table 1. From the DSC analysis only the glass transition temperature is observed, which indicates that POCs, as obtained from the synthesis, are amorphous polymers, with glass transition temperatures depending on the length of aliphatic segments in the main chain. As expected, shorter aliphatic chains lead to higher T_g while intermediate values are observed for the copolymers with mixed length of chains.

Glass transition temperature in the range 115–125°C ensures good stability of film morphology at room temperature. The only exception is POC(6), which shows a poor solubility and higher T_g (170°C), due to its shorter aliphatic chain portion. As an example, DSC trace of POC(8,4) is reported in Figure 2.

Table 1: Features of POC(n,m).

Polymer	T_g (°C)*	T_d (°C)**	Solvent***
POC(12)	122	314	$CHCl_3$
POC(6)	169	359	DMF
POC(12,6)	115	374	$CHCl_3$
POC(8,4)	124	318	$CHCl_3$

* Glass transition temperature, from DSC, N_2 flow at 10°C/min rate; ** 5% weight loss temperature, from TGA, air flow at 20°C/min rate. *** The polymer POC(6) has higher solubility in DMF than $CHCl_3$.

The X-ray diffraction pattern of virgin samples of POC, recorded at room temperature is reported in Figure 3. It shows a broad halo, confirming the amorphous nature of the polymers.

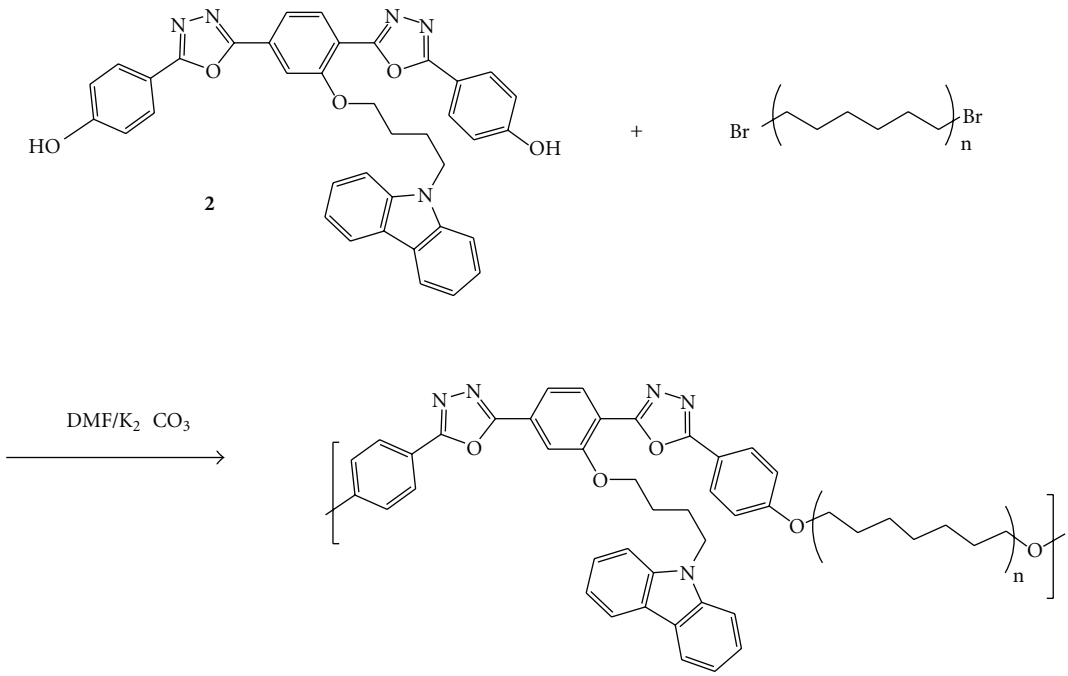

Scheme 3: Synthesis of the polymers (POC).

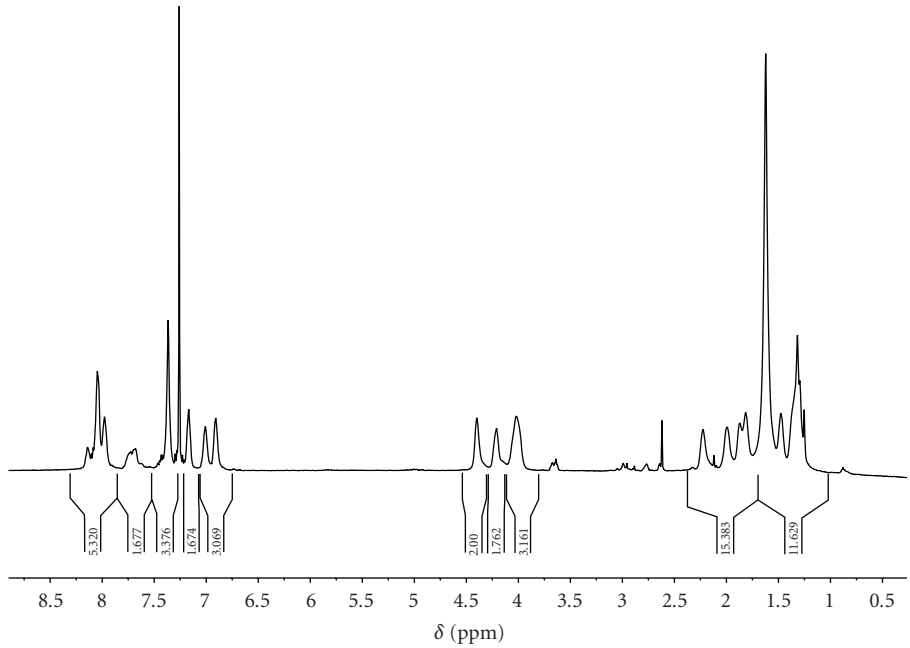

Figure 1: ^{1}H NMR spectrum of POC(12,6) in deuterated chloroform solution.

In the thermogravimetric plots of POC, the degradation process, indicated with a single shoulder, is observed starting at a temperature of about 400°C. This indicates stability of POC at temperatures lower than about 350°C (Table 1). As an example, thermogravimetric trace of POC(12,6) is reported in Figure 4.

POCs are easily soluble in a series of organic solvents; in particular, good-optical-quality films are obtained from chloroform or DMF (Table 1).

3.2. Optical and Photoluminescence Characterization. All POC polymers show similar absorption and emission spectra. As a representative example, UV and fluorescence spectra of POC(12,6) in chloroform solution are reported in Figure 5.

In analogy with our previous paper on low-molecular-weight carbazole/oxadiazole compounds [18] and on oxadiazole-containing polymers [19–21], the carbazole moiety absorbs at lower wavelength (strong peak at 292 nm) with

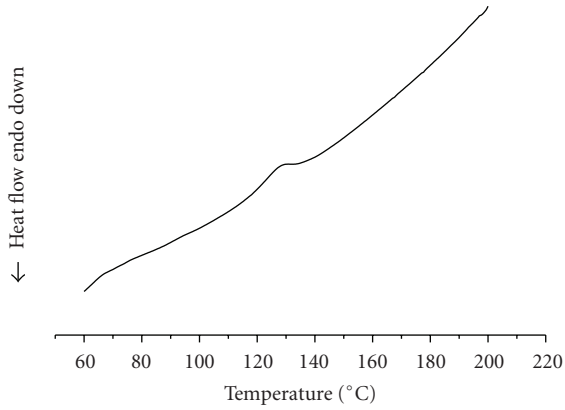

Figure 2: Calorimetric trace of virgin samples of POC(8,4), as obtained from the synthesis, first heating run.

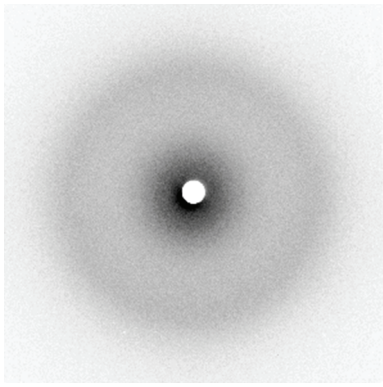

Figure 3: X-ray diffraction pattern of POC(12,6).

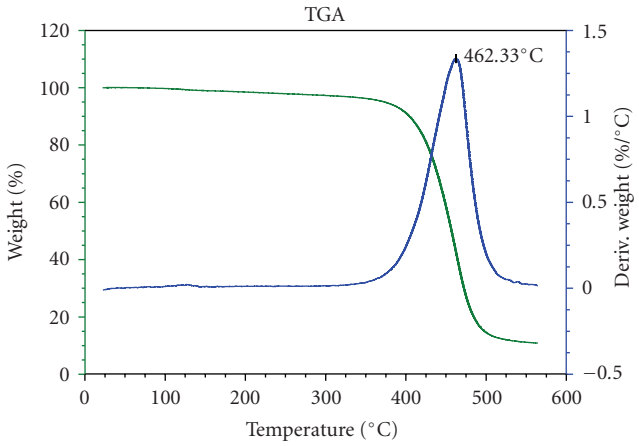

Figure 4: Thermogravimetric trace of POC(12,6).

respect to the oxadiazole unit (two strong and broad peaks at 322 and 345 nm) and emits in the wavelength range (two strong peaks at 354 and 369 nm) where the oxadiazole unit strongly absorbs. The result is that POCs show a strong blue emission, identical to that of analogue oxadiazole-containing polymers; in particular, the emission occurs at 407 nm (main peak, sharp) and at 460 nm (lower peak, broad band).

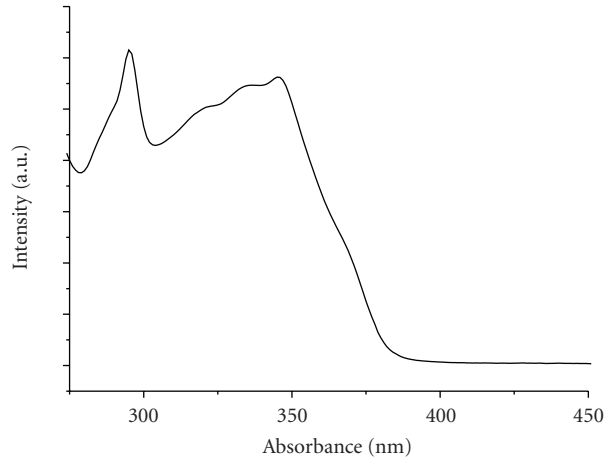

(a)

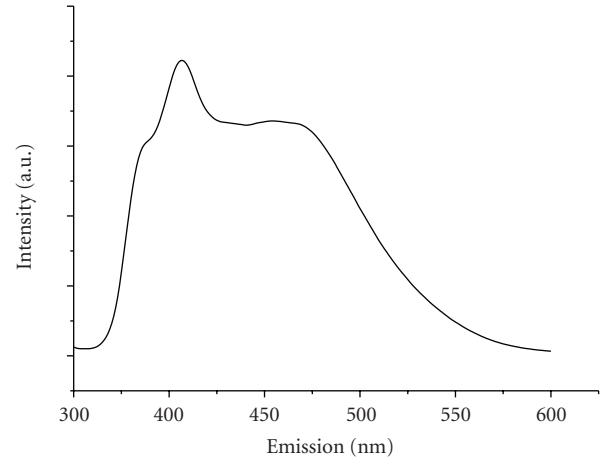

(b)

Figure 5: (a) Absorption and (b) photoluminescence of POC(12,6), irradiated at 345 nm, in chloroform solution.

The good solubility in chlorinate solvents and DMF allows the preparation of films with homogeneous thickness by spin coating.

4. Conclusions

The new synthesized carbazole/oxadiazole-containing polymers (POCs) are blue photoluminescent materials. Taking advantage of the steric constraints due to the side insertion of carbazole unit to the oxadiazole moiety and to the insertion of flexible aliphatic segments in the main polymer chain, POCs are soluble in chlorinate organic solvents or DMF and they can be easily processed to homogenous films. The synthesized polymers show strong photoemission in the blue region of the visible spectrum. Taking advantage from these features, POC could be good candidate materials for the realization of single-layer organic LED.

References

[1] J. H. Burroughes, D. D. C. Bradley, A. R. Brown, et al., "Light-emitting diodes based on conjugated polymers," *Nature*, vol. 347, no. 6293, pp. 539–541, 1990.

[2] A. B. Holmes, D. D. C. Bradley, A. R. Brown, et al., "Photoluminescence and electroluminescence in conjugated polymeric systems," *Synthetic Metals*, vol. 57, no. 1, pp. 4031–4040, 1993.

[3] M. Berggren, O. Inganas, G. Gustafsson, et al., "Light emitting diodes with variable colours from polymer blends," *Nature*, vol. 372, no. 6505, pp. 444–446, 1994.

[4] G. Grem, G. Leditzky, B. Ullrich, and G. Leising, "Realization of a blue-light-emitting device using poly(p-phenylene)," *Advanced Materials*, vol. 4, no. 1, pp. 36–37, 1992.

[5] C. Adachi, T. Tsutsui, and S. Saito, "Blue light-emitting organic electroluminescent devices," *Applied Physics Letters*, vol. 56, no. 9, pp. 799–801, 1990.

[6] J.-I. Lee, G. Klaerner, and R. D. Miller, "Oxidative stability and its effect on the photoluminescence of poly(fluorene) derivatives: end group effects," *Chemistry of Materials*, vol. 11, no. 4, pp. 1083–1088, 1999.

[7] Z. Peng and J. Zhang, "New oxadiazole-containing conjugated polymer for single-layer light-emitting diodes," *Chemistry of Materials*, vol. 11, no. 4, pp. 1138–1143, 1999.

[8] F.-C. Chen, G. He, and Y. Yang, "Triplet exciton confinement in phosphorescent polymer light-emitting diodes," *Applied Physics Letters*, vol. 82, no. 7, pp. 1006–1008, 2003.

[9] C. Adachi, R. C. Kwong, P. Djurovich, et al., "Endothermic energy transfer: a mechanism for generating very efficient high-energy phosphorescent emission in organic materials," *Applied Physics Letters*, vol. 79, no. 13, pp. 2082–2084, 2001.

[10] R. J. Holmes, S. R. Forrest, Y.-J. Tung, et al., "Blue organic electrophosphorescence using exothermic host-guest energy transfer," *Applied Physics Letters*, vol. 82, no. 15, pp. 2422–2424, 2003.

[11] H.-J. Su, F.-I. Wu, C.-F. Shu, Y.-L. Tung, Y. Chi, and G.-H. Lee, "Polyfluorene containing diphenylquinoline pendants and their applications in organic light emitting diodes," *Journal of Polymer Science Part A*, vol. 43, no. 4, pp. 859–869, 2005.

[12] Z. Liu, Y. Zhang, Y. Hu, et al., "Novel bipolar light-emitting copolymer containing triazole and triphenylamine moieties," *Journal of Polymer Science Part A*, vol. 40, no. 8, pp. 1122–1126, 2002.

[13] F.-I. Wu, P.-I. Shih, C.-F. Shu, Y.-L. Tung, and Y. Chi, "Highly efficient light-emitting diodes based on fluorene copolymer consisting of triarylamine units in the main chain and oxadiazole pendent groups," *Macromolecules*, vol. 38, no. 22, pp. 9028–9036, 2005.

[14] X.-C. Li, Y. Liu, M. S. Liu, and A. K.-Y. Jen, "Synthesis, properties, and application of new luminescent polymers with both hole and electron injection abilities for light-emitting devices," *Chemistry of Materials*, vol. 11, no. 6, pp. 1568–1575, 1999.

[15] Z. Peng, Z. Bao, and M. E. Galvin, "Polymers with bipolar carrier transport abilities for light emitting diodes," *Chemistry of Materials*, vol. 10, no. 8, pp. 2086–2090, 1998.

[16] J. Lu, A. R. Hlil, Y. Sun, et al., "Synthesis and characterization of a blue light emitting polymer containing both hole and electron transporting units," *Chemistry of Materials*, vol. 11, no. 9, pp. 2501–2507, 1999.

[17] M. B. Casu, P. Imperia, S. Schrader, B. Schulz, M. Jandke, and P. Strohriegl, "Valence electronic structure of oxadiazoles and quinoxalines model compounds," *Synthetic Metals*, vol. 121, no. 1–3, pp. 1397–1398, 2001.

[18] V. Bugatti, S. Concilio, P. Iannelli, et al., "Synthesis and characterization of new electroluminescent molecules containing carbazole and oxadiazole units," *Synthetic Metals*, vol. 156, no. 1, pp. 13–20, 2006.

[19] D. Acierno, E. Amendola, S. Bellone, et al., "Synthesis and luminescent properties of a new class of nematic oxadiazole containing poly-ethers for PLED," *Journal of Non-Crystalline Solids*, vol. 338–340, no. 1, pp. 278–282, 2004.

[20] D. Acierno, S. Concilio, A. Diodati, P. Iannelli, S. P. Piotto, and P. Scarfato, "Synthesis and liquid crystalline properties of low molecular mass compounds containing the 1,4-bis (5-phenyl-1,3,4-oxadiazolyl) benzene unit," *Liquid Crystals*, vol. 29, no. 11, pp. 1383–1392, 2002.

[21] D. Acierno, E. Amendola, S. Bellone, et al., "Synthesis and characterization of a new class of nematic photoluminescent oxadiazole-containing polyethers," *Macromolecules*, vol. 36, no. 17, pp. 6410–6415, 2003.

Hindawi Publishing Corporation
International Journal of Polymer Science
Volume 2010, Article ID 908128, 9 pages
doi:10.1155/2010/908128

Research Article

New Type of Donor-Acceptor Through-Space Conjugated Polymer

Lin Lin, Yasuhiro Morisaki, and Yoshiki Chujo

Department of Polymer Chemistry, Graduate School of Engineering, Kyoto University, Katsura, Nishikyo-ku, Kyoto 615-8510, Japan

Correspondence should be addressed to Yasuhiro Morisaki, ymo@chujo.synchem.kyoto-u.ac.jp and Yoshiki Chujo, chujo@chujo.synchem.kyoto-u.ac.jp

Received 2 November 2009; Accepted 21 February 2010

Academic Editor: Jinying Yuan

We report the synthesis and properties of a novel through-space conjugated polymer with a [2.2]paracyclophane skeleton. The obtained polymer possessed donor (fluorene) and acceptor (2,1,3-benzothiadiazole) segments that were alternately π-stacked in proximity via the [2.2]paracyclophane moieties. The good overlap between the emission peak of the donor unit (fluorene) and the CT band of the acceptor unit (2,1,3-benzothiadiazole) caused fluorescence resonance energy transfer, and the visible green light emission from the acceptor unit was observed.

1. Introduction

Since [2.2]paracyclophane was first prepared by Brown and Farthing in 1949 [1], [2.2]paracyclophane consisting of two benzene rings closely linked (distance of approximately 2.8–3.1 Å) by two ethylene bridges at *para* positions, it has been attracting attention [2–4]. However, even though cyclophane compounds have been receiving considerable attention in the field of organic chemistry, only several reports [5–23] on the synthesis of [2.2]paracyclophane-containing polymers have been published in the field of polymer chemistry. In particular, only a few reports on conjugated polymers containing [2.2]paracyclophane in the polymer main chain have been published [5–7, 20–23]. Recently, we successfully synthesized novel through-space conjugated polymers possessing [2.2]paracyclophanes as a repeating unit into the main chain [5–7, 24–38]. We elucidated their properties and found that the conjugation lengths of these polymers extend via the stacked π-electron systems. In addition, we synthesized [2.2]paracyclophane-layered polymers by treating pseudo-*p*-diethynyl[2.2]paracyclophane with diiodoxanthene as a scaffold [39–42].

A one-dimensional π-stacked structure can be readily obtained by incorporating a [2.2]paracyclophane unit into a conjugated polymer backbone. As shown in Scheme 1, for example, copolymerization of pseudo-*p*-diethynyl[2.2]paracyclophane with 2,5-dialkoxy-1,4-diiodobenzene yields a through-space conjugated polymer comprising a stacked π-electron system, that is, a stacked xylyl-phenylene-xylyl unit. Therefore, the properties of through-space conjugated polymers synthesized by using a [2.2]paracyclophane monomer depend on this stacked π-electron system (Scheme 1). We elucidated that the polymer emitted efficiently (Φ_F = 82% in diluted $CHCl_3$ solution) [35] not from the excimer of the stacked xylyl-phenylene-xylyl segments but from the xylyl-phenylene-xylyl segment itself, irrespective of the π-stacked structure of the polymer chain [6, 7, 43–45].

The use of [2.2]paracyclophane as a monomer for the synthesis of a conjugated polymer enables the development of π-stacked structures of various π-electron systems. Such through-space conjugated polymers can be expected to transfer charge and/or energy effectively via the through-space interaction. Here, we report the synthesis of a new type of donor-acceptor through-space conjugated polymer with fluorene as a donor component and 2,1,3-benzothiadiazole as an acceptor component. The obtained polymer comprises donor and acceptor π-electron systems that are alternately π-stacked in proximity and held by covalent bonds, while the construction of π-stacked donor-acceptor systems has been achieved by a supramolecular approach [46–50].

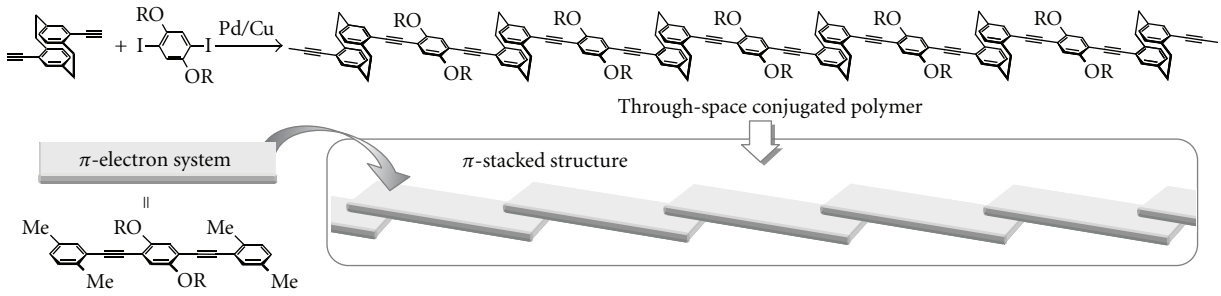

Scheme 1: π-Stacked structure of a through-space conjugated polymer based on [2.2]paracyclophane.

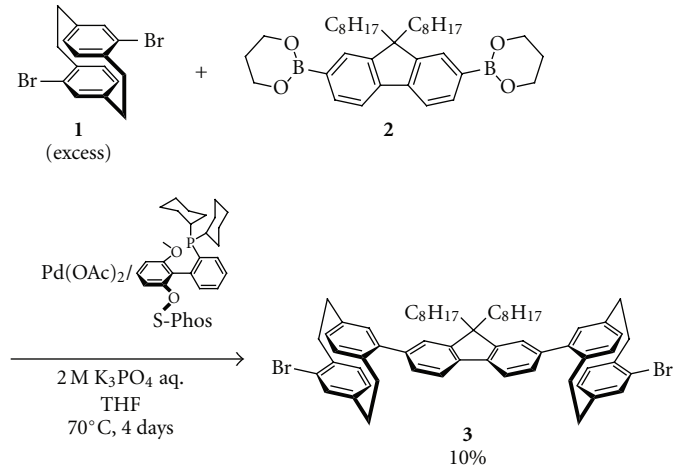

Scheme 2: Synthesis of monomer **3**.

2. Experimental Section

2.1. General. ^{1}H and ^{13}C NMR spectra were recorded on a JEOL JNM-EX400 instrument at 400 and 100 MHz, respectively. The chemical shift values were expressed relative to Me_4Si as an internal standard. FTIR spectra were obtained on a Perkin-Elmer 1600 spectrometer. High-resolution mass spectra (HRMS) were obtained on a JEOL JMS-SX102A spectrometer. Analytical thin-layer chromatography (TLC) was performed with silica gel 60 Merck F_{254} plates. Column chromatography was performed with Wakogel C-300 silica gel. Gel permeation chromatography (GPC) was carried out on a TOSOH 8020 (TSKgel α-3000 column) instrument using $CHCl_3$ as an eluent after calibration with standard polystyrene samples. Recyclable preparative high-performance liquid chromatography (HPLC) was performed in Japan Analytical Industry Co. Ltd., Model 918R (JAIGEL-2.5H and 3H columns) using $CHCl_3$ as an eluent. UV-Vis absorption spectra were obtained on a Shimadzu UV3600 spectrometer. Photoluminescence spectra were obtained on a HORIBA Jobin Yvon FluoroMax-4 luminescence spectrometer. For cyclic voltammetry, a polymer thin film was obtained by spin-coating from a toluene solution on an indium-tin-oxide (ITO) coated-glass electrode. Cyclic voltammetry (CV) was carried out on a BAS CV-50W electrochemical analyzer in CH_3CN containing 0.1 M Et_4NBF_4 with a glassy carbon working electrode, a Pt counter electrode, an Ag/Ag^+ reference electrode, and ferrocene (Fc/Fc^+) as an external standard at a scan rate of 100 mV/s. Thermogravimetric analysis (TGA) was made on a Seiko EXSTAR 6000 instrument (10°C/min). Elemental analyses were performed with an Elementar Analysensysteme varioMICRO V1.5.8 system using the CHN mode or performed at the Microanalytical Center of Kyoto University.

2.2. Materials. Dehydrated toluene was purchased and used without further purification. THF was purchased and purified by passage through purification column under Ar pressure [51]. $Pd(PPh_3)_4$, $Pd(OAc)_2$, 2-dicyclohexylphosphino-2′,6′-dimethoxybiphenyl (S-Phos), K_2CO_3, and K_3PO_4 were used as received. 9,9-Dioctylfluorene-2,7-diboronic acid bis(1,3-propanediol)ester (**2**), 1-bromo-2,5-dimethylbenzene (**5**), and 2,5-dimethylphenylboronic acid (**6**) were purchased and used without further purification. Pseudo-*p*-dibromo[2.2]paracyclophane (**1**) [52, 53], 4,7-bis(4,4,5,5-tetramethyl-1,3,2-dioxaborolan-2-yl)-2,1,3-benzothiadiazole (**4**) [54], and 4,7-dibromo-2,1,3-benzothiadiazole (**7**) [55] were prepared according to the literature. All reactions were performed under Ar atmosphere.

*2.3. 9,9-Dioctyl-2,7-bis(pseudo-p-bromo[2.2]paracyclophanyl)fluorene (**3**).* A mixture of pseudo-*p*-dibromo[2.2]paracyclophane (**1**) (366 mg, 1.0 mmol), 9,9-dioctylfluorene-2,7-diboronic acid bis(1,3-propanediol)ester (**2**) (150 mg,

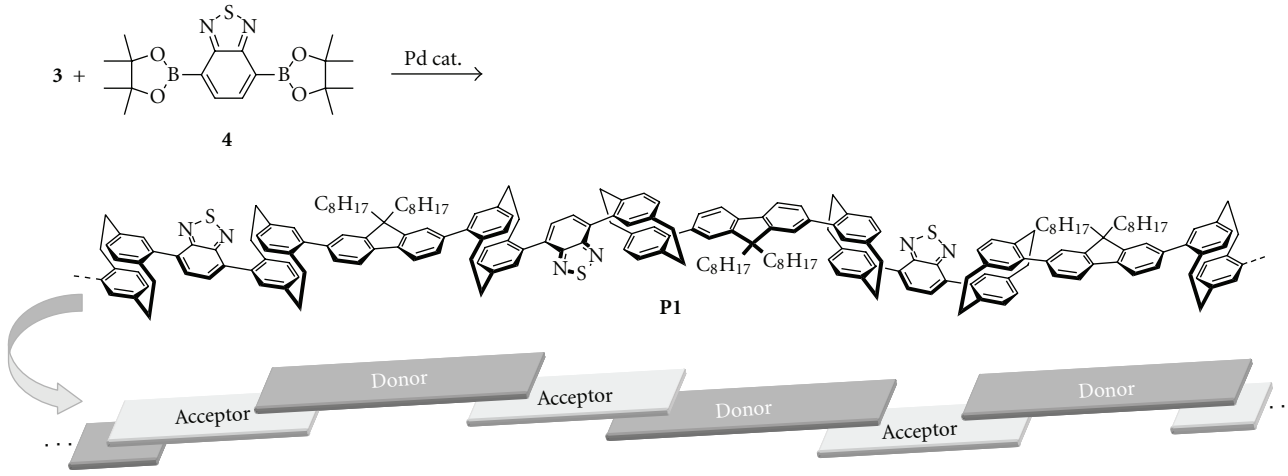

Scheme 3: Synthesis of polymer **P1**.

Table 1: Polymerization results.

Run	Catalyst system Inorganic base,* solvent	Temperature/°C	Time/h	Yield**/%	M_w***	M_n***
1	$Pd(PPh_3)_4$ K_2CO_3, toluene	80	96	14	3700	3300
2	$Pd(OAc)_2$/S-Phos**** K_3PO_4, THF	reflux*****	24	68	49000	17000

*2.0 M Aqueous solution, **isolated yield after reprecipitation, ***estimated by GPC ($CHCl_3$ eluent, polystyrene standards), ****2-dicyclohexylphosphino-2′,6′-dimethoxybiphenyl, and *****oil bath temperature: 75°C.

0.30 mmol), $Pd(OAc)_2$ (6.7 mg, 0.030 mmol), and S-Phos (24 mg, 0.060 mmol) was placed in a Schlenk tube equipped with a magnetic stirring bar. THF (9.0 mL) and aqueous 2.0 M K_3PO_4 (0.45 mL) were added, and the reaction was carried out for 4 days at 70°C. After the reaction, the reaction mixture was poured into H_2O, and extraction with $CHCl_3$ was carried out. The organic layer was dried over $MgSO_4$. After $MgSO_4$ was filtered off, solvent was removed in vacuo. The crude solid was purified by column chromatography on silica gel (eluent: $CHCl_3$/hexane, v/v = 1/3). Further purification by HPLC yielded monomer **3** as a white solid (30 mg, 0.030 mmol, 10%).

R_f = 0.40 (hexane/$CHCl_3$, v/v = 1/3); ^{1}H NMR (CD_2Cl_2, 400 MHz) δ 0.61 (t, J = 6.8 Hz, 3H), 0.7 (br, 8H), 0.73 (t, J = 6.8 Hz, 6H), 0.79, J = 7.0 Hz, 3H), 1.0–1.3 (m, 40H), 2.0 (m, 4H), 2.1 (m, 4H), 2.54 (m, 4H), 2.68 (m, 4H), 2.90 (m, 8H), 3.01 (m, 4H), 3.19 (m, 4H), 3.45 (m, 8H), 6.54 (m, 16H), 6.61 (s, 4H), 7.08 (d, J = 7.8 Hz, 4H), 7.36 (s, 4H), 7.44 (d, J = 8.0 Hz, 4H), 7.80 (d, J = 7.8 Hz, 4H) ppm; ^{13}C NMR (CD_2Cl_2, 100 MHz) δ14.2, 22.9, 24.5, 29.6, 29.8, 30.4, 30.5, 32.0, 32.1, 32.3, 33.6, 34.4, 34.5, 35.8, 41.0, 55.6, 120.2, 125.1, 126.8, 128.6, 128.8, 129.3, 132.4, 134.2, 135.5, 137.3, 137.6, 139.3, 139.9, 140.2, 140.4, 142.3, 143.0, 147.2, 151.6 ppm. HRMS (EI): calcd. for $C_{61}H_{68}Br_2$ $[M]^+$: 958.3688, found 958.3668. Anal. calcd. for $C_{61}H_{68}Br_2$: C 76.24; H 7.13; Br 16.63, found: C 76.08; H 7.12; Br 16.82.

2.4. Polymerization. A typical procedure is as follows. A mixture of **3** (30 mg, 0.030 mmol), 4,7-bis(4,4,5,5-tetramethyl-1,3,2-dioxaborolan-2-yl)-2,1,3-benzothiadiazole (**4**) (12 mg, 0.030 mmol), $Pd(OAc)_2$ (1.4 mg, 0.006 mmol), and S-Phos (5.0 mg, 0.012 mmol) was placed in a Schlenk tube equipped with a magnetic stirring bar. THF (3.0 mL) and aqueous 2.0 M K_3PO_4 (0.10 mL) were added, and the reaction was carried out for 24 hours at reflux temperature (bath temp.: 75°C). After the reaction mixture was cooled to room temperature, the mixture was filtered to remove precipitated salts and washed with $CHCl_3$. The filtrate was washed with 28% aqueous NH_3 solution, and the organic layer was poured into a large amount of MeOH to obtain polymer **P1** (19 mg, 0.080 mmol, 68%) as a yellow powder.

^{1}H NMR (CD_2Cl_2, 400 MHz) δ 0.8–1.0 (br m), 1.0–1.4 (br m), 1.7 (br), 2.2 (br), 2.8–3.2 (br m), 3.7 (br), 6.7–7.1 (m), 7.6–7.7 (br), 8.0 (m) ppm; ^{13}C NMR (CD_2Cl_2, 100 MHz) δ 13.5, 22.2, 23.8, 29 (m), 31 (m), 34 (m), 40.3, 55.0, 119.6, 124.3, 129.4, 131-134 (m), 139 (m), 142.1, 151.0, 153.8 ppm.

*2.5. 9,9-Dioctyl-2,7-dixylylfluorene (**M1**).* A mixture of **2** (420 mg, 0.75 mmol), 1-bromo-2,5-dimethylbenzene (**5**) (276 mg, 1.5 mmol), $Pd(OAc)_2$ (1.12 mg, 0.005 mmol), and S-Phos (4.1 mg, 0.010 mmol) were placed in a Schlenk tube equipped with a magnetic stirring bar. THF (1.0 mL) and

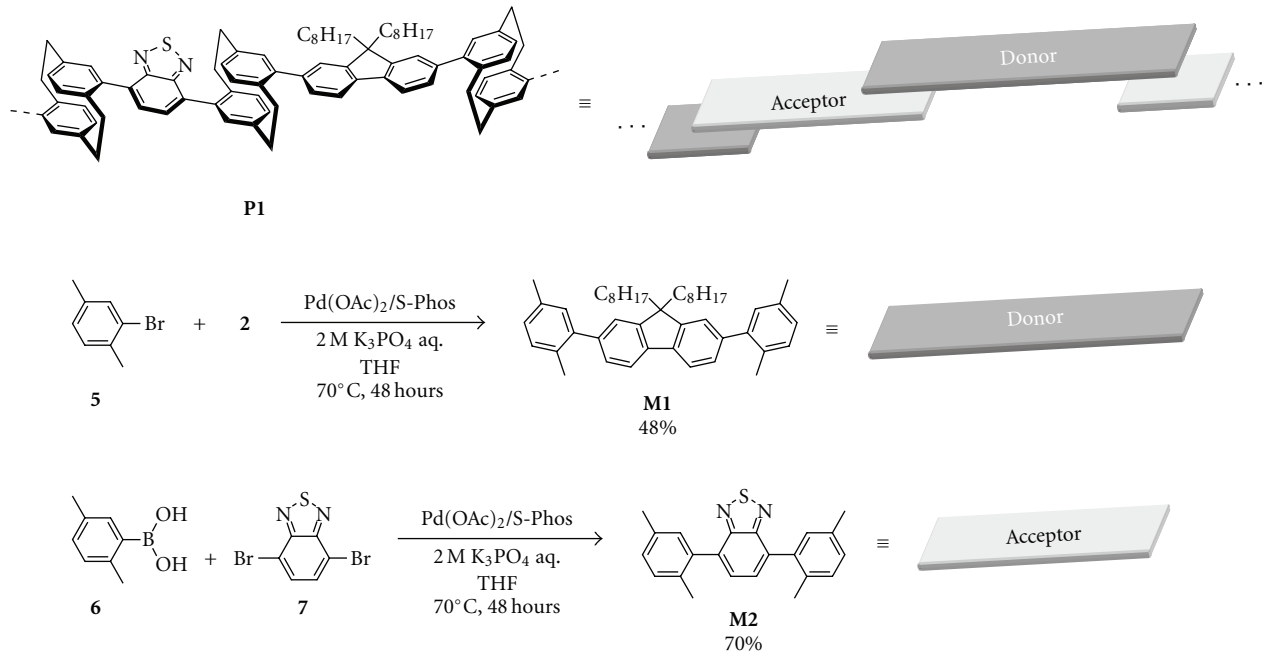

Scheme 4: Synthesis of model compounds **M1** and **M2**.

aqueous 2.0 M K_3PO_4 (0.10 mL) was added, and the reaction was carried out for 48 hours at 70°C. After the reaction mixture was cooled to room temperature, the mixture was filtered to remove precipitated salts and washed with $CHCl_3$. The organic layer was dried over $MgSO_4$. $MgSO_4$ was removed, and the solvent was dried in vacuo. The solid was purified by column chromatography on silica gel (eluent: $CHCl_3$/hexane, v/v = 3/1) to yield model compound **M1** as a white solid (217 mg, 0.36 mmol, 48%).

R_f = 0.85 ($CHCl_3$/hexane, v/v = 3/1); ^{1}H NMR ($CDCl_3$, 400 MHz) δ 0.74 (br, 4H), 0.81 (t, J = 7.1 Hz, 6H), 1.06 (m, 16H), 1.19 (t, J = 6.8 Hz, 4H), 1.98 (m, 4H), 2.27 (s, 6H), 2.38 (s, 6H), 7.09 (d, J = 7.6 Hz, 2H), 7.15 (s, 2H), 7.18 (d, J = 7.8 Hz, 2H), 7.28 (d, J = 7.8 Hz, 2H), 7.29 (s, 2H), 7.74 (d, J = 7.6 Hz, 2H) ppm; ^{13}C NMR ($CDCl_3$, 100 MHz) δ 14.1, 20.1, 20.9, 22.6, 23.8, 29.1, 29.2, 30.0, 31.8, 40.4, 55.1, 119.2, 123.8, 127.79, 127.84, 130.3, 130.5, 132.3, 135.1, 139.5, 140.7, 142.3, 150.6 ppm. HRMS (EI): calcd. for $C_{45}H_{58}$ $[M]^+$: 598.4539, found 598.4541. Anal. calcd. for $C_{45}H_{58}$: C 90.24; H 9.76, found: C 90.18; H 9.73.

*2.6. 4,7-Dixylyl-2,1,3-benzothiadiazole (**M2**).* A mixture of 2, 5-dimethylphenylboronic acid (**6**) (375 mg, 2.5 mmol), 4,7-dibromo-2,1,3-benzothiadiazole (**7**) (293 mg, 1.0 mmol), $Pd(OAc)_2$ (8.98 mg, 0.040 mmol), and S-Phos (32.8 mg, 0.080 mmol) were placed in a Schlenk tube equipped with a magnetic stirring bar. THF (2.0 mL) and aqueous 2.0 M K_3PO_4 (0.20 mL) was added, and the reaction was carried out for 48 hours at 70°C. After the reaction mixture was cooled to room temperature, the mixture was filtered to remove precipitated salts and washed with $CHCl_3$. The organic layer was dried over $MgSO_4$. $MgSO_4$ was removed, and the solvent was dried in vacuo. The solid was purified by column chromatography on silica gel (eluent: $CHCl_3$/hexane, v/v = 1/1) to yield model compound **M2** as a white solid (240 mg, 0.70 mmol, 70%).

R_f = 0.43 (hexane/$CHCl_3$, v/v = 1/1); ^{1}H NMR (CD_2Cl_2, 400 MHz) δ 2.14 (s, 6H), 2.39 (s, 6H), 7.21 (s, 4H), 7.26 (d, J = 8.3 Hz, 2H), 7.54 (s, 2H), ppm; ^{13}C NMR ($CDCl_3$, 100 MHz) δ 19.2, 20.2, 128.5, 128.7, 129.7, 130.4, 133.1, 134.0, 134.8, 137.1, 153.7 ppm. HRMS (EI): calcd. for $C_{22}H_{20}N_2S$ $[M]^+$: 344.1347, found 344.1344. Anal. calcd. for $C_{22}H_{20}N_2S$: C 76.71; H 5.85; N 8.13; S 9.31, found: C 76.52; H 5.86; N 7.82; S 9.07.

^{1}H and ^{13}C NMR spectra of all compounds described above are shown in Supplementary Material available online doi:10.115/2010/908128 Information.

3. Results and Discussion

The synthesis of monomer **3** is outlined in Scheme 2. The treatment of the excess amount (>2.5 equivalent) of pseudo-*p*-dibromo[2.2]paracyclophane **1** with fluorene diboronic acid ester **2** in the presence of a catalytic amount of $Pd(OAc)_2$ and 2-dicyclohexylphosphino-2′,6′-dimethoxybiphenyl (S-Phos) in THF with aqueous K_3PO_4 [56, 57] afforded the corresponding bis(pseudo-*p*-bromo[2.2]paracyclophanyl)fluorene **3** in 10% isolated yield. The purification of monomer **3** by column chromatography using SiO_2 and recyclable HPLC resulted in this low isolated yield (10%). The ^{1}H NMR spectrum of monomer **3** exhibited two peaks at around 2.1 ppm (approximately 1:1), as shown in Figure S1; these peaks were assigned to the methylenes of octyl groups at the 9-position of fluorene. This result suggests that the existence of two isomers was

attributed to the two diastereomers (racemi and meso) derived from two planar chiral [2.2]paracyclophane units in monomer **3**.

Polymer **P1** was synthesized by the palladium-catalyzed polymerization of **3** and 4,7-bis(4,4,5,5-tetramethyl-1,3,2-dioxaborolan-2-yl)-2,1,3-benzothiadiazole **4**, as shown in Scheme 3. The palladium-catalyzed coupling reaction of monomers **3** and **4** was carried out to obtain the corresponding through-space conjugated polymer **P1**; the polymerization results are listed in Table 1. An appropriate catalytic system was critically important for achieving successful polymerization. The standard Suzuki-Miyaura coupling reaction [56] with a $Pd(PPh_3)_4$ catalyst and aqueous K_2CO_3 in toluene at 80°C for 96 hours was ineffective for polymerization. Polymer **P1** was obtained in 14% isolated yield with a number-average molecular weight (M_n) of 3300 and a weight-average molecular weight (M_w) of 3700 by GPC analysis ($CHCl_3$, polystyrene standards, Run 1 in Table 1). $Pd(OAc)_2$ with S-Phos catalytic system considerably increased the catalytic activity for the polymer synthesis as well as the monomer synthesis to afford polymer **P1** in 68% isolated yield, and the M_n and M_w were estimated to be 17000 and 49000, respectively (Run 2 in Table 1).

The obtained polymer **P1** is a new type of donor-acceptor conjugated polymer in which a donor π-electron system and an acceptor π-electron system are linked alternately via the through-space interaction in the single polymer main chain (Scheme 3). The structure of **P1** was confirmed by ^1H and ^{13}C NMR spectra (Figures S3 and S4 in Supplementary Material). Polymer **P1** was highly soluble in common organic solvents such as THF, $CHCl_3$, CH_2Cl_2, toluene, and DMF. In addition, it could be processed into a thin film by casting or spin-coating from toluene solution, and it was found to be air stable in solution and in the solid state. The thermal stability of **P1** was evaluated by carrying out thermogravimetric analysis (TGA) under air (Figure S9 in Supplementary Material). The TGA results showed that **P1** exhibited good thermal stability with a 10% weight loss and temperature at 408°C.

In order to elucidate the optical properties of polymer **P1**, we designed and prepared model compounds **M1** and **M2**. These compounds **M1** and **M2** represent the donor and acceptor unit layers of **P1**, respectively, as shown in Scheme 4. Figure 1 shows UV-Vis absorption spectra and photoluminescence spectra of **M1**, **M2**, and **P1** in diluted $CHCl_3$ (1.0×10^{-5} M for UV and 1.0×10^{-6} M for photoluminescence). As shown in Figure 1(a), the typical π-π^* transition band of a fluorene compound was observed at around 300 nm, and blue emission was observed at 364 nm with a vibrational structure.

As shown in Figure 1(b), **M2** exhibited a broad absorption band at around 360 nm, which was attributed to a charge-transfer (CT) band from the benzene to the thiadiazole moieties, in addition to a π-π^* transition band of xylyl-phenylene-xylyl backbone at around 310 nm. When the CT band at 360 nm was excited, the photoluminescence spectrum of **M2** showed a maximum peak at 467 nm. The shape and the peak top of the photoluminescence spectrum of **M2** were independent of the excitation wavelength (308 nm and 360 nm), indicating that the spectrum is characteristic of the benzothiadiazole moiety.

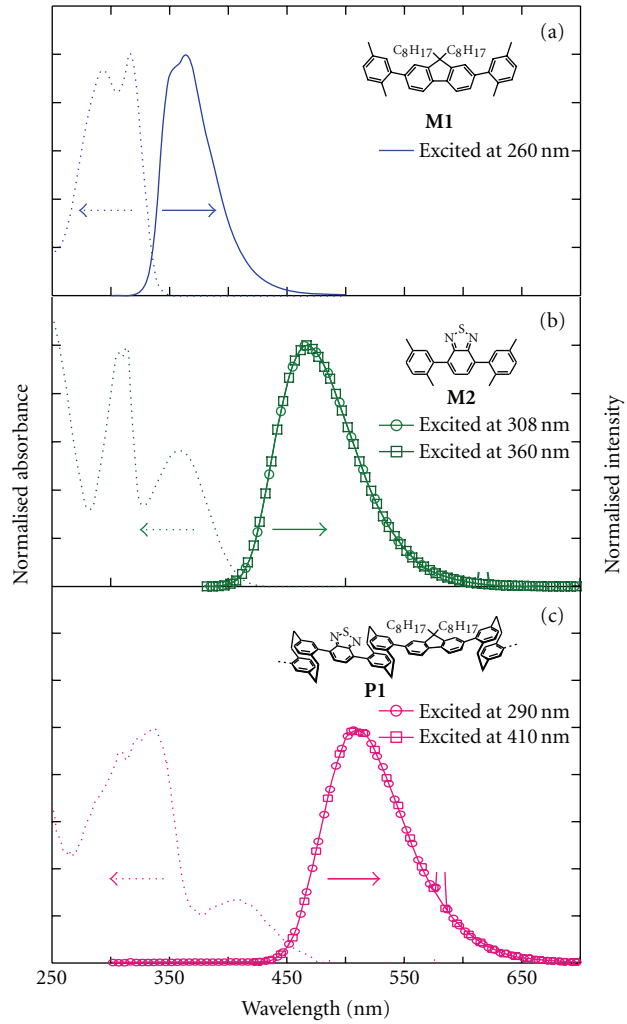

Figure 1: UV-Vis absorption spectra and photoluminescence spectra of (a) model compounds **M1**, (b) **M2**, and (c) polymer **P1** in $CHCl_3$ (1.0×10^{-5} M for UV and 1.0×10^{-6} M for photoluminescence). Scattered light was deleted from the spectra.

As shown in Figure 1(c), polymer **P1** exhibited a UV spectrum with two absorption bands at around 330 nm and 400 nm. According to the UV-Vis absorption spectra of **M1** and **M2** (Figures 1(b) and 1(c), resp.), it was observed that the spectrum of **P1** comprises the π-π^* bands of **M1** and **M2** segments and the CT band of the benzothiadiazole moiety. In contrast, the absorption spectrum of **P1** exhibited a red shift of approximately 50 nm in comparison with the absorption spectra of **M1** and **M2**, because of the through-space conjugation. As in the case of **M2**, the photoluminescence spectrum of **P1** exhibited a broad peak at around 505 nm. The photoluminescence spectra obtained at excitation wavelengths of 290 nm and 410 nm were identical, as shown in Figure 1(c). In other words, even if the fluorene segments in **P1** were excited, only the benzothiadiazole segments emitted. In addition, from the excitation spectrum of polymer **P1**,

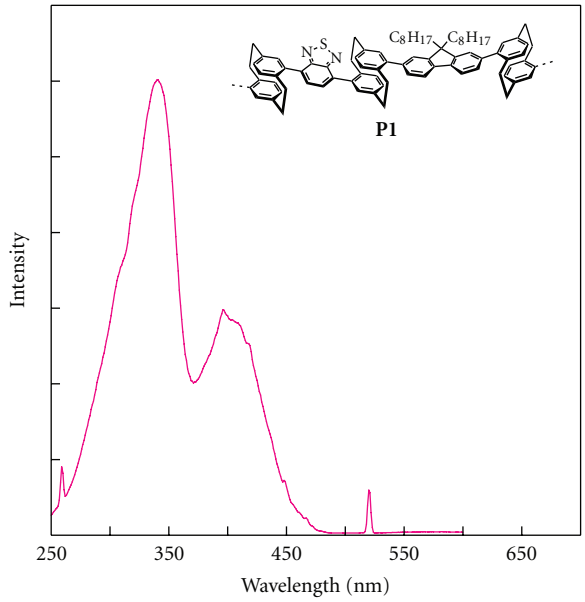

Figure 2: Excitation spectrum of polymer **P1** in $CHCl_3$ (1.0×10^{-5} M), monitoring wavelength at 520 nm.

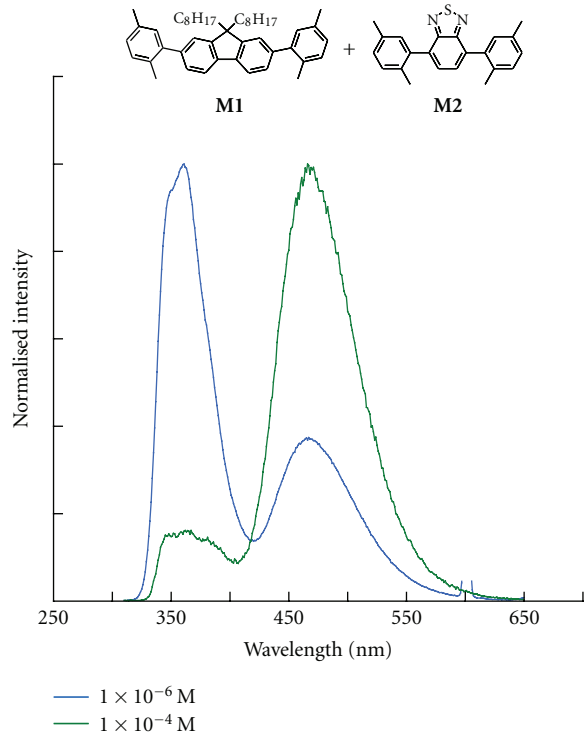

Figure 3: Photoluminescence spectrum of the 1:1 mixture of **M1** and **M2** in $CHCl_3$ (1.0×10^{-6} M and 1.0×10^{-4} M) excited at 300 nm. Scattered light (600 nm) was deleted from the spectrum.

it was confirmed that the benzothiadiazole segments were the emitting species (Figure 2). We confirmed that this concentration (1.0×10^{-6} M) was sufficiently diluted to avoid intermolecular interactions according to the concentration effect of the photoluminescence spectra (Figures S11) due to peak shift saturation. These results and the good overlap between the emission peak of **M1** and the CT band of **M2** suggest the occurrence of fluorescence resonance energy transfer (FRET) [58] from the donor-fluorene segments to the acceptor-benzothiadiazole segments.

Figure 3 shows the photoluminescence spectrum of a mixture of compounds **M1** and **M2** (concentration of each compound: 1.0×10^{-6} M)in a diluted $CHCl_3$ solution excited at 300 nm. Emissions from both **M1** and **M2** were observed at 361 nm and 467 nm, respectively. Increasing the concentration from 1.0×10^{-6} M to 1.0×10^{-4} M resulted in an increase in the intensity of emission from **M2** due to the intermolecular interaction. The closely π-stacked structure of alternate donor-fluorene and acceptor-benzothiadiazole segments in the polymer main chain caused FRET. The absolute photoluminescence quantum efficiency (Φ_{PL}) of **P1** was calculated to be 0.49, which was lower than that of **M2** ($\Phi_{PL} = 0.75$). The solvent effect on the photoluminescence of **P1** was examined, and the Φ_{PL} in more polar solvents such as DMF was 0.42 (Figure S12). This result implies that photo-excited electron transfer as well as energy transfer causes a decrease in the photoluminescence quantum efficiency. Incidentally, the Commission Internationale de L'Eclairage (CIE 1931) coordinates (x,y) of **P1** were (0.2827, 0.5192) in solution and in the thin film, indicating visible green light emission.

The HOMO and LUMO energy levels of polymer **P1** were estimated from the cyclic voltammogram as well as UV-Vis absorption spectrum. The cyclic voltammogram

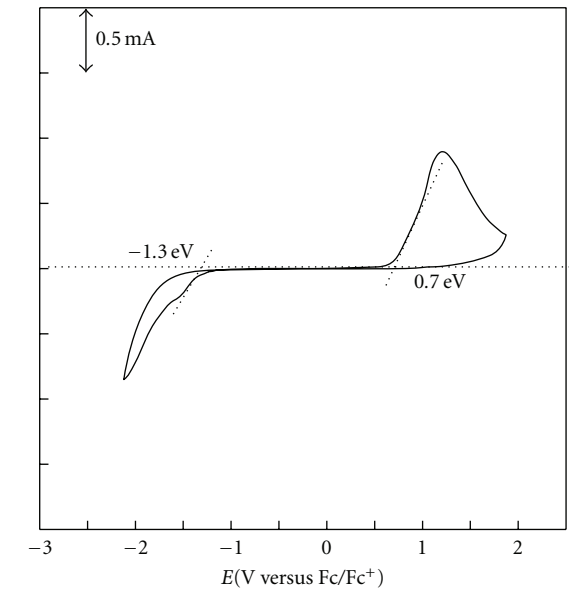

Figure 4: Cyclic voltammogram of polymer **P1** on an ITO electrode in CH_3CN containing 0.1 M Et_4NBF_4 (versus Fc/Fc^+) at a scan rate of 100 mV/s.

was obtained by fabricating thin films on an ITO glass electrode in CH_3CN solution of 0.1 M Et_4NBF_4 using a three-electrode cell with a Pt counter electrode, an Ag/Ag^+ reference electrode, and ferrocene (Fc/Fc^+) as an external

standard. Figure 4 shows the cyclic voltammogram of **P1** at a scan rate of 100 mV/s. The oxidation process of **P1** resulted in an onset peak at approximately 0.7 V; in the cathodic scan, the onset reduction potential was observed at approximately –1.3 V (versus Fc/Fc^+). The HOMO and LUMO energy levels of **5** were roughly estimated to be –5.5 eV and –3.5 eV, respectively. The bandgap energy was approximately 2.0 eV, which was in agreement with the optical band gap energy (approximately 2.2 eV) estimated from the absorption spectrum of a thin film made of **P1** (onset λ = 575 nm, as shown in Figure S10 in Supplementary Material). On the other hand, density functional theory (DFT) calculations at the B3LYP/6-31G* level were carried out for model compounds. As can be seen in Figure S13 in Supplementary Material, the HOMO and LUMO of the polymer comprise the fluorene unit and the benzothiadiazole unit, respectively. Thus, it can be reasonably concluded that both of the electron transfer and the energy transfer from the fluorene unit to the benzothiadiazole unit occurs in the polymer chain (vide supra).

4. Conclusion

In summary, we successfully synthesized a novel through-space conjugated polymer with a [2.2]paracyclophane skeleton. The obtained polymer possessed donor and acceptor segments that were alternately π-stacked in proximity via the [2.2]paracyclophane moieties. The polymer was soluble in common organic solvents, and a homogeneous thin film was readily obtained by casting or spin-coating techniques. The conjugation length of the polymer was extended by the through-space interaction. The polymer exhibited green emission with Φ_{PL} of 0.49 and CIE coordinates of (0.2827, 0.5192) in a diluted solution. This emission was attributed to the benzothiadiazole moieties; in other words, the benzothiadiazole moieties emitted due to FRET even when the fluorene moieties were excited. The polymer exhibited oxidation and reduction potentials at 0.7 V and –1.3 V (versus Fc/Fc^+), respectively. Finally, it should be emphasized that the polymer is a novel donor-acceptor conjugated polymer that combines the donor and acceptor units alternately through π-π stacking and not through a bond. Further studies on the synthesis of through-space conjugated polymers containing the donor and acceptor units at each polymer chain end are currently in progress.

Acknowledgments

This work was supported by Grant-in-Aid for Young Scientists (A) (no. 21685012) from the Ministry of Education, Culture, Sports, Science and Technology, Japan. Financial support from the Mazda Foundation is also acknowledged.

References

[1] C. J. Brown and A. C. Farthing, "Preparation and structure of di-*p*-xylylene," *Nature*, vol. 164, no. 4178, pp. 915–916, 1949.

[2] R. Cleiter and H. Hopf, Eds., *Modern Cyclophane Chemistry*, Wiley-VCH, Weinheim, Germany, 2004.

[3] H. Hopf, "[2.2]Paracyclophanes in polymer chemistry and materials science," *Angewandte Chemie International Edition*, vol. 47, no. 51, pp. 9808–9812, 2008.

[4] F. Vögtle, *Cyclophane Chemistry*, John Wiley & Sons, New York, NY, USA, 1993.

[5] Y. Morisaki and Y. Chujo, "Through-space conjugated polymers based on cyclophanes," *Angewandte Chemie International Edition*, vol. 45, no. 39, pp. 6430–6437, 2006.

[6] Y. Morisaki and Y. Chujo, "Cyclophane-containing polymers," *Progress in Polymer Science*, vol. 33, no. 3, pp. 346–364, 2008.

[7] Y. Morisaki and Y. Chujo, "Synthesis of π-stacked polymers on the basis of [2.2]paracyclophane," *Bulletin of the Chemical Society of Japan*, vol. 82, no. 9, pp. 1070–1082, 2009.

[8] S. Iwatsuki, T. Itoh, M. Kubo, and H. Okuno, "Synthesis and polymerization of 4-vinyl [2.2]paracyclophane," *Polymer Bulletin*, vol. 32, no. 1, pp. 27–34, 1994.

[9] J. Nishimura and S. Yamashita, "C3 cyclopolymerization: cationic cyclopolymerization of 1,3-bis(*p*-vinylphenyl)propane and its derivatives," in *Cyclopolymerization and Polymers with Chain-Ring Structures*, G. B. Butler and J. E. Kresta, Eds., pp. 177–195, American Chemical Society, Washington, DC, USA, 1982.

[10] J. Furukawa and J. Nishimura, "Cyclopolymerization of α,ω-bis(4-vinylphenyl)alkane—polymer containing [3.3]paracyclophane unit in main chain," *Journal of Polymer Science, Part B*, vol. 14, no. 2, pp. 85–90, 1976.

[11] J. Furukawa and J. Nishimura, "Cationic cyclopolymerization of α,ω-bis(4-vinylphenyl)alkanes—polymer containing [3.3]paracyclophane units in main chain," *Journal of Polymer Science Polymer Symposium*, no. 56, pp. 437–446, 1976.

[12] J. Nishimura and S. Yamashita, "Polymerization of α,ω-bis(para-isopropenylphenyl)alkanes by means of stannic chloride," *Polymer Journal*, vol. 11, no. 8, pp. 619–627, 1979.

[13] J. Nishimure, M. Mimura, N. Nakazawa, and S. Yamashita, "C3 cyclopolymerization. II. Charge-transfer cyclopolymerization of 1,3-bis(*p*-vinylphenyl)propane," *Journal of Polymer Science, Part A*, vol. 18, no. 7, pp. 2071–2084, 1980.

[14] J. Nishimura, M. Furukawa, S. Yamashita, T. Inazu, and T. Yoshino, "C3 cyclopolymerization. IV. Cationic polymerization of 1,3-bis(4-vinylnaphthyl)propane and the polymer structure yielded," *Journal of Polymer Science, Part A*, vol. 19, no. 12, pp. 3257–3268, 1981.

[15] D. T. Glatzhofer and D. T. Longone, "Extended cooperative electronic effects in poly((*E*,*E*)-[6.2]paracyclophane-1,5-diene)," *Journal of Polymer Science, Part A*, vol. 24, no. 5, pp. 947–954, 1986.

[16] D. T. Longone and D. T. Glatzhofer, "Cyclopolymerization of (*E*,*E*)-[6.2]paracyclophane-1,5-diene," *Journal of Polymer Science, Part A*, vol. 24, no. 8, pp. 1725–1733, 1986.

[17] J. Ulański, J. Sielski, D. T. Galtzhofer, and M. Kryszewski, "Poly(paracyclophane)—high-mobility photoconducting polymer," *Journal of Physics D*, vol. 23, no. 1, pp. 75–78, 1990.

[18] J. Ulański, J. Kubacki, I. Glowacki, M. Kryszewski, and D. T. Glatzhofer, "Photoconductivity of poly((E,E)-[6.2]paracyclophane-1,5-diene) and its complex with TCNE," *Journal of Applied Polymer Science*, vol. 44, no. 12, pp. 2103–2106, 1992.

[19] D. J. Guerrero and D. T. Glatzhofer, "Synthesis and electronic properties of poly((*E*,*E*)-[6.2]-(2,5)thiophenophane-1,5-diene)," *Journal of Polymer Science, Part A*, vol. 32, no. 3, pp. 457–464, 1994.

[20] L. Guyard and P. Audebert, "Synthesis and electrochemical polymerization of bis-dithienyl cyclophane," *Electrochemistry Communications*, vol. 3, no. 4, pp. 164–167, 2001.

[21] L. Guyard, P. Audebert, W. R. Dolbier Jr., and J.-X. Duan, "Synthesis and electrochemical polymerization of new oligothiophene functionalized fluorocyclophanes," *Journal of Electroanalytical Chemistry*, vol. 537, no. 1-2, pp. 189–193, 2002.

[22] F. Salhi, B. Lee, C. Metz, L. A. Bottomley, and D. M. Collard, "Influence of π-stacking on the redox properties of oligothiophenes: (α-alkyloligo-thienyl)para[2.2]cyclophanes," *Organic Letters*, vol. 4, no. 19, pp. 3195–3198, 2002.

[23] F. Salhi and D. M. Collard, "π-stacked conjugated polymers: the influence of paracyclophane π-stacks on the redox and optical properties of a new class of broken conjugated polythiophenes," *Advanced Materials*, vol. 15, no. 1, pp. 81–85, 2003.

[24] Y. Morisaki and Y. Chujo, "Synthesis of novel π-conjugated polymers having [2.2]paracyclophane skeleton in the main chain. Extension of π-conjugated length via the through-space," *Macromolecules*, vol. 35, no. 3, pp. 587–589, 2002.

[25] Y. Morisaki and Y. Chujo, "Synthesis of novel alternating π-conjugated copolymers having [2.2]paracyclophane and fluorene units in the main chain leading to the blue light-emitting materials," *Chemistry Letters*, no. 2, pp. 194–195, 2002.

[26] Y. Morisaki, T. Ishida, and Y. Chujo, "Synthesis and properties of novel through-space π-conjugated polymers based on poly(*p*-phenylenevinylene)s having a [2.2]paracyclophane skeleton in the main chain," *Macromolecules*, vol. 35, no. 21, pp. 7872–7877, 2002.

[27] Y. Morisaki and Y. Chujo, "Synthesis and optical properties of the [2.2]paracyclophane-containing π-conjugated polymer with a diacetylene unit," *Polymer Bulletin*, vol. 49, no. 4, pp. 209–215, 2002.

[28] Y. Morisaki, F. Fujimura, and Y. Chujo, "Synthesis and properties of novel σ-π-conjugated polymers with alternating organosilicon and [2.2]paracyclophane units in the main chain," *Organometallics*, vol. 22, no. 17, pp. 3553–3557, 2003.

[29] Y. Morisaki and Y. Chujo, "Synthesis and properties of a novel through-space conjugated polymer with [2.2] paracyclophane and ferrocene in the main chain," *Macromolecules*, vol. 36, no. 25, pp. 9319–9324, 2003.

[30] Y. Morisaki and Y. Chujo, "Novel [2.2]paracyclophane-fluorene-based conjugated copolymers: synthesis, optical, and electrochemical properties," *Macromolecules*, vol. 37, no. 11, pp. 4099–4103, 2004.

[31] Y. Morisaki, T. Ishida, H. Tanaka, and Y. Chujo, "Synthesis and properties of the [2.2]paracyclophane-containing conjugated polymer with benzothiadiazole as an electron acceptor," *Journal of Polymer Science, Part A*, vol. 42, no. 23, pp. 5891–5899, 2004.

[32] Y. Morisaki, N. Wada, and Y. Chujo, "Novel conjugated polymers containing [2.2]paracyclophane and carbazole units with efficient photoluminescence," *Polymer Bulletin*, vol. 53, no. 2, pp. 73–80, 2005.

[33] Y. Morisaki, N. Wada, and Y. Chujo, "Novel π-conjugated cyclophane polymers containing phenylamine moieties with strong blue-light emission," *Polymer*, vol. 46, no. 16, pp. 5884–5889, 2005.

[34] Y. Morisaki and Y. Chujo, "Novel through-space conjugated polymers consisting of alternate [2.2]paracyclophane and fluorene," *Bulletin of the Chemical Society of Japan*, vol. 78, no. 2, pp. 288–293, 2005.

[35] Y. Morisaki, N. Wada, M. Arita, and Y. Chujo, "Synthesis of through-space conjugated polymers containing the pseudo-ortho-linked [2.2]paracyclophane moiety," *Polymer Bulletin*, vol. 62, no. 3, pp. 305–314, 2009.

[36] Y. Morisaki, L. Lin, and Y. Chujo, "Through-space conjugated polymer containing [2.2]paracyclophane and dithiafulvene units in the main chain," *Polymer Bulletin*, vol. 62, no. 6, pp. 737–747, 2009.

[37] Y. Morisaki, L. Lin, and Y. Chujo, "Synthesis of cyano-substituted through-space poly(*p*-arylenevinylene)," *Chemistry Letters*, vol. 38, no. 7, pp. 734–735, 2009.

[38] Y. Morisaki, L. Lin, and Y. Chujo, "Synthesis and properties of through-space conjugated polymers based on cyano-substituted poly(*p*-arylenevinylene)s," *Journal of Polymer Science, Part A*, vol. 47, no. 22, pp. 5979–5988, 2009.

[39] Y. Morisaki and Y. Chujo, "Construction of benzene ring-layered polymers," *Tetrahedron Letters*, vol. 46, no. 15, pp. 2533–2537, 2005.

[40] Y. Morisaki, T. Murakami, and Y. Chujo, "Synthesis and properties of [2.2]paracyclophane-layered polymers," *Macromolecules*, vol. 41, no. 16, pp. 5960–5963, 2008.

[41] Y. Morisaki, T. Murakami, and Y. Chujo, "Synthesis, structure, and properties of aromatic ring-layered polymers containing ferrocene as a terminal unit," *Journal of Inorganic and Organometallic Polymers and Materials*, vol. 19, no. 1, pp. 104–112, 2009.

[42] Y. Morisaki, T. Murakami, T. Sawamura, and Y. Chujo, "[2.2]Paracyclophane-layered polymers end-capped with fluorescence quenchers," *Macromolecules*, vol. 42, no. 10, pp. 3656–3660, 2009.

[43] W. J. Oldham Jr., Y.-J. Miao, R. J. Lachicotte, and G. C. Bazan, "Stilbenoid dimers: effect of conjugation length and relative chromophore orientation," *Journal of the American Chemical Society*, vol. 120, no. 2, pp. 419–420, 1998.

[44] G. C. Bazan, W. J. Oldham Jr., R. J. Lachicotte, S. Tretiak, V. Chernyak, and S. Mukamel, "Stilbenoid dimers: dissection of a paracyclophane chromophore," *Journal of the American Chemical Society*, vol. 120, no. 36, pp. 9188–9204, 1998.

[45] S. Wang, G. C. Bazan, S. Tretiak, and S. Mukamel, "Oligophenylenevinylene phane dimers: probing the effect of contact site on the optical properties of bichromophoric pairs," *Journal of the American Chemical Society*, vol. 122, no. 7, pp. 1289–1297, 2000.

[46] I. Yamaguchi and T. Yamamoto, "Self-assembly of donor and acceptor π-conjugated molecules via complexation with γ-cyclodextrin to give a pseudorotaxane type macromolecular adduct with an expanded π-conjugation system," *Chemistry Letters*, no. 9, pp. 938–939, 2002.

[47] R. S. Lokey and B. L. Iverson, "Synthetic molecules that fold into a pleated secondary structure in solution," *Nature*, vol. 375, no. 25, pp. 303–305, 1995.

[48] X. Zhao, M.-X. Jia, X.-K. Jiang, L.-Z. Wu, Z.-T. Li, and G.-J. Chen, "Zipper-featured δ-peptide foldamers driven by donor-acceptor interaction. Design, synthesis, and characterization," *Journal of Organic Chemistry*, vol. 69, no. 2, pp. 270–279, 2004.

[49] S. Ghosh and S. Ramakrishnan, "Structural fine-tuning of (–donor–*spacer*–acceptor–*spacer*–)$_n$ type foldamers. Effect of spacer segment length, temperature, and metal-ion complexation on the folding process," *Macromolecules*, vol. 38, no. 3, pp. 676–686, 2005.

[50] W. Zhang, W. R. Dichtel, A. Z. Stieg, et al., "Folding of a donor-acceptor polyrotaxane by using noncovalent bonding interactions," *Proceedings of the National Academy of Sciences of the United States of America*, vol. 105, no. 18, pp. 6514–6519, 2008.

[51] A. B. Pangborn, M. A. Giardello, R. H. Grubbs, R. K. Rosen, and F. J. Timmers, "Safe and convenient procedure for solvent

purification," *Organometallics*, vol. 15, no. 5, pp. 1518–1520, 1996.

[52] H. J. Reich and D. J. Cram, "Macro rings. XXXVI. Ring expansion, racemization, and isomer interconversions in the [2.2]paracyclophane system through a diradical intermediate," *Journal of the American Chemical Society*, vol. 91, no. 13, pp. 3517–3526, 1969.

[53] A. Izuoka, S. Murata, T. Sugawara, and H. Iwamura, "Molecular design and model experiments of ferromagnetic intermolecular interaction in the assembly of high-spin organic molecules. Generation and characterization of the spin states of isomeric bis(phenylmethylenyl)[2.2]paracyclophanes," *Journal of the American Chemical Society*, vol. 109, no. 9, pp. 2631–2639, 1987.

[54] M. Zhang, H. N. Tsao, W. Pisula, C. Yang, A. K. Mishra, and K. Müllen, "Field-effect transistors based on a benzothiadiazole-cyclopentadithiophene copolymer," *Journal of the American Chemical Society*, vol. 129, no. 12, pp. 3472–3473, 2007.

[55] Z. Dominguez, T.-A. V. Khuong, H. Dang, C. N. Sanrame, J. E. Nuñez, and M. A. Garcia-Garibay, "Molecular compasses and gyroscopes with polar rotors: synthesis and characterization of crystalline forms," *Journal of the American Chemical Society*, vol. 125, no. 29, pp. 8827–8837, 2003.

[56] N. Miyaura and A. Suzuki, "Palladium-catalyzed cross-coupling reactions of organoboron compounds," *Chemical Reviews*, vol. 95, no. 7, pp. 2457–2483, 1995.

[57] S. D. Walker, T. E. Barder, J. R. Martinelli, and S. L. Buchwald, "A rationally designed universal catalyst for Suzuki-Miyaura coupling processes," *Angewandte Chemie International Edition*, vol. 43, no. 14, pp. 1871–1876, 2004.

[58] Th. Förster, "Energiewanderung und fluoreszenz," *Naturwissenschaften*, vol. 33, no. 6, pp. 166–175, 1946.

Hindawi Publishing Corporation
International Journal of Polymer Science
Volume 2010, Article ID 612180, 8 pages
doi:10.1155/2010/612180

Research Article

Photoluminescent Patterned Papers Resulting from Printings of Polymeric Nanoparticles Suspension

Pierre Sarrazin,[1] Davide Beneventi,[1] Aurore Denneulin,[1] Olivier Stephan,[2] and Didier Chaussy[1]

[1] *Laboratory of Pulp and Paper Science and Graphic Arts (LGP2), Grenoble Institute of Technology, 461 rue de la Papeterie, BP65-38402 Saint Martin d'Hères, France*
[2] *Laboratory of Spectrometry and Physics (LSP), Grenoble University, 140 Avenue de la Physique, BP87-38402 Saint Martin d'Hères, France*

Correspondence should be addressed to Didier Chaussy, didier.chaussy@efpg.inpg.fr

Received 23 October 2009; Accepted 21 February 2010

Academic Editor: Jinying Yuan

The printability of a copolyfluorene-fluorenone (PFFO) photoluminescent nanoparticle aqueous suspension on commercial tracing paper was here investigated. The nanoparticles suspension was obtained by miniemulsification of a suitable preformed photoluminescent organic polymer. The structural, physicochemical, and rheological characteristics of the nanoparticles suspension were first studied before considering its printability by inkjet and flexography techniques. The native properties of the nanoparticles suspension revealed to be more suitable for inkjet printing which was successfully used to print photoluminescent patterns using a very low amount of PFFO.

1. Introduction

Since the middle of the last century the interest towards photoluminescent inks increased steadily either in the interior and packaging decorations (e.g., printing paper and cardboard) or mostly in the paper security sector [1, 2]. In the last domain, inks are composed of chromophores which: (i) are not visible under solar light to provide printed images that can not be photocopied, (ii) are readable only under special environments (e.g., ultraviolet light), (iii) can be thermally erasable for rewriting [3]. The luminescence of the majority of these inks originates from pigments [2], metal complexes [3], or specific organic compounds [4]. In the last decade it was demonstrated that a new material class such as organic semiconductors can be used to achieve luminescence [5] offering new opportunities for light-emitting sources [6] and a multitude of other electronic devices. Especially organic conjugated polymers have an excellent processability, since they are soluble in common organic solvents when functionalized with side chains. Thus, conjugated polymer organic solutions were easily processed by spin- or drop-casting, screen-printing [7–9] or inkjet printing [4, 10–13] for the treatment of several kinds of surfaces.

To tune luminescent properties, sophisticated control of the polymer luminescence colour, efficiency, and charge-transport properties are required. The emission wavelength depends on the extent of conjugation/delocalization, and can be controlled by the modification of the configuration or conformation of the polymer and by interactions with the local environment. This can be achieved by grafting functional moieties such as electron donor or acceptor groups, which allow the modulation of the electronic structure of the conjugated backbone. Studies, focused on semiconducting polymer chemistry, showed that polymer backbone substitutions or copolymerisation with other active or no-active monomer allow controlling the final conducting property of the material [14]. Finally, electronic interactions between neighbouring polymer chains may lead to the creation of new excited state species (excimers) [15–18] which can be beneficial if they are emissive [19, 20] or detrimental if they are nonemissive [21]. Such strategies have already been

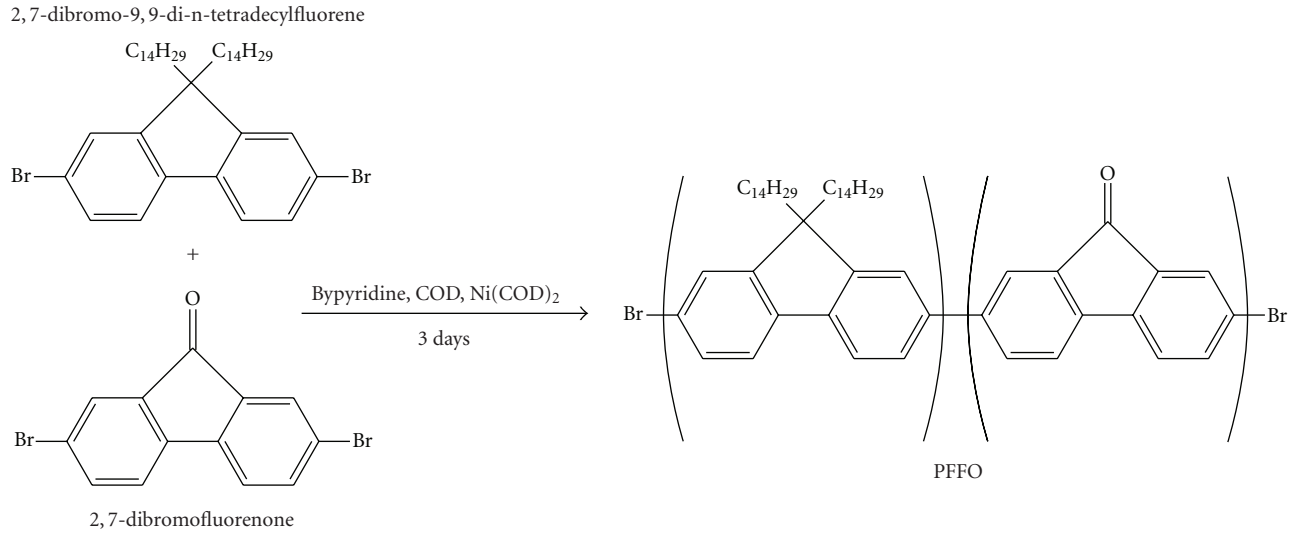

Figure 1: Polymerisation of modified 2,7-dibromofluorene and 2,7-dibromofluorenone monomers by Yamamoto route.

reported to enhance the transport of energy and/or charge, thereby influencing or drastically changing the polymer performances [22].

In the paper industry, screen printing are relatively slow, limiting the productivity and use in high volume manufacturing [23]. For this reason high volume printing processes such as flexography are also typically used as contact deposition techniques. On an other hand, the inkjet printing process (technique without contact with the substrate) reveals several advantages for the deposition of precise material at well-defined positions.

Both printing processes require suitable ink characteristics such as: (i) solvent evaporation to optimize printing speed, (ii) rheology, surface tension and pigment size matching with printing device requirements. For these reasons, organic solvent-based inks were, for long time, the most employed. But, since the early 1980s, the overriding concern of inkmakers and printers has been the replacement the solvent by water. More precisely water-based emulsions are emerged as outstanding candidates to obtain very stable water-based ink which combine the intrinsic properties of the emulsified compound with those of nanostructured matter. Recently, several authors showed that aqueous organic conjugated polymer nanoparticles suspension exhibit unaltered luminescence properties and can be deposed on glassy or plastic substrates by inkjet printing in the manufacturing of thin film single and multilayer OLED or PLED [24–26]. At this time no studies are yet focused on the paper surface treatment by printing this kind of water-based nanoparticles suspension.

Basically, organic semiconducting polymer nanoparticles can be prepared by miniemulsion polymerization, where the monomer is polymerized to form polymer particles without changing the droplets identity [27]. Other possibilities are the formation of artificial latexes by reprecipitation of hydrophobic polymers in water [28, 29] or by solubilization of a preformed polymer in organic/aqueous mixtures and its miniemulsification in water to give stable emulsions with droplets size ranging between 50 and 500 nm [30, 31]. In the miniemulsification process, after evaporation of the solvent, a polymer dispersion is obtained in less restrictive conditions and without the presence of residual polymerisation byproducts.

A fairly recent investigation has shown that an orange 2,7-poly(9,9-dialkylfluorene-*co*-fluorenone) (PFFO) could be synthesized by Nickel(0) coupling (using the Yamamoto route) of the corresponding dibromo-monomers [32] (Figure 1) to obtain an efficient yellowish photoluminescence (PL) [33]. Previous studies showed that this polymer can be successfully miniemulsified to obtain aqueous particles suspension and these cationic nanoparticles are able to be adsorbed on cellulose fibres in one-step process to obtain bulky activated paper sheets [34, 35].

The purpose of this investigation was to show that a yellowish photoluminescent water-based ink can be formulated in one step by miniemulsification of a preformed polymer. As well as stable, free hazardous solvent, and easily handling, this nanoparticles suspension has the properties of inks commonly used in flexography and inkjet printing processes.

2. Materials and Methods

2.1. Materials. 2, 7-dibromofluorene, 2, 7-dibromofluorenone, sodium hydride, tetradecyl bromide, bipyridine and cyclooctadiene were provided by Aldrich. Tetradecyltrimethylammonium bromide (TTAB) was obtained from Fluka and Bis(1,5-cyclooactadiene)Nickel(0) from Strem. Toluene, methanol, acetone, HCl, $CHCl_3$, NaCl, NaOH, and N,N-dimethylformamide used in experiments were of analytical grade.

A commercial tracing paper supplied by Clairefontaine was used as printing support. The grammage (mass per unit area) and thickness of tracing paper sheet were measured according to the norms ISO 534:2005 and ISO 536:1995,

respectively. The surface topography (roughness) was estimated using the Parker Print Surf (PPS) instrument which measures the leakage of a low pressure air between the sample surface and the edge of the head reading ring. The PPS instrument operates using clamp at various pressure (0.5, 1 or 2 MPa) which allows studying paper surface in function of the pressure to reach the roughness (in μm). The porosity (ε) of the tracing paper was estimated by using the following equation:

$$\varepsilon = \frac{V_{\text{void}}}{V_{\text{tot}}} = \frac{V_{\text{tot}} - V_{\text{cell}}}{V_{\text{tot}}} = 1 - \frac{V_{\text{cell}}/w_{\text{sample}}}{V_{\text{tot}}/w_{\text{sample}}}, \quad (1)$$

where w_{sample} is the sample weight, $V_{\text{tot}}/w_{\text{sample}}$ is the specific volume of the tracing paper and $V_{\text{cell}}/w_{\text{sample}}$ is the density of the solid part. As the tracing paper is composed only with cellulose fibres ($\rho_{\text{cell}} = 1.54\ \text{g/cm}^3$):

$$\frac{V_{\text{cell}}}{\text{w}_{\text{sample}}} = \frac{1}{\rho_{\text{cell}}}. \quad (2)$$

The surface energy of paper was obtained from contact angle measurements performed with a DataPhysics OCA20 using the sessile drop method. For that, the initial resting drop image was acquired by a CDD camera and the corresponding contact angle was calculated after fitting the drop contour line to an ellipse. To determine the surface energy four liquids were used as probe: demineralised water, glycerol, ethylene glycol, and diiodomethane. By applying the Owens, Wendt, Kaelbe and Uy (OWKU) approximation of the dispersive and the polar interactions between the two phases by a geometric mean expression, the surface energy was calculated as the sum of the dispersive and polar solid surface energies.

2.2. Synthesis of the Photoluminescent Polymer. The monomer was synthesised starting from 10 mmol of 2,7-dibromofluorene dissolved in 50 mL of N,N-dimethylformamide. 20 mmol of sodium hydride was added to the mixture at room temperature. After 4 hours under stirring, 30 mmol of tetradecyl bromide were slowly added and the mixture stirred for an additional period of 12 hours. Then, the 2,7-dibromo-9,9-di-n tetradecylfluorene was purified by column chromatography using pentane as eluant. The copolymer was synthesised by mixing 2,7-dibromo-9,9-di-n-tetradecylfluorene (1.8 mmol) and 2,7-dibromofluorenone (0.2 mmol), Bipyridine (2 mmol), cyclooctadiene (2.5 mmol) and Bis(1,5-cyclooctadiene)Nickel(0) (2 mmol) (Figure 1). Toluene (16 mL) and N,Ndimethylformamide (6 mL) were added via syringe and the mixture was stirred at 80°C for 3 days. After cooling the polymer was precipitated by pouring the solution in a methanolacetone-concentrated HCl mixture. The solid was collected by filtration and purified by subsequent precipitation in methanol mixture.

2.3. Preparation of the Aqueous Nanoparticles Suspension. The synthesised copolyfluorene-fluorenone, PFFO, (10 mg) was dissolved in 1 mL $CHCl_3$ (CF) and added to 5 mL of an aqueous Tetradecyltrimethylammonium bromide (TTAB) (17 mg, 6 times higher than c.m.c) solution. After stirring 15 minutes for pre-emulsification, the miniemulsion was prepared by ultrasonicating the mixture for 15 minutes (bath, 150 W). After ultrasonication, the sample was stirred in a regulated bath at 50°C for 30 minutes to evaporate the

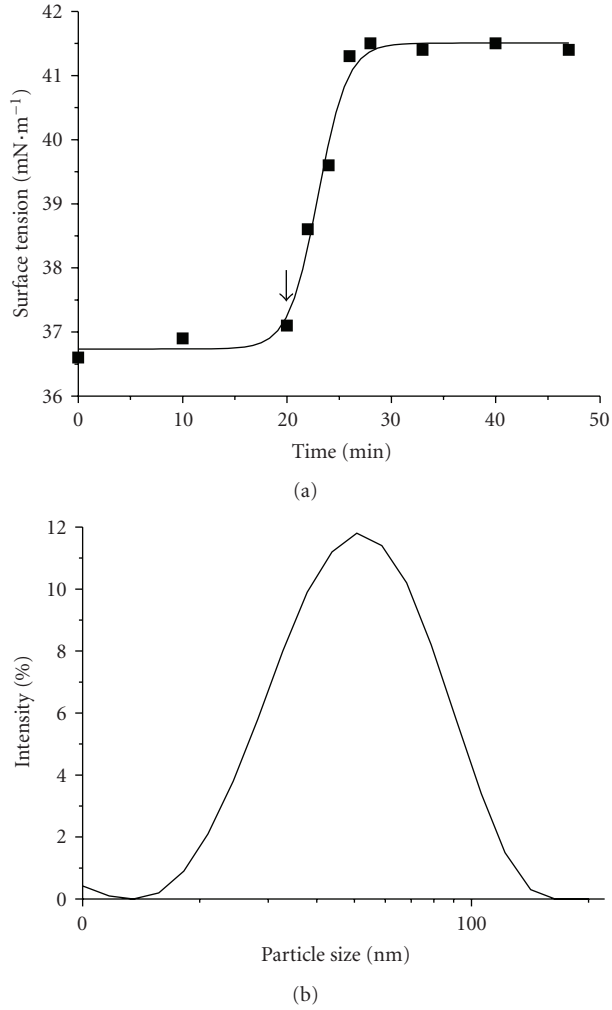

Figure 2: (a) Variation of the surface tension of water-TTAB-PFFO-CF systems during ultrasonication (arrow indicates the beginning of ultrasonication). (b) Intensity weighed particle size distribution of PFFO nanoparticles.

Figure 3: Inkjet drop formation of the PFFO nanoparticles suspension.

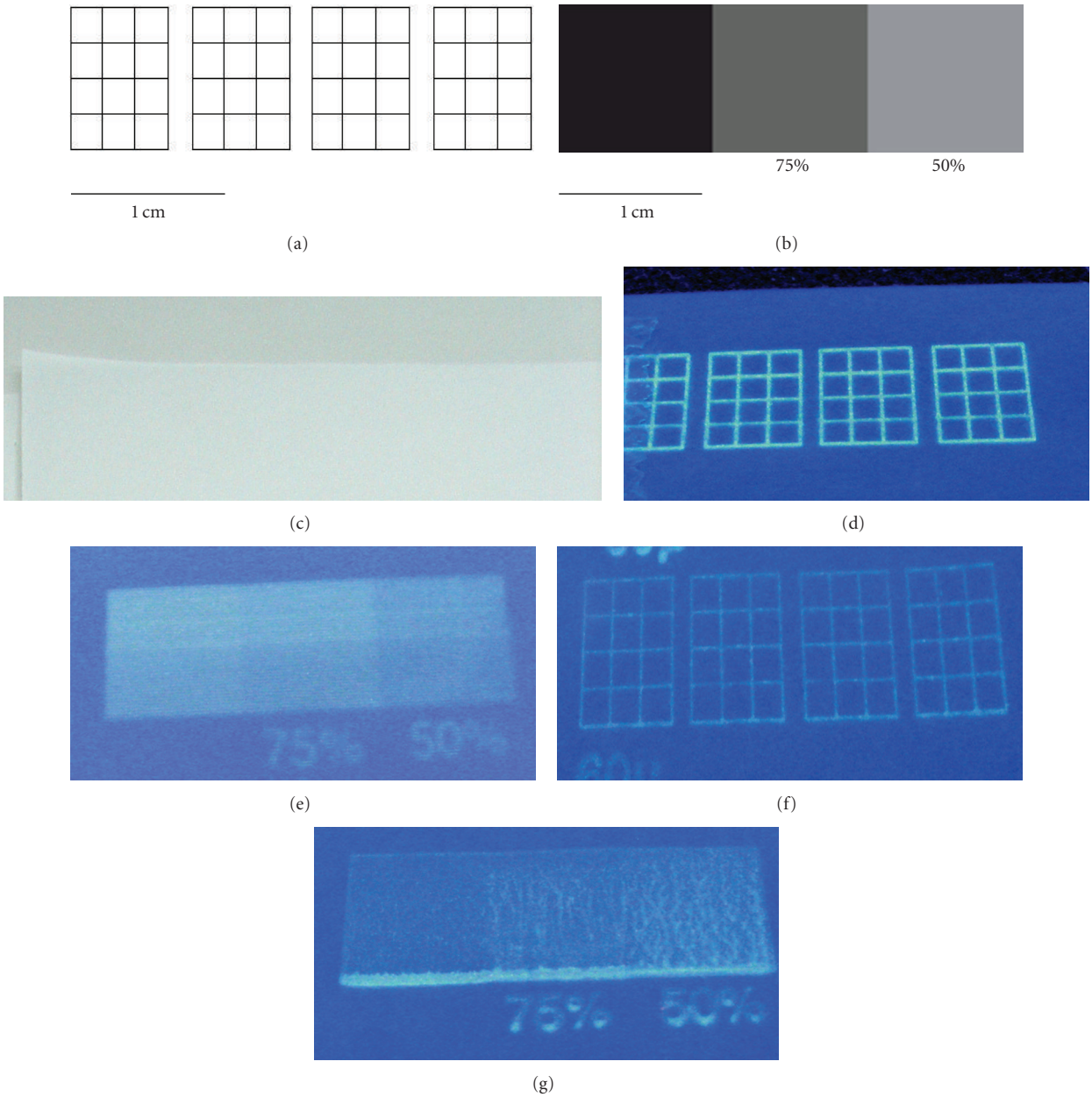

Figure 4: Printed patterns: grids of squares (a), full tones (b); printed tracing paper under room light (c); inkjet printed patterns under UV-light (d and e); flexography printed patterns under UV-light (f and g).

$CHCl_3$. The polymer particles size was cut off at 1.2 μm by filtrating the solution using a 1.2 μm syringe filter.

The Zeta-potential and the intensity weighted particle size distribution of photoluminescent PFFO particles were measured by electrophoresis and dynamic light scattering (DLS) (Malvern Zetasizer nanoZS) in a 10^{-2} M NaCl solution. The surface tension of the PFFO particles suspension was measured using the Wilhelmy plate technique (Kruss, K 100, Germany). The viscosity of the PFFO nanoparticles suspension was determined with a rheometer (Anton Paar, Physica MCR 301) measuring the evolution of the shear stress (Pa) in function of the shear rate (0–1500 s^{-1}).

2.4. Inkjet and Flexography Printings. The same pattern was printed by inkjet and flexography. For inkjet process the drop and demand (DOD) technology was applied and the PFFO nanoparticles suspension was printed onto tracing paper samples using a laboratory piezoelectric inkjet printer (Fujifilm-Dimatix DMP 2831 with 10 pL nominal drop size cartridge). Jetting of the fluid was controlled by a voltage pulse to deform the piezoelectric actuator in the ink cavity and eject a drop from the nozzle. A drop-watch camera included in the printer allowed checking the jettability of fluids. Flexography printing was realised with a Flexiproof 100 device supplied by RK Print Coat Instruments. This printing

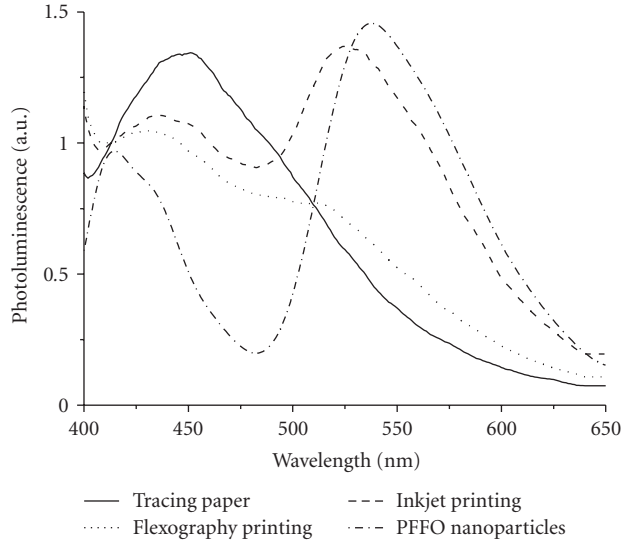

Figure 5: Photoluminescence of full tone printed patterns and PFFO nanoparticles suspension.

process is based on a rotary relief method of printing. The image pattern plate made of rubber or plastic is attached to a plate cylinder. Ink is applied to the printing plate using an engraved roller called anilox. Printing experiments were realised on paper strips of 105 × 297 cm, with an anilox of 5 cm^3/m^2 and a print speed of 25 m/min. The pressure of the anilox on the printing plate and the pressure of the printing plate on the paper were progressively modified by changing the position between elements by 4 μm incrementation.

Printed pattern morphology and the water stability of printings were studied using a Zeiss Axiovert 200 confocal laser scanning microscope. Photoluminescence measurements of printed area were performed using a spectrofluorometer (Fluorolog, Horiba Jobin Yvon) after an excitation at 365 nm. Photoluminescence spectra were recorded at room temperature and ambient atmosphere.

3. Results and Discussion

3.1. Polymer, Ink, and Support Preparations. The photoluminescent copolyfluorene-fluorenone (PFFO) was obtained with a reactive yield around 40%. This polymer is mainly amorphous (Tg = −20°C) with a liquid crystal transition at 45°C. The solution of the polymer in chloroform (CF) was successfully miniemulsified in water by using an excess (8 times cmc) of tetradecyltrimethylammonium bromide (TTAB) to obtain a photoluminescent yellowish nanoparticles suspension. Surface tension measurements taken during the miniemulsification process showed an initial increase in surface tension from 36.8 to 41.6 $mN \cdot m^{-1}$ followed by a plateau, which reflected the progressive TTAB adsorption to the surface of freshly formed PFFO/chloroform droplets (Figure 2(a)). Even after prolonged ultrasonication, surface tension remained constant indicating that after 6 minutes ultrasonication TTAB adsorption reached the equilibrium and therefore that free surfactant remains in the aqueous phase with a concentration close to the c.m.c. At this concentration, the final PFFO nanoparticle suspension is stabilized by the strong positive charge associated to the presence of adsorbed surfactants on particles surface. DLS measurements showed an intensity weighed particle size distribution centered on 60 nm with bigger particles closed to 200 nm (Figure 2(b)). The surface tension and particle size values suggested, according to several previous studies [25, 36–39], that the PFFO nanoparticles suspension prepared by miniemulsification seems to have intrinsically suitable properties to be printed with inkjet printing process. Besides the nanoparticles suspension showed a Newtonian behaviour and a low viscosity of 1.12 $mPa \cdot s^{-1}$, which is necessary in flexography printing process for which the ink needs to flow into the cells of the anilox rolls of the press (Table 1).

The surface analysis of the tracing paper (thickness = 68 μm) with Parker Print Surf instrument confirmed its low roughness (5.7 μm). The estimated porosity revealed the slight porous (32%) structure of this 71.5 g/m^2 density fibres sheet. Finally the surface energy of the paper was estimated from the measurement of the contact angle between several liquids and the support (Table 1). It had a polar component of 5.7 $mN \cdot m^{-1}$ and a dispersive one of 31.2 $mN \cdot m^{-1}$. The low roughness and the rather hydrophobic surface of this support allowed assuming that during the printing process this support should be treated only on the surface because of the difficulty of the water-based ink to penetrate in the paper. The contact angle of the native PFFO nanoparticles suspension on the tracing paper (67.1°) was lower than with water (90.4°) (Table 1). It is attributed to the presence of free surfactant molecules which decrease the surface tension of the miniemulsion and improve its spreading onto the support.

3.2. Printing. With inkjet printing system, the aqueous dispersion was directly DOD inkjet printed by applying the Dymatix printer parameters used during previous investigations realised by co-workers with a similar water-based ink [40].

Figure 3 displays the droplet formation of the PFFO nanoparticles suspension printed by the three nozzles printer. During the ejection, the droplet forms a thread before droplet detaches the nozzle. This phenomenon can be associated, in comparison with some other investigations, to the bead-on-a-string effect of a polymer-based solution used as ink [25, 41]. Nevertheless, the inkjet printing process remained stable during the entire paper treatment meaning that the formation of the droplet does not alter with time and that the native suspension has almost suitable ink properties (e.g., viscosity, surface tension).

With the flexography process, before processing to the printing of the native PFFO nanoparticles suspension, printing parameters of the Flexiproof device were optimized with a commercial blue water-based ink. Experiments showed that, for one millilitre of ink, the highest pressure of the anilox on the printing plate and the highest pressure of the printing plate on the paper were required to print patterns without deforming the printing plate.

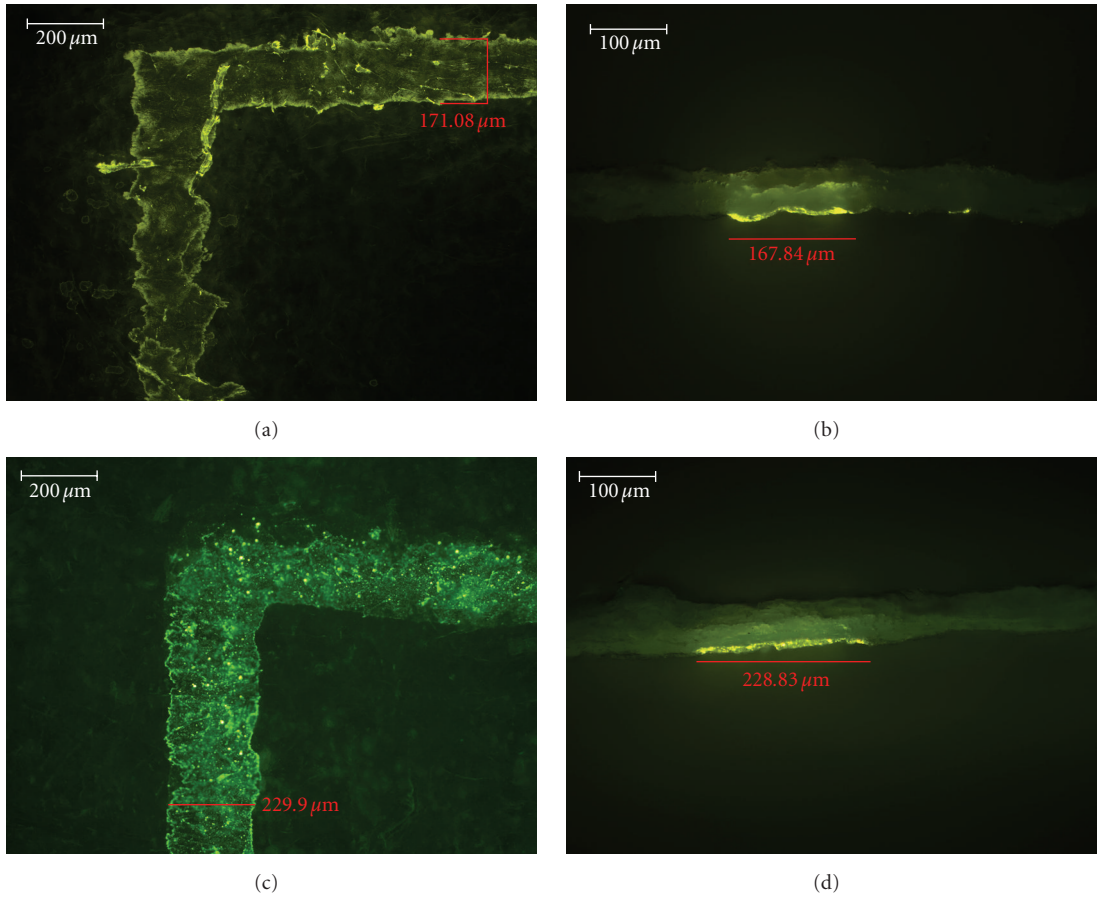

Figure 6: Fluorescence microscopy pictures of one right angle and of the slide of printed square on the tracing paper. Inkjet printing (a and b); Flexography (c and d).

Table 1: Ink and support characteristics.

Ink		Tracing paper			
				Contact Angle (deg°)	
Viscosity ($mPa \cdot s^{-1}$)	Surface Tension ($mN \cdot m^{-1}$)	Roughness PPS (μm)	Surface Energy ($mN \cdot m^{-1}$)	Water	PFFO nanoparticles suspension
1.12	41.5	5.7	36.9	90.4	67.1

After studying the efficiency of the ejected drop in inkjet printing (jettability performance) and optimizing the transfer conditions in flexography process, the interaction between the printed nanoparticles suspension and the substrate was taken under consideration. In both printing processes, one millilitre of PFFO nanoparticles suspension was used to print two different patterns such as grids of 12 squares and full tone (Figures 4(a) and 4(b)). The printed patterns were room air dried after less than two minutes before their characterisation. Camera pictures of the treated paper under UV-light showed globally an efficient photoluminescence of printed patterns by flexography and inkjet printing whereas nothing appeared under room light (Figures 4(c), 4(d), 4(e), 4(f), 4(g)). Photoluminescent PFFO nanoparticles were successfully deposit on the tracing paper because of their affinity with the negative charged cellulose fibres surface due to their positive surface charge provided by cationic surfactant [34, 35]. As demonstrated in these latter investigations, the adsorption of PFFO nanoparticles on the cellulose fibre surface of the tracing paper remains stable even the prolonged wetting of the printed paper (1 minute) in deionised water.

Concerning flexography printed full tone pattern, nanoparticles accumulation occurred at the bottom of the model (Figure 4(g)) assuming an inhomogeneous pressure of the printing plate either on the anilox or on the paper itself. Whereas, with inkjet printing, a more homogeneous (no ink accumulation) printed pattern was obtained (Figure 4(e)). It seems that the horizontal treatment of the tracing paper by a technique without contact between the substrate and a

low viscosity ink is more suitable. Figure 5 shows that the commercial tracing paper has a native photoluminescence in the UV-visible blue region whereas the 100% full tone printed areas have a yellowish photoluminescence corresponding to the activity of PFFO nanoparticles deposited on tracing paper surface. Because of the contribution of the tracing paper, the photoluminescence of these both patterns was slightly shifted to the bluish region. Inkjet printed full tone displayed a higher photoluminescence than those obtained by flexography because the flexography technique led to a heterogeneous printed pattern with a lower amount of nanoparticles spread out on the studied surface.

In both cases, fluorescence microscopy pictures showed that the grids of squares were printed with a similar film thickness (around $8\,\mu$m) but with a more homogeneous film morphology with the inkjet technique (Figure 6). Furthermore, the line width of squares was 3 and 4 times higher for inkjet and flexography, respectively, than the designed pattern on the polymeric printing plate ($\approx 60\,\mu$m). For flexography, this difference was ascribed to the high pressure used between the printing plate and the paper which led to the compression and deformation of the printing plate on the support. Whereas for inkjet printing this gap can come from the spreading of suspension droplets on the substrate (contact angle = 67.1°). To understand more efficiently these phenomena and to control the printed pattern aspects (pattern size and photoluminescence intensity), the influence of PFFO nanoparticles suspension characteristics (nanoparticles size and concentration) and printing processes parameters (e.g., jet frequency or ink volume) is currently yet deeply studied.

4. Conclusion

In summary, we have pointed out that a photoluminescent nanoparticles suspension obtained by miniemulsification of preformed semiconducting polymer (PFFO) can be used as an effective water-based ink for paper treatment. This suspension was suited to inkjet or flexography printing techniques because it is composed of nanosized "pigments" (nanoparticles) and it showed suitable properties such as low viscosity ($\sim 1\,\text{mPa}\cdot\text{s}^{-1}$) and surface tension ($\sim 40\,\text{mN}\cdot\text{m}^{-1}$). The better printed patterned tracing papers (printed shape, photoluminescence quality, etc.) were obtained with the inkjet process with a lower amount of PFFO nanoparticles suspension. However, a thorough survey of the parameters of the printing process is necessary to consider the use of this specific ink in different domains such as security papers.

Acknowledgments

The authors wish to thank the microscopy team workers of the LGP2 laboratory for their expertise in taking fluorescence imaging measurements. This work was supported by a MEN Grant.

References

[1] R. W. Phillips and A. F. Bleikolm, "Optical coatings for document security," *Applied Optics*, vol. 35, no. 28, pp. 5529–5534, 1996.

[2] M. Yousaf and M. Lazzouni, "Formulation of an invisible infrared printing ink," *Dyes and Pigments*, vol. 27, no. 4, pp. 297–303, 1995.

[3] A. Kishimura, T. Yamashita, K. Yamaguchi, and T. Aida, "Rewritable phosphorescent paper by the control of competing kinetic and thermodynamic self-assembling events," *Nature Materials*, vol. 4, no. 7, pp. 546–549, 2005.

[4] T. R. Hebner, C. C. Wu, D. Marcy, M. H. Lu, and J. C. Sturm, "Ink-jet printing of doped polymers for organic light emitting devices," *Applied Physics Letters*, vol. 72, no. 5, pp. 519–521, 1998.

[5] M. Pope, H. P. Kallmann, and P. Magnante, "Electroluminescence in organic crystals," *The Journal of Chemical Physics*, vol. 38, no. 8, pp. 2042–2043, 1963.

[6] R. H. Friend, R. W. Gymer, A. B. Holmes, et al., "Electroluminescence in conjugated polymers," *Nature*, vol. 397, no. 6715, pp. 121–128, 1999.

[7] Z. Bao, Y. Feng, A. Dodabalapur, V. R. Raju, and A. J. Lovinger, "High-performance plastic transistors fabricated by printing techniques," *Chemistry of Materials*, vol. 9, no. 6, pp. 1299–1301, 1997.

[8] K. Mori, T. Ning, M. Ichikawa, T. Koyama, and Y. Taniguchi, "Organic light-emitting devices patterned by screen-printing," *Japanese Journal of Applied Physics*, vol. 39, no. 9, pp. L942–L944, 2000.

[9] S. E. Shaheen, R. Radspinner, N. Peyghambarian, and G. E. Jabbour, "Fabrication of bulk heterojunction plastic solar cells by screen printing," *Applied Physics Letters*, vol. 79, no. 18, pp. 2996–2998, 2001.

[10] T. R. Hebner and J. C. Sturm, "Local tuning of organic light-emitting diode color by dye droplet application," *Applied Physics Letters*, vol. 73, no. 13, pp. 1775–1777, 1998.

[11] L. M. Leung, C. F. Kwong, C. C. Kwok, and S. K. So, "Organic polymer thick film light emitting diodes (PTF-OLED)," *Displays*, vol. 21, no. 5, pp. 199–201, 2000.

[12] Y. Yang, S.-C. Chang, J. Bharathan, and J. Liu, "Organic/polymeric electroluminescent devices processed by hybrid ink-jet printing," *Journal of Materials Science: Materials in Electronics*, vol. 11, no. 2, pp. 89–96, 2000.

[13] C. N. Hoth, S. A. Choulis, P. Schilinsky, and C. J. Brabec, "High photovoltaic performance of inkjet printed polymer:fullerene blends," *Advanced Materials*, vol. 19, no. 22, pp. 3973–3978, 2007.

[14] X. Qiao, X. Wang, and Z. Mo, "Effects of different alkyl substitution on the structures and properties of poly(3-alkylthiophenes)," *Synthetic Metals*, vol. 118, no. 1–3, pp. 89–95, 2001.

[15] M. Yan, L. J. Rothberg, E. W. Kwock, and T. M. Miller, "Interchain excitations in conjugated polymers," *Physical Review Letters*, vol. 75, no. 10, pp. 1992–1995, 1995.

[16] C. L. Chochos, J. K. Kallitsis, and V. G. Gregoriou, "Rod-coil block copolymers incorporating terfluorene segments for stable blue light emission," *The Journal of Physical Chemistry B*, vol. 109, no. 18, pp. 8755–8760, 2005.

[17] C. L. Chochos, D. Papakonstandopoulou, S. P. Economopoulos, V. G. Gregoriou, and J. K. Kallitsis, "Synthesis and optical properties on a series of polyethers incorporating terfluorene segments and methylene spacers," *Journal of Macromolecular Science Part A*, vol. 43, no. 3, pp. 419–431, 2006.

[18] C. L. Chochos, N. P. Tzanetos, S. P. Economopoulos, V. G. Gregoriou, and J. K. Kallitsis, "Synthesis and characterization of random copolymers combining terfluorene segments and hole or electron transporting moieties," *Journal of Macromolecular Science Part A*, vol. 44, no. 9, pp. 923–930, 2007.

[19] M. W. Wu and E. M. Conwell, "Effect of interchain coupling on conducting polymer luminescence: excimers in derivatives of poly(phenylene vinylene)," *Physical Review B*, vol. 56, no. 16, pp. 10060–10062, 1997.

[20] C. L. Chochos, J. K. Kallitsis, P. E. Keivanidis, S. Baluschev, and V. G. Gregoriou, "Thermally stable blue emitting terfluorene block copolymers," *The Journal of Physical Chemistry B*, vol. 110, no. 10, pp. 4657–4662, 2006.

[21] R. Jakubiak, L. J. Rothberg, W. Wan, and B. R. Hsieh, "Reduction of photoluminescence quantum yield by interchain interactions in conjugated polymer films," *Synthetic Metals*, vol. 101, no. 1–3, pp. 230–233, 1999.

[22] T.-Q. Nguyen, I. B. Martini, J. Liu, and B. J. Schwartz, "Controlling interchain interactions in conjugated polymers: the effects of chain morphology on exciton-exciton annihilation and aggregation in MEH-PPV films," *The Journal of Physical Chemistry B*, vol. 104, no. 2, pp. 237–255, 2000.

[23] P. Calvert, "Inkjet printing for materials and devices," *Chemistry of Materials*, vol. 13, no. 10, pp. 3299–3305, 2001.

[24] E. Fisslthaler, S. Sax, U. Scherf, et al., "Inkjet printed polymer light-emitting devices fabricated by thermal embedding of semiconducting polymer nanospheres in an inert matrix," *Applied Physics Letters*, vol. 92, no. 18, Article ID 183305, 2008.

[25] G. Mauthner, K. Landfester, A. Köck, et al., "Inkjet printed surface cell light-emitting devices from a water-based polymer dispersion," *Organic Electronics*, vol. 9, no. 2, pp. 164–170, 2008.

[26] T. Piok, S. Gamerith, C. Gadermaier, et al., "Organic light-emitting devices fabricated from semiconducting nanospheres," *Advanced Materials*, vol. 15, no. 10, pp. 800–804, 2003.

[27] M. Omastová, M. Trchová, J. Kovarova, and J. Stejskal, "Synthesis and structural study of polypyrroles prepared in the presence of surfactants," *Synthetic Metals*, vol. 138, no. 3, pp. 447–455, 2003.

[28] F. Kong, X. L. Wu, G. S. Huang, R. K. Yuan, and P. K. Chu, "Tunable emission from composite polymer nanoparticles based on resonance energy transfer," *Thin Solid Films*, vol. 516, no. 18, pp. 6287–6292, 2008.

[29] M. Zhao, J. Li, E. Mano, et al., "Oxidation of primary alcohols to carboxylic acids with sodium chlorite catalyzed by TEMPO and bleach," *Journal of Organic Chemistry*, vol. 64, no. 7, pp. 2564–2566, 1999.

[30] M. Antonietti and K. Landfester, "Polyreactions in miniemulsions," *Progress in Polymer Science*, vol. 27, no. 4, pp. 689–757, 2002.

[31] K. Landfester, R. Montenegro, U. Scherf, et al., "Semiconducting polymer nanospheres in aqueous dispersion prepared by a miniemulsion process," *Advanced Materials*, vol. 14, no. 9, pp. 651–655, 2002.

[32] T. Yamamoto, A. Morita, Y. Miyazaki, et al., "Preparation of pi-conjugated poly(Thiophene-2,5-Diyl), poly(Para-Phenylene), and related polymers using zero valent nickel-complexes—linear structure and properties of the pi-conjugated polymers," *Macromolecules*, vol. 25, no. 4, pp. 1214–1223, 1992.

[33] S. Panozzo, J.-C. Vial, Y. Kervella, and O. Stéphan, "Fluorene-fluorenone copolymer: stable and efficient yellow-emitting material for electroluminescent devices," *Journal of Applied Physics*, vol. 92, no. 7, pp. 3495–3502, 2002.

[34] P. Sarrazin, D. Beneventi, D. Chaussy, L. Vurth, and O. Stephan, "Adsorption of cationic photoluminescent nanoparticles on softwood cellulose fibres: effects of particles stabilization and fibres' beating," *Colloids and Surfaces A*, vol. 334, no. 1–3, pp. 80–86, 2009.

[35] P. Sarrazin, L. Valecce, D. Beneventi, D. Chaussy, L. Vurth, and O. Stephan, "Photoluminescent paper based on poly(fluorene-co-fluorenone) particles adsorption on modified cellulose fibers," *Advanced Materials*, vol. 19, no. 20, pp. 3291–3294, 2007.

[36] R. Mannerbro, M. Ranlöf, N. Robinson, and R. Forchheimer, "Inkjet printed electrochemical organic electronics," *Synthetic Metals*, vol. 158, no. 13, pp. 556–560, 2008.

[37] O. Ngamna, A. Morrin, A. J. Killard, S. E. Moulton, M. R. Smyth, and G. G. Wallace, "Inkjet printable polyaniline nanoformulations," *Langmuir*, vol. 23, no. 16, pp. 8569–8574, 2007.

[38] M. D. Croucher and M. L. Hair, "Design criteria and future directions in inkjet ink technology," *Industrial and Engineering Chemistry Research*, vol. 28, no. 11, pp. 1712–1718, 1989.

[39] B.-J. De Gans, E. Kazancioglu, W. Meyer, and U. S. Schubert, "Ink-jet printing polymers and polymer libraries using micropipettes," *Macromolecular Rapid Communications*, vol. 25, no. 1, pp. 292–296, 2004.

[40] A. Denneulin, J. Bras, A. Blayo, B. Khelifi, F. Roussel-Dherbey, and C. Neuman, "The influence of carbon nanotubes in inkjet printing of conductive polymer suspensions," *Nanotechnology*, vol. 20, no. 38, pp. 1–10, 2009.

[41] R. P. Mun, J. A. Byars, and D. V. Boger, "The effects of polymer concentration and molecular weight on the breakup of laminar capillary jets," *Journal of Non-Newtonian Fluid Mechanics*, vol. 74, no. 1–3, pp. 285–297, 1998.

Hindawi Publishing Corporation
International Journal of Polymer Science
Volume 2010, Article ID 264781, 7 pages
doi:10.1155/2010/264781

Research Article

Prevention of H-Aggregates Formation in Cy5 Labeled Macromolecules

Jing Kang,[1] Oliver Kaczmarek,[2] Jürgen Liebscher,[2] and Lars Dähne[1]

[1] *Surflay Nanotec GmbH, Schwarzschildstr. 8, 12489 Berlin, Germany*
[2] *Institute of Chemistry, Humboldt University, of Brook-Taylor-Str. 2, 12489 Berlin, Germany*

Correspondence should be addressed to Lars Dähne, l.daehne@surflay.com

Received 13 November 2009; Revised 23 February 2010; Accepted 14 March 2010

Academic Editor: Jinying Yuan

H-aggregates of the cyanine dye Cy5 are formed during covalent linkage to the cationic macromolecule Poly(allylamine) (PAH). The nonfluorescent H-aggregates strongly restrict the usage of the dye for analytical purposes and prevent a quantitative determination of the labeled macromolecules. The behavior of the H-aggregates has been studied by investigation of the absorption and fluorescence spectra of the dye polymer in dependence on solvent, label degree and additional sulfonate groups. H-aggregate formation is caused by an inhomogeneous distribution of the Cy5 molecules on the polymer chain. The H-aggregates can be destroyed by conformational changes of the PAH induced by interactions with polyanions or in organic solvents. It has been found that the polymer labeling process in high content of organic solvents can prevent the formation of H-aggregates. The results offer a better understanding and improvement of the use of the Cy5 dye for labeling purposes in fluorescence detection of macromolecules.

1. Introduction

The labeling of biological or technical materials with fluorescent dyes has gained a great importance in connection with the development of new modern fluorescence-based analytical techniques such as Fluorescence Correlation Spectroscopy (FCS) [1, 2], Single Molecule Spectroscopy (SMS) [3], Confocal Laser Scanning Microscopy (CLSM) [4], Fluorescence Resonance Energy Transfer (FRET) [5], Fluorescence Recovery after Photobleaching (FRAP) [6], or time resolved spectroscopic methods down to femtoseconds [7, 8]. For all of these processes the spectroscopic parameters of the dye molecules such as excitation and emission spectra, lifetime and fluorescence quantum yield are important but often change in an unpredictable way by the labeling procedure [9–12]. Especially in the case of proteins high label degrees or label sites in close neighborhood lead to a strong decrease of the fluorescence quantum yield as well as a shift of absorption and fluorescence energy [13–15]. We investigated these processes on the well-known chromophore Bis(indolenyl)pentamethincyanine that is commercially available under the label name Cy5 (Figure 1). Strong changes in the spectroscopic properties of the dye have been observed earlier by simple adsorption of the positively charged chromophore to negatively charged macromolecules, namely, polyanions [16, 17]. In this paper we studied the spectroscopic behavior of the dye after covalent linkage to the cationic macromolecule PAH. The polyelectrolyte PAH of molecular weight 70 kDa can not only serve as a simple model for proteins below their isoelectric point (IEP) but also it is an important material used in Layer-by-Layer technology allowing the formation of multilayers of alternatively charged polyelectrolytes on planar and colloidal substrates [18, 19].

Formation of Cy5 H-aggregates was observed after the labeling procedure. Such non-fluorescent H-aggregates remarkably restrict the applicability of fluorescent dyes in analytical methods. Therefore, efforts have been made to investigate the factors that could reduce H-aggregates

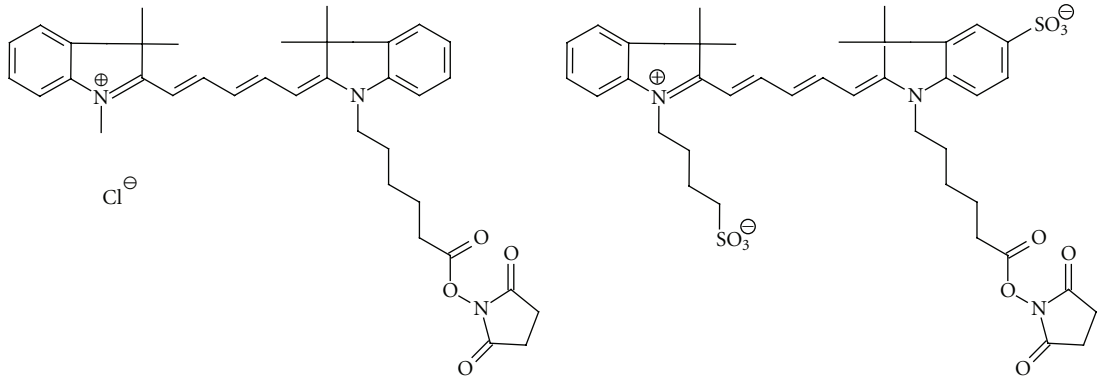

(a) Cy5 (b) Sulfo-Cy5 (Cy5 with two additional sulfonate groups)

Figure 1: Chromophore structures of Bis(indolenyl)pentamethincyanine.

formation such as solvent, ion strength and complexation with oppositely charged polymers in order to improve the cyanine dye labeling process.

2. Experimental Part

2.1. Materials. PAH (Mw 70.000), poly(styrenesulfonate) (PSS, Mw 70.000), dimethylformamide (DMF), methanol, acetone, dimethyl sulfoxide (DMSO) and buffer materials were purchased from Aldrich (Germany); poly(methacrylic acid) (PMAA, Mw 100.000) was purchased from PolyScience Inc. (USA). All chemicals were in high purity (spectroscopic grade) and were used as received. The Sulfo-Cy5 was received from FEW Wolfen (Germany) for research purposes.

2.2. Absorption and Fluorescence Masurements. Absorption spectroscopy was obtained using a Varian Cary 50 UV/Vis spectrophotometer. The fluorescence spectra were taken using a Varian Cary Eclipse. Spectra were taken with samples in quartz cuvettes of 1 cm in thickness.

2.3. Preparation of Cy5 (2-(3-{1-[5-(2,5-Dioxopyrrolidin-1-Yloxycarbonyl)-Pentyl]-3,3-Dimethyl-1,3-Dihydro-Indol-2-Ylidene}-Propenyl-1,3,3-Trimethyl-3H-Indolium Tetrafluoroborate). The corresponding Cy5-carboxylic acid Tetrafluoroborate (756 mg, 1.38 mmol) was dissolved in dry dichloromethane (25 mL) and stirred under argon. Ethyl- diisopropylamine (258 mg, 2.77 mmol) and N, N′-disuccinylcarbonate (392 mg, 1.53 mmol) were added under argon. The mixture was stirred at room temperature for 20 hours, then diluted with dichloromethane (20 mL) and washed successively with water, 32% aqueous Tetrafluoroboronic acid and water. The organic layer was separated, dried (Na_2SO_4) and concentrated. The remainder was stirred in diethylether (40 mL). The ethereal phase was separated and the ether stripped off to give the product (780 mg, 88% yield).

NMR Analysis of This Synthesized Compound. ^{1}H-NMR ($CDCl_3$) δ (ppm): 1.50 (m, 2H, $2CH_2$), 1.59 (s, 12H, $4CH_3$), 1.70 (m, 4H, $2CH_2$), 2.49 (t, 2H, CH_2COO), 2.69 (s, 4H, $COCH_2CH_2CO$), 3.55 (s, 3H, NCH_3), 3.98 (t, 2H, NCH_2), 6.46 (t, 2H, 2CH=), 7.04 (t, 2H, aryl), 7.12 (t, 2H, aryl), 7.26 (m, 4H, aryl), 8.29 (t, 1H, CH=). ^{13}C-NMR ($CDCl_3$) δ (ppm): 24.7 (CH_2), 25.3 (CH_2), 25.4 (CH_2), 26.7 (CH_2), 27.8 (CH_3), 27.9 (CH_3), 30.4 (CH_2), 31.3 (CH_3), 44.0 (CH_2), 48.9 (C), 49.0 (C), 103.3 (CH), 103.8 (CH), 110.8 (CH), 122.0 (CH), 122.1 (CH), 125.3 (CH), 125.4 (CH), 128.7 (CH), 128.8 (CH), 140.3 (C), 140.4 (C), 141.7(C), 142.4(C), 150.6(CH), 168.5(C), 169.3(C), 173,8(C), 174.5(C).

Mass Spectrometry.

Calculated for $C_{36}H_{42}N_3O_4$: 580.3175 g/mol

Determined: 580.3210 g/mol for Mol Peak

UV/Vis Spectroscopy.

Literature [20]: $\varepsilon_{640\,nm}$(MetOH) $= 250\,000\,l\,mol^{-1}\,cm^{-1}$

Determined: $\varepsilon_{640\,nm}(MetOH) = 256\,700\,l\,mol^{-1}\,cm^{-1}$

Determined: $\varepsilon_{640\,nm}(H_2O) = 230\,400\,l\,mol^{-1}\,cm^{-1}$

2.4. Preparation of PAH-Cy5. PAH was dissolved in borate buffer (50 mM, pH 8.0) to a final concentration of 1.0 mol/L and Cy5 (or Sulfo-Cy5) was dissolved in DMF to a final concentration of 0.1 mol/l. A solvent mixture consisting of 75% borate buffer and 25% DMF was used to synthesize PAH-Cy5 A and PAH-Cy5 C (when Sulfo-Cy5 is in use). A mixture of 25% borate buffer and 75% DMF was used to synthesize PAH-Cy5 B. Molar ratio between monomer unit of the polymer and dye molecules was controlled for producing PAH-Cy5 with different label degrees. The reaction was performed under stirring at room temperature overnight (24 hours). The product was dialyzed with membrane of Mwco <15,000 for one week against deionized water and thereafter filtered and lyophilized. The label degree of dye molecules on the polymer chain was determined by UV spectroscopy in 10 mM Tris buffer, pH 7.0. The extinction coefficient for Cy5, ε_{Cy5} was determined and taken as $230.400\,M^{-1}\,cm^{-1}$ at 640 nm, while ε_{Cy5} for Sulfo-Cy5

is 187.000 $M^{-1}\,cm^{-1}$ (FEW Wolfen) at 645 nm in water. For calculation of the label degree, only the absorption maximum at 640 nm and 645 nm (for Sulfo-Cy5) has been used, respectively.

3. Results and Discussion

The absorption spectrum of the dye labeled polymer PAH-Cy5 A is remarkably different to the spectrum of the free dye Cy5 (Figure 2).

A new absorption band appears at 590 nm close to the vibrational transition of the dye at 602 nm. In contrast, the fluorescence spectra of the free dye and the polymer bound dye have the same shape and peak wavelength (Figure 2), although the free dye has a 14.8% higher fluorescence intensity. These experimental results can have two different origins: either a new species is formed by the labeling procedure or the vibrational structure of the dye has changed, which is well known for certain dyes such as for example, pyrene [21]. In order to distinguish between these possibilities the fluorescence excitation spectra have been measured for the free and the immobilized dye (Figure 3). They are identical but do not show the peak at 590 nm. Hence the UV/Vis spectrum of the PAH-Cy5 shows the superposition of the single Cy5 molecule and another none-fluorescent species.

The spectrum of the new species is estimated by the difference of the spectra of labeled polymer and the free dye. The 14.8% lower fluorescence intensity of PAH-Cy5 compared to that of the free dye reveals the percentage of spectrum contribution of the new non-fluorescent species in PAH-Cy5 at the maximum at 640 nm. Taken this into account, the absorption spectrum of the new species is estimated. Its spectrum has an absorption maximum at 588 nm and a broad shoulder around 645 nm. Such hypsochromic shift of absorption to higher energy could have its origin in the formation of dye H-aggregates or dimers [22]. Formation of pure H-aggregate from the Cy5 dye has been observed earlier when it was adsorbed to PSS (Cy5/PSS) in a 1 : 1 dye to monomer ratio [16, 17]. However, the spectrum of Cy5-H-aggregate on PSS (Cy5/PSS) has a quite different shape compared to that of PAH-Cy5 (Figure 3) pointing to a different arrangement and orientation of the dye molecules to each other. The maximum is at 556 nm and the shoulder around 645 nm is less pronounced as negligible.

The formation of H-aggregates and the observed differences can be explained in terms of the Kasha-theory and the Davydov splitting (Scheme 1) [22–24]. The hypsochromic absorption shift is caused by transition dipole interactions between two or more chromophores arranged parallel to each other (H-aggregates) with a large slip angle α [23, 24]. The interaction of two transition dipoles M1 and M2 yield an energetic splitting of the excited state in two components m_+ and m_-. In the case of parallel alignment of dye molecules, the absorption and emission from one energy level is forbidden because the resulting transition moment $m_- = M1 - M2 = 0$. Only the state $m_+ = M1 + M2$ can be populated. In H-aggregates, the allowed m_+ state has a higher energy than the m_- state and the monomer. This leads to the observed hypsochromic shift of the absorption energy with respect to the monomer. In this case the m_+ state shows no fluorescence due to fast internal conversion process to the nonemitting m_- state, in which the radiative decay is forbidden. In agreement with that, the Cy5 H-aggregates show no fluorescence.

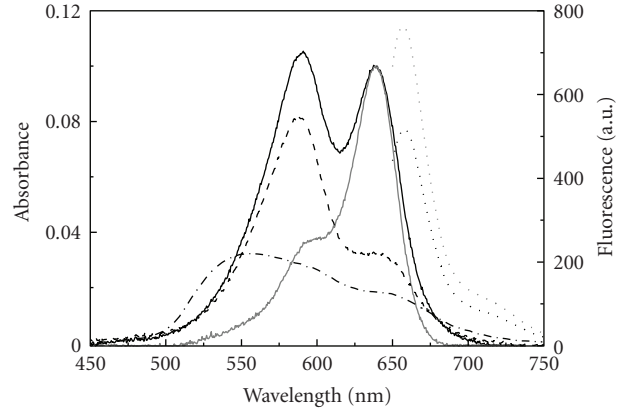

Figure 2: Absorption (solid lines) and fluorescence spectra (dotted lines) of PAH-Cy5 A (black) and Cy5 (grey). The fluorescence spectra were taken for excitation in the maximum $\lambda_{ex} = 638$ nm. The absorption spectrum of the new species is calculated (dashed line). For comparison, the H-aggregate spectrum of Cy5/PSS is given (dash-dotted line) [16, 17].

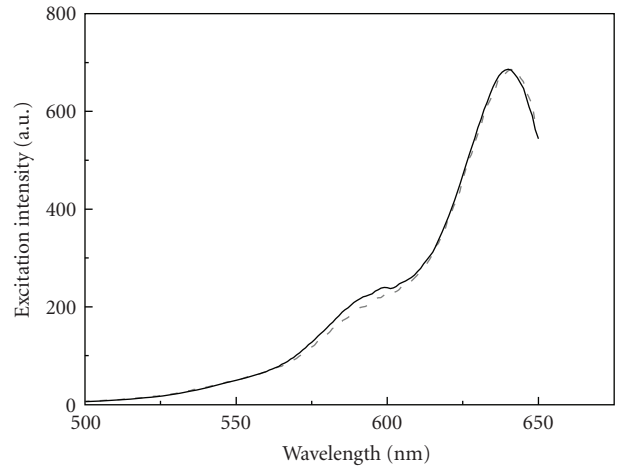

Figure 3: Excitation spectra of Cy5 (black lines) and PAH-Cy5 A (dashed grey line).

The two absorptions found for the PAH-Cy5 could be caused by a slightly inclined orientation of dye molecules to each other like in a herringbone aggregate. Then, both transitions become allowed and can be observed as Davydov components at different wavelength. The intensity ratio between the peaks depends on the angle between the molecule axes (transition dipoles). This could cause the observed shoulder at 642 nm.

The difference of the Cy5/PSS to the PAH-Cy5 spectrum can be explained by the high 1 : 1 ratio of dye molecules to

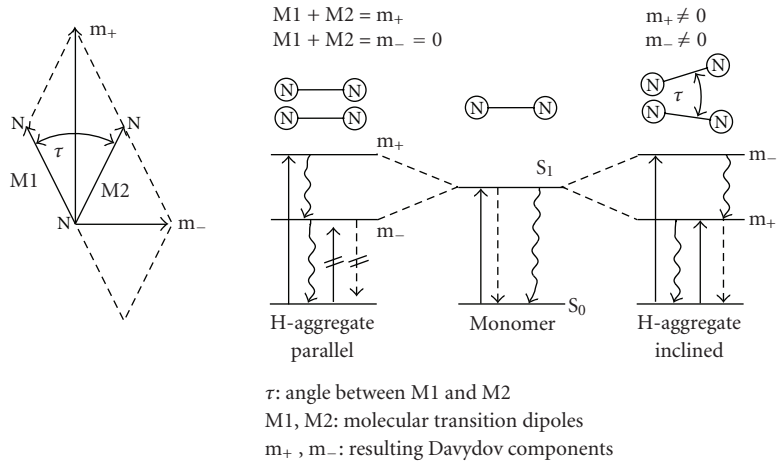

Scheme 1: Left: scheme of Davydov splitting; Right: model of molecule orientation and transition dipole interactions in dye H-aggregates and their absorption and fluorescence properties. The dumbbells model the dye molecules, solid arrows mark the absorption, broken arrows the fluorescence and wavy arrows the internal conversion, crossed lines are forbidden transitions.

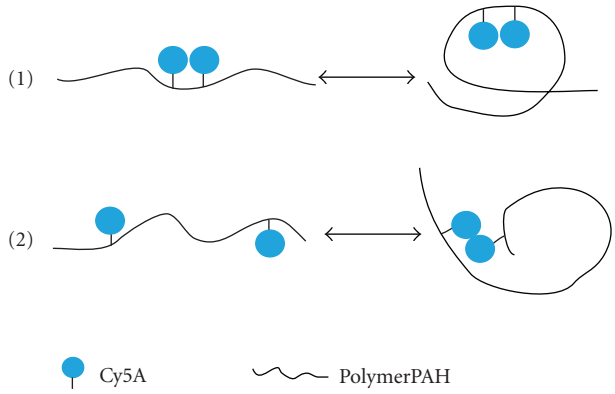

Scheme 2: Two possible ways of dye aggregates formation on PAH-Cy5.

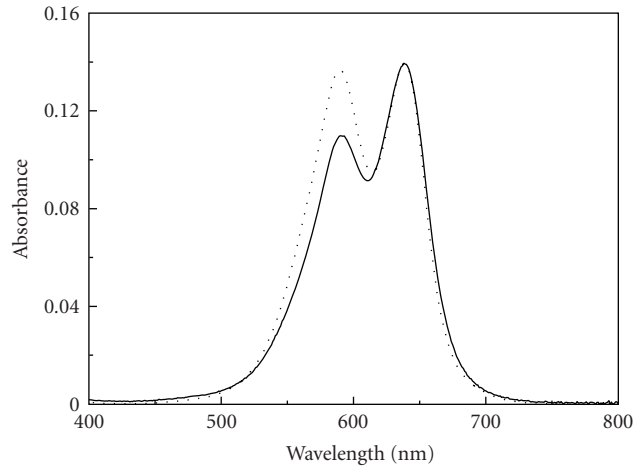

Figure 4: Absorption spectra of PAH-Cy5 A with dye label degree of 1 : 1500 (solid line) and 1 : 840 (dotted line).

monomer units on the polymer in Cy5/PSS and by the less spatial constraints compared to the covalently linked PAH-Cy5. The concentration of the dye molecules adsorbed on PSS is more than 600 times higher, yielding almost complete vanishing of the monomer absorption and the fluorescence. The dye molecules are obviously all in parallel alignment that is, the long wavelength absorption is not present. In contrast, the large constraints of Cy5 in PAH-Cy5 and the lower dye concentration result in a relatively high content of nonaggregated dye molecules. The aggregates consists of inclined molecules, producing the shoulder around 645 nm as second Davydov-component [22].

In order to eliminate the H-aggregates on the polymer, PAH-Cy5 A with lower label degrees have been synthesized (Figure 4). The aggregate band becomes smaller with decreasing label degree, which proves less dye interactions and aggregate formation. However, even at low label degree of 1 : 1500, theoretically with less than half a dye molecule bound to one polymer molecule, aggregates still exist. Hence, the formation of H-aggregate on the chain can have two possible reasons (Scheme 2):

(1) The dye molecules are not statistically distributed along the PAH chain. This could be due to a preferred attachment of the dyes in direct neighborhood on the PAH chains during the reaction.

(2) The dye molecules are statistically evenly distributed but due to well-known tangling of polyelectrolyte in aqueous solution, even dye molecules located far from each other could form aggregates.

The tangling level of polyelectrolyte depends highly on the ion strength of the surrounding aqueous solution due to shielding of the charges [25, 26]. In pure water, the polymer chain is stretched, which should bring statistically distributed dye molecules far away from each other. We investigated

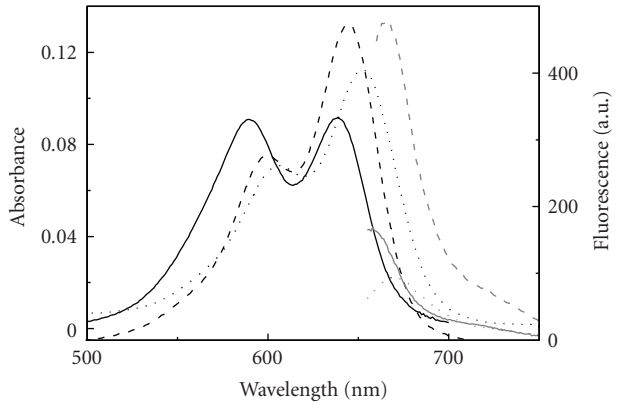

Figure 5: Absorption (black lines) and fluorescence spectra (grey lines) of PAH-Cy5 A (1 : 840) in various solvent: DMF (dashed line), H_2O (solid line) and PSS solution (C_{PSS} = 5 mg/mL) (dotted line). (Monomer ratio between PAH and PSS is 1 : 12.) The fluorescence spectra are taken with λ_{ex} = 638 nm and a slit width of 5/10 nm.

the absorption spectrum of the PAH-Cy5 solution in dependence on NaCl concentration in the range 0 and 0.25 M (data not shown). The negligible changes in the absorption spectra exclude reason 2 and reveal reason 1: the Cy5 molecules are bound in very close neighborhood on the PAH chain and cause formation of H-aggregates.

It is well known that dye aggregates can be dissolved by addition of organic solvents [27]. Furthermore, complexation of the PAH-Cy5 with a polycation can strongly change the conformation of the polymer and possibly destruct the aggregates. The interaction of PAH-Cy5 with PSS yielded a strong decrease of the band at 588 nm, showing the disappearance of the H-aggregate (Figure 5). Nevertheless, the fluorescence intensity decreased, probably due to the formation of polyelectrolyte complexes and an increase of dye density to the range where self-quenching exists. Furthermore, a bathochromic shift of absorption energy of the monomer dye molecules is observed, caused by the negative charge of the surrounding molecules (Table 1). This effect is also visible for the introduction of the sulfonate groups on the chromophor and it is not related to the aggregation phenomena.

Addition of 75% of organic solvents to the aqueous PAH-Cy5 A solution yielded an increase of the absorption in the monomer dye range at the cost of the H-aggregate band. Simultaneously, the fluorescence intensity increased by almost three times. These findings prove the inhomogeneous distribution of the dye molecules in the PAH chain.

In order to minimize the formation of H-aggregates on the PAH chain, we tried to reduce the interactions between the Cy5 molecules during the labeling reaction by the addition of different organic solvents, like methanol, acetone, DMSO and DMF. DMF has been identified as the optimal solvent for the labeling process. By such synthesis PAH-Cy5 B was prepared that showed remarkable less H-aggregates. Also this dye has been used for labelling PAH in aqueous solution yielding PAH-Cy5 C. As shown absorbance and fluorescence

Table 1: Shift of absorption maxima λ_{abs} (in nm) of Cy5 monomer band in different media.

	Monomer λ_{abs}	Monomer λ_{abs} in DMF	Monomer λ_{abs} in PSS solution
Cy5	638	644	648
PAH-Cy5	638	644	652
PAH-(SulfoCy5)	644	650	655

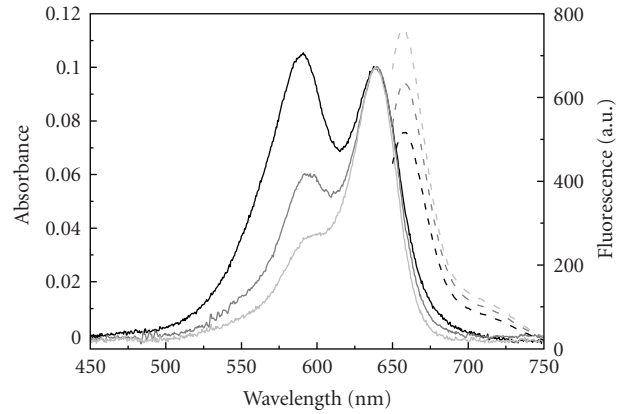

Figure 6: Absorption (solid lines) and fluorescence spectra (dashed lines) of PAH-Cy5 A (black), PAH-Cy5 B (grey) and Cy5 free dye (light grey) measured in aqueous solution. The concentration of the solutions is set to the absorption maximum. The fluorescence spectra are taken with λ_{ex} = 638 nm and a slit width of 5/5 nm.

spectra measured in aqueous solution show that the H-aggregate peak of PAH-Cy5 B is much smaller compared to that of PAH-Cy5 A, and the fluorescence quantum yield is significantly improved (Figure 6). However, the fluorescence quantum yield of free dye is still higher compared to the immobilized ones in PAH-Cy5 B.

For labeling of biological molecules the commercially available Cy5 chromophore is functionalized with two additional sulfonate groups increasing the solubility in water (Sulfo-Cy5, Figure 1). Hence, hydrophobic interactions supporting the formation of dye aggregates are less pronounced. This dye has been taken for the labeling procedure in aqueous solution. As shown in Figure 7, formation of H-aggregates is less pronounced compared to the Cy5 without sulfonate groups, but they were still present and the content increased with the label degree. Hence, our findings are also valid for better understanding of the spectroscopic properties and usage of the more hydrophilic, sulfonated Cy5 chromophores.

4. Conclusions

In this paper, H-aggregates of cyanine dye Cy5 covalently linked to the polymer PAH have been observed and the behavior of the "H-aggregate band" at different solvent and synthesis conditions has been investigated. In the PAH-Cy5 H-aggregates, the absorption wavelength is shifted from

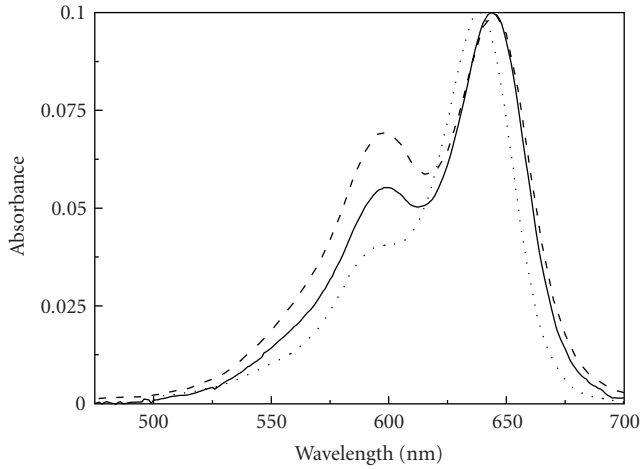

Figure 7: Absorption spectra measured from PAH-Cy5 C with label degrees 1 : 490 (solid line), 1 : 320 (dashed line), and the free dye Cy5 (dotted line).

638 nm to 588 nm. The H-aggregates show no fluorescence, which remarkably reduces the sensitivity and applicability of the dye labeled materials for analytical methods. The behavior of the coupled dye can be described well by the KASHA-theory and the Davydov-splitting. It was found that H-aggregates were formed during the synthesis by interactions between dye molecules, leading to an inhomogeneous distribution along the polymer chain even at low label concentrations. In order to reduce this undesired effect a different synthetic route in 75% organic solvent has been developed yielding much higher label degrees and remarkable less H-aggregates on the polymer. These findings open the door for better and wider use of Cy5 dyes in sensing and fluorescence detection applications.

Acknowledgments

This work was supported by a grant of the Federal Ministry of Education and Research (BMBF Project INUNA FKZ 0312027A).

References

[1] D. Pristinski, V. Kozlovskaya, and S. A. Sukhishvili, "Fluorescence correlation spectroscopy studies of diffusion of a weak polyelectrolyte in aqueous solutions," *Journal of Chemical Physics*, vol. 122, no. 1, article 014907, pp. 1–9, 2005.

[2] C. Reznik, Q. Darugar, A. Wheat, T. Fulghum, R. C. Advincula, and C. F. Landes, "Single ion diffusive transport within a poly(styrene sulfonate) polymer brush matrix probed by fluorescence correlation spectroscopy," *Journal of Physical Chemistry B*, vol. 112, no. 35, pp. 10890–10897, 2008.

[3] K. Becker and J. M. Lupton, "Efficient light harvesting in dye-endcapped conjugated polymers probed by single molecule spectroscopy," *Journal of the American Chemical Society*, vol. 128, no. 19, pp. 6468–6479, 2006.

[4] A. P. R. Johnston, A. N. Zelikin, L. Lee, and F. Caruso, "Approaches to quantifying and visualizing polyelectrolyte multilayer film formation on particles," *Analytical Chemistry*, vol. 78, no. 16, pp. 5913–5919, 2006.

[5] C.-Y. Zhang, H.-C. Yeh, M. T. Kuroki, and T.-H. Wang, "Single-quantum-dot-based DNA nanosensor," *Nature Materials*, vol. 4, no. 11, pp. 826–831, 2005.

[6] V. E. Keuren and W. Schrof, "Fluorescence recovery after two-photon bleaching for the study of dye diffusion in polymer systems," *Macromolecules*, vol. 36, no. 13, pp. 5002–5007, 2003.

[7] K. Ray, H. Nakahara, A. Sakamoto, and M. Tasumi, "Excitation energy transfer from symmetric cyanine dyes to unsymmetric merocyanine aggregated in functionalized Langmuir-Blodgett films by time-resolved fluorescence spectroscopy," *Chemical Physics Letters*, vol. 342, no. 1-2, pp. 58–64, 2001.

[8] K. Becker, J. M. Lupton, J. Feldmann, et al., "On-chain fluorenone defect emission from single polyfluorene molecules in the absence of intermolecular interactions," *Advanced Functional Materials*, vol. 16, no. 3, pp. 364–370, 2006.

[9] E. E. Jelly, "Spectral absorption and fluorescence of dyes in the molecular state," *Nature*, vol. 138, p. 1009, 1936.

[10] G. Scheibe, "Uber die veranderlichkeit der absorptionsspektren in losungen und die nebenvalenzen als ihre ursache," *Angewandte Chemie*, vol. 49, no. 31, p. 563, 1936.

[11] W. West, S. P. Lovell, and W. Cooper, "Electronic spectra of cyanine dyes at low temperature. 1," *Photographic Science and Engineering*, vol. 14, no. 1, pp. 52–62, 1970.

[12] U. Roesch, S. Yao, R. Wortmann, and F. Wuerthner, "Fluorescent H-aggregates of merocyanine dyes," *Angewandte Chemie - International Edition*, vol. 45, no. 42, pp. 7026–7030, 2006.

[13] R. W. Chambers, T. Kajiwara, and D. R. Kearns, "Effect of dimer formation of the electronic absorption and emission spectra of ionic dyes. Rhodamines and other common dyes," *Journal of Physical Chemistry*, vol. 78, no. 4, pp. 380–387, 1974.

[14] M. Van Der Auweraer, G. Biesmans, and F.-C. De Schryver, "On the photophysical properties of aggregates of 3-(2-phenyl)-indolocarbocyanines," *Chemical Physics*, vol. 119, no. 2-3, pp. 355–375, 1988.

[15] H. J. Gruber, C. D. Hahn, G. Kada, et al., "Anomalous fluorescence enhancement of Cy3 and Cy3.5 versus anomalous fluorescence loss of Cy5 and Cy7 upon covalent linking to IgG and noncovalent binding to avidin," *Bioconjugate Chemistry*, vol. 11, no. 5, pp. 696–704, 2000.

[16] C. S. Peyratout, E. Donath, and L. Daehne, "Electrostatic interactions of cationic dyes with negatively charged polyelectrolytes in aqueous solution," *Journal of Photochemistry and Photobiology A*, vol. 142, no. 1, pp. 51–57, 2001.

[17] C. S. Peyratout, E. Donath, and L. Daehne, "Aggregation of thiacyanine derivatives on polyelectrolytes," *Physical Chemistry Chemical Physics*, vol. 4, no. 13, pp. 3032–3039, 2002.

[18] G. Decher, "Fuzzy nanoassemblies: toward layered polymeric multicomposites," *Science*, vol. 277, no. 5330, pp. 1232–1237, 1997.

[19] C. S. Peyratout and L. Daehne, "Tailor-Made Polyelectrolyte Microcapsules: From Multilayers to Smart Containers," *Angewandte Chemie-International Edition*, vol. 116, no. 29, pp. 3762–3783, 2004.

[20] R. B. Mujumdar, L. A. Ernst, S. R. Mujumdar, C. J. Lewis, and A. S. Waggoner, "Cyanine dye labeling reagents: sulfoindocyanine succinimidyl esters," *Bioconjugate Chemistry*, vol. 4, no. 2, pp. 105–111, 1993.

[21] F. M. Winnik, "Photophysics of preassociated pyrenes in aqueous polymer solutions and in other organized media," *Chemical Reviews*, vol. 93, no. 2, pp. 587–614, 1993.

[22] A. S. Davydov, *Theory of Molecular Excitons*, McGraw-Hill, New York, NY, USA, 1962.

[23] M. Kasha, H. R. Rawls, and M. A. El-Bayoumi, "The exciton model in molecular spectroscopy," *Pure and Applied Chemistry*, vol. 11, pp. 371–392, 1965.

[24] D. Moebius, "Scheibe-aggregates: highly ordered systems of strongly interacting chromophores," *Advanced Materials*, vol. 7, pp. 437–444, 1995.

[25] A. Fery, B. Scholer, and T. Cassagneau, "Nanoporous thin films formed by salt-induced structural changes in multilayers of poly(acrylic acid) and poly(allylamine)," *Langmuir*, vol. 17, no. 3-4, pp. 3779–3783, 2001.

[26] R. Georgieva, R. Dimova, and G. Sukhorukov, "Influence of different salts on micro-sized polyelectrolyte hollow capsules," *Journal of Materials Chemistry*, vol. 15, no. 40, pp. 4301–4310, 2005.

[27] A. Mishra, G. B. Behera, M. M. G. Krishna, and N. Periasamy, "Time-resolved fluorescence studies of aminostyryl pyridinium dyes in organic solvents and surfactant solutions," *Journal of Luminescence*, vol. 92, no. 3, pp. 175–188, 2001.

Hindawi Publishing Corporation
International Journal of Polymer Science
Volume 2010, Article ID 379286, 10 pages
doi:10.1155/2010/379286

Research Article

Polymersomes and Wormlike Micelles Made Fluorescent by Direct Modifications of Block Copolymer Amphiphiles

Karthikan Rajagopal, David A. Christian, Takamasa Harada, Aiwei Tian, and Dennis E. Discher

Department of Chemical and Biomolecular Engineering, University of Pennsylvania, Philadelphia, PA 19104, USA

Correspondence should be addressed to Karthikan Rajagopal, kr@seas.upenn.edu

Received 23 December 2009; Accepted 20 April 2010

Academic Editor: Jinying Yuan

Wormlike micelles and vesicles prepared from diblock copolymers are attracting great interest for a number of technological applications. Although transmission electron microscopy has remained as the method of choice for assessing the morphologies, fluorescence microscopy has a number of advantages. We show here that when commercially available fluorophores are covalently attached to diblock copolymers, a number of their physicochemical characteristics can be investigated. This method becomes particularly useful for visualizing phase separation within polymer assemblies and assessing the dynamics of wormlike micelles in real time. Near-IR fluorophores can be covalently conjugated to polymers and this opens the possibility for deep-tissue fluorescence imaging of polymer assemblies in drug delivery applications.

1. Introduction

In aqueous solution, amphiphilic diblock copolymers can spontaneously self-assemble to form supramolecular morphologies such as spherical and worm-like micelles and vesicles (polymersomes) [1–3]. Due to their unique physicochemical characteristics these polymeric assemblies have shown potential for various applications such as drug delivery. Wormlike micelles ("worms") increase the delivered dose of water-insoluble drugs such as Taxol [4, 5], and vesicles (polymersomes) can be used for the encapsulation and delivery of both water-insoluble (Taxol) and water-soluble therapeutics that range from drugs to proteins [6] to siRNA [7]. An understanding of morphologies from amphiphilic diblock copolymers in dilute solution as well as their characteristics would facilitate the generation of even more robust and useful supra-molecular materials. Seminal experiments of Eisenberg and Bates helped to show that classic ideas of surfactant-based morphologies also apply to block copolymers upon varying the relative sizes of the two dissimilar blocks [8, 9]. While such studies used TEM to visualize frozen nano-morphologies, we have emphasized and exploited fluorescence imaging, including the use of dyes covalently conjugated to block copolymers as described here. Fluorescence microscopy helps to clarify many of the unique physical characteristics of polymer assemblies, including the diversity in sizes, shapes, flexibilities and lateral segregation.

Fluoroscence microscopy is widely used in cell biology and biophysics for understanding the structure and function of molecules within cells and organelles [10–12]. Although one cannot infer structural information below the diffraction limit, this method nevertheless enables the visualization of spatial and temporal evolution of processes within the cell. As a result, numerous fluorescent dyes have become commercially available for ready conjugation to biomolecules [13]. A number of these fluorophores have been specifically designed for aqueous phase reaction with various functional groups on amino acid side chains such as thiols, amines, hydroxyls and acids. On the other hand, TEM is particularly useful for identifying structures down to nanometer length scale and therefore has remained the method of choice for assessing the morphologies of polymer assemblies [14–17]. However, TEM imaging is performed on samples after drying, which can be an issue with water-based assemblies, and while

cryo-TEM of vitrified samples partially circumvents the issue, the films are nano, contrast can be problematic, and information on dynamics of these structures in solution is simply not obtainable. Equipment costs, sample preparation complexities, and specialized training all limit the utility of TEM. Alternatively, fluorescence microscopy is a robust and simpler method that enables rapid assessment of structures as well as the dynamics of polymeric assemblies in real time. Because wormlike micelles and polymersomes formed from diblock copolymers are often microns in size, they can be easily identified and quantified using fluorescence microscopy—although it should be stated at the outset that one cannot unequivocally decipher differences between spherical micelles and submicron sized worm micelles and vesicles.

Visualization of polymer assemblies by fluorescence microscopy can be accomplished by adding a small amount of lipophilic dye (e.g., PKH26, Sigma) to a solution of the polymer sample. Such a dye molecule immediately partitions into the hydrophobic core of the polymer assemblies and therefore the shapes of the assemblies can be directly observed under the microscope. Using this approach, we have extensively characterized the physical properties and degradation of polymeric worm-like micelles and vesicles [18–22]. While these studies demonstrate that the externally added dye is minimally perturbing to the polymeric structures, their utility in some instances seems limited. For example, chemical incompatibility between the hydrophobic core and dye molecules may result in poor labeling and in some cases the dye molecule has been shown to leach out [23] or transfer to a different environment such as cell membranes [24]. We envisioned that covalent conjugation of a fluorophore to diblock copolymers may not only overcome some of these limitations, but it may also be useful, as we show here, in investigating phase separation within polymer assemblies as well as tracking their intracellular transport for drug delivery applications. We show here that several commercially available dyes can be readily conjugated to diblock copolymers using established chemistries, and when the modified polymers were blended with diblock copolymers in small proportions, their morphologies are retained and dynamics in real time can be observed using fluorescence microscopy. Finally, we show that near-IR emissive fluorophores can be attached to diblock copolymers and this will be particularly important for in vivo tracking of these assemblies via deep-tissue fluorescence imaging.

2. Experimental Methods

2.1. Materials. Polyethyleneoxide-b-polybutadiene (PEO-b-PBD; 10,500 g/mole), polyacrylic acid–b-polyethyleneoxide (PEO-b-PAA; 10,500 g/mole), polycaprolactone-b-polyethyleneoxide (PCL-b-PEO; 15,500 g/mole), and polycaprolactone (PCL-OH; 7,700 g/mole) were obtained from Polymer Source, Canada. Thiol-terminated polycaprolactone (PCL-SH) was synthesized as described before from hydroxyl-terminated polycaprolactone (PCL-OH). Fluorescent dyes, cascade blue ethylenediamine trisodium salt (C621), fluorescein-5-carbonyl azide diacetate (F6218), rhodamine maleimide (R6029), and Alexa fluor 750 C5 maleimide (A30459) were obtained from Molecular Probes, Eugene, OR and 3,3′-dioctadecyloxacarbocyanine perchlorate (DiO) was obtained from Sigma.

2.2. Conjugation of Fluorescein Azide Carboxylate to PBD-b-PEO. In a 5 mL RB flask 30 mg (2.86×10^{-3} mMoles) of PBD-b-PEO (10, 500 g/mole) and 6.9 mg (14.3×10^{-3} mM) of fluorescein azide carboxylate (485.41 g/mole) were taken and dissolved in 1.0 mL anhydrous toluene. The contents were stirred overnight on an oil bath at 85°C. The reaction was stopped next day and 1.0 mL of anhydrous DMF and 200 μL of hydroxylamine (50%) were added to the flask. The contents of the flask turn dark orange and after stirring for 2 hours were transferred to a Spectrapor dialysis membrane (MWCO 3500) and dialysed against DMSO for 2 hours. This was followed by dialysis against DI water for two days and water was changed every 12 hours. The dye-conjugated polymer in dry form was recovered by freeze-drying.

2.3. Conjugation of Cascade Blue to PBD-b-PAA. To a solution of polybutadiene-b-polyacrylic acid (PBD-b-PAA) polymer (10 mg, 0.905×10^{-3} mMoles) in anhydrous DMF (0.7 mL), 3 equivalents of EDAC (0.52 mg, 2.7×10^{-3} mMoles) and HOBt (0.42 mg, 2.7×10^{-3} mMoles) were added and the contents were stirred under argon for 1 hour. A solution of cascade blue etylenediamine (1.7 mg, 625 g/mole, 2.7×10^{-3} mMoles) in anhydrous DMF (0.3 mL) was prepared separately and added to the reaction mixture. The contents were stirred for 36 hours and the dye-conjugated polymer was separated by dialysis against Millipore water (18.2 M ω.cm) using a Slide-A-Lyzer (Thermo Scientific) dialysis cassette (MWCO : 10 kD). After 4 days of dialysis, the aqueous polymer solution was frozen and lyophilized to yield the dry polymer conjugated with the dye. To remove any residual and unreacted dye, the polymer was further washed with water and methanol and dried under vacuum. Covalent conjugation was established by thin layer chromatography using methanol as eluent.

2.4. Conjugation of Maleimide Dyes to PCL-SH. Thiol-terminated polycaprolactone (PCL-SH) (7700 g/mole, 36 mg, 4.7×10^{-3} mMoles) was taken in a clean 5 mL RB flask and dissolved in 0.7 mL of freshly distilled DCM. Separately 1.2 equivalents of rhodamine maleimide (680.8 g/mole, 3.82 mg, 5.61×10^{-3} mMoles) was dissolved in 40 μL of anhydrous DMSO and added to the RB flask. The contents were stirred overnight at room temperature under argon. The dye-conjugated polymer was separated by dialysing (Spectrapor membrane, MWCO: 3500) for a day against DCM followed by dialysis against DMSO for a day. The purified polymer in dry form was obtained after freeze-drying from DMSO solution. For the conjugation of Alexa Flour C5 750 maleimide (1350 g/mole), PCL-SH (5.7 mg, 7700 g/mole, 0.74×10^{-3} mMoles) was dissolved in freshly distilled DCM in a 5 mL RB flask. Separately 1.0 equivalent of Alexa Flour dye (1 mg, 0.74×10^{-3} mMoles)

was dissolved in 10 μL DMSO and transferred to the flask containing PCL-SH. The contents were stirred overnight under argon. The dye-conjugated polymer was separated by dialysing (Spectrapor membrane, MWCO: 3500) against DCM for a day followed by dialyzing against DMSO for a day. The purified polymer in dry form was obtained after freeze-drying.

2.5. Preparation of Polymer Assemblies. Polymer assemblies were prepared using one of two methods. In the solvent evaporation method, a 1 mM stock of the unlabeled and labeled polymer was first prepared in chloroform separately. In a 4 mL amber vial 95 μL of the unlabeled polymer and 5 μL of the labeled polymer were added and mixed well. To the vial 1 mL of DI water was added and the contents were stirred gently (~200 rpm) on a magnetic stir plate using a micro stir bar with the cap open at room temperature. Stirring was continued for 48 hours or until no chloroform layer was observed. The final polymer concentration after chloroform evaporation was 100 mM. In the film rehydration method, 100 μL of 1 mM polymer stock solution containing 5 μL of labeled polymer was diluted to 800 μL with chloroform in a 4 mL amber glass vial. Chloroform was evaporated by gently purging nitrogen into the vial until a thin film of the polymer was formed on the inner surface and the vial was further dried in vacuum for at least 8 hours. To the dried vial, 1 mL of DI water was added, placed in a preheated oven at 60°C with cap closed and gently stirred (~100 rpm) for 12 hours. Phase separated polymersomes were formed by film rehydration method using 0.05 mg of polymer (0.033 mg of TMRCA labeled PBD-b-PEO, 0.015 mg of unlabeled PBD-b-PAA, 0.0017 mg of cascade blue labeled PBD-b-PAA) hydrated with 500 μL of DI water at pH 3.5 and 0.1 mM Ca^{2+}.

2.6. Fluorescence Microscopy. Morphologies were assessed using epifluorescence microscopy on an Olympus IX71. In an Eppendorf tube 10 μL of the sample after self-assembly was taken and diluted to 100 μL with DI water. A small amount of sample (~3 μL) was spotted on a precleaned glass slide and 18 mm circular cover slip was placed on top and gently pressed so as to form a thin film of the sample. The circular end of the cover slip was sealed using vacuum grease. The sample was placed on the microscope stage and imaged through the cover slip. For time lapse imaging a sequence of images from the same field of view was captured at 4s interval. Two color phase separated polymersomes were imaged by laser-scanning confocal microscopy on an Olympus Fluoview 300 with 405 nm and 543 nm laser excitation sources. Laser scanning confocal microscopy on an Olympus Fluoview 1000 was used to image AlexaFluor 750-labeled polymersomes with a 748 nm laser excitation source.

2.7. Intracellular Tracking of Fluorescent Polymersomes. Approximately 50,000 A549 human lung carcinoma cells were seeded on 35 mm Matek dish 24 hours prior to the addition of polymersome sample. Ham's F12 (Invitrogen) with 10% FBS and 1% penicillin/streptomycin was used for culturing A549 cells. After exchanging with fresh medium and adding the sample, cells were incubated 24 hours for PCL-b-PEO/PCL-Rhodamine and 12 hours for PCL-b-PEO/DiO at 37°C with 5% CO_2. At the end of incubation, Hoechst 33342 in PBS was added 5000-fold dilution. After 10-minute incubation with Hoechst 33342, cells were washed with PBS three times and fresh medium was added. Cells were observed under fluorescent microscope without fixation.

2.8. Near IR Imaging Using Licor. Assemblies labeled with the AlexaFluor 750 fluorophore were diluted 10 fold in PBS and dispensed into a 96 well plate. The 96-well plate containing these solutions was then imaged on a Licor Odyssey using the 800 nm laser excitation source.

3. Results and Discussion

3.1. Covalent Attachment of Fluorophores to Diblock Copolymers Polymers. Two different diblock polymers were chosen for covalent conjugation to fluorescent dyes. The reaction schemes for dye conjugation are presented in Scheme 1 and the details of fluorophores used are shown in Table 1. Polybutadiene-b-poly(ethylene oxide) (PBD-b-PEO) diblock copolymer was made fluorescent by reacting the terminal hydroxyl group of the PEO block with fluorescein-5-carbonyl azide. In anhydrous organic solvents, alcohols react with isocyanates to form urethane linkage. However, due to the limited stability of isocyanates, acyl-azide bearing fluorophores that are converted to isocyanates in situ can be used to label hydroxyls [25, 26]. PBD-b-PEO was dissolved in anhydrous toluene along with fluorescein acyl azide and heated to 85°C. The acyl azide first undergoes a Curtius rearrangement to form an isocyanate that subsequently reacts with the terminal hydroxyl on the PEO block to form a stable urethane linkage. The resulting product becomes fluorescent only after hydrolyzing the carbonyl ester using hydroxylamine.

Polybutabiene-b-polyacrylic acid (PBD-b-PAA) was made fluorescent by coupling an amine containing fluorescent dye, cascade blue ethylenediamine, to acid groups on PAA using EDAC chemistry. EDAC is a water-soluble reagent that is used for the activation of carboxylic acids for reaction to amines. Since the diblock copolymer is not directly soluble in water this reaction was performed in anhydrous DMF. The first step in the reaction is the formation of O-acylurea intermediate that is relatively unstable and slow to react with amines. However, the stability of the intermediate and the yield of amide bonds can be enhanced by including hydroxybenzotriazole (HOBT) in the reaction. This results in the formation of HOBT ester that readily reacts with amines. In order to couple cascade blue ethylenediamine to PBD-b-PAA, 3 equivalents of dye was used resulting in efficient coupling as established using TLC. However, it is important to note that for fuorescence microscopy yield of the reaction is not of a major concern as long as one can image these assemblies.

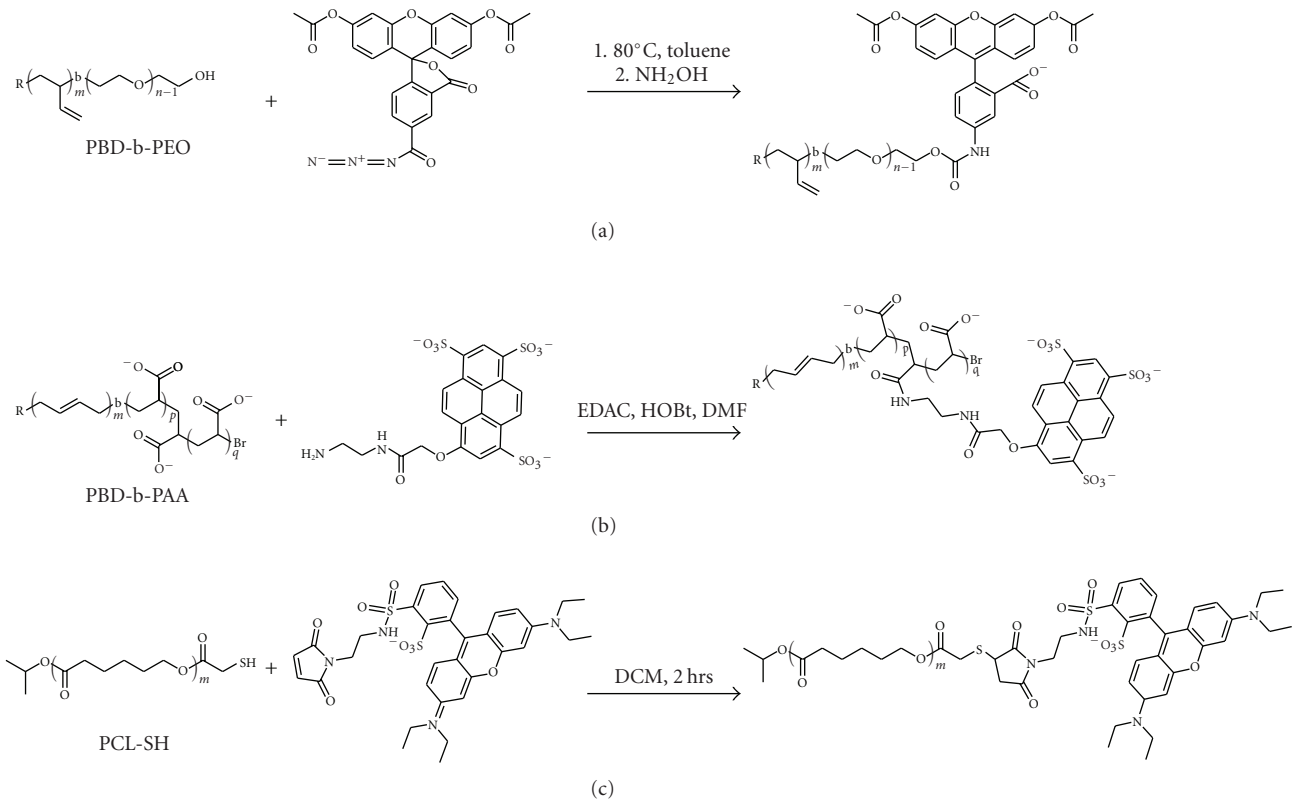

Scheme 1: The conjugation of various reactive fluorophores to polymers is shown.

Table 1: Details of fluorophores used.

Fluorophore	MW (g/mole)	Absorption (nm)	Extinction coefficient	Emission (nm)
Cascade blue ethylenediamine trisodium salt	624.49	399	30,000	423
Fluorescein-5-carbonyl azide diacetate*	485.41	490	>70,000	510
Rhodamine maleimide	680.8	560	119,000	580
Alexa Fluor 750 C5-maleimide	1350	753	290,000	783

* Becomes fluorescent after hydrolysis of carbonyl group.

3.2. Fluorescence Microscopy Visualization of Polymer Assemblies. In order to visualize the morphologies by fluorescence microscopy, 5 mol% of the labeled polymer was blended with the unlabeled polymer prior to self-assembly. The unlabeled and labeled polymers were first dissolved separately in chloroform, a good solvent for both the hydrophobic and hydrophilic blocks, and mixed prior to self-assembly. Self-assembly was initiated using one of two standard methods. In the first method, referred to as solvent evaporation, 100 μL of the stock containing 5% of labeled polymer was taken in a vial and hydrated by adding 1 mL of DI water at room temperature. Upon gentle stirring as the chloroform evaporates, the polymers spontaneously self-assemble. The second method used was standard film-rehydration, where 100 μL of the polymer stock solution containing 5% of labeled polymer was added to a vial and diluted to 1 mL by adding chloroform and then cast into a thin film on the surface by drying. The vials were then hydrated at 60°C to induce self-assembly.

The morphologies obtained from the self-assembly of diblock copolymers were visualized directly using fluorescence microscopy. Figures 1(a) and 1(b) show vesicles formed from PBD-b-PAA and PBD-b-PEO diblock copolymers respectively. Labeling of the vesicle membrane gives vesicles an edge-bright fluorescence, although the membrane thickness is not resolvable by fluorescence microscopy. The edge brightness cannot be seen in vesicles with submicron diameters and thus they usually appear as bright spots. Since the amount of polymer incorporated within a spherical micelle is much less than that of a sub-micron sized vesicle, vesicles can be distinguished from spheres as they appear as much brighter structures. Nevertheless, This method allows us to identify the formation of multilamellar vesicles as shown in the left panel of Figure 2(a).

3.3. Blending PCL-Rhodamine for Imaging PEO-b-PCL Assemblies. The morphologies of PCL-b-PEO assemblies were visualized by blending in rhodamine conjugated to the

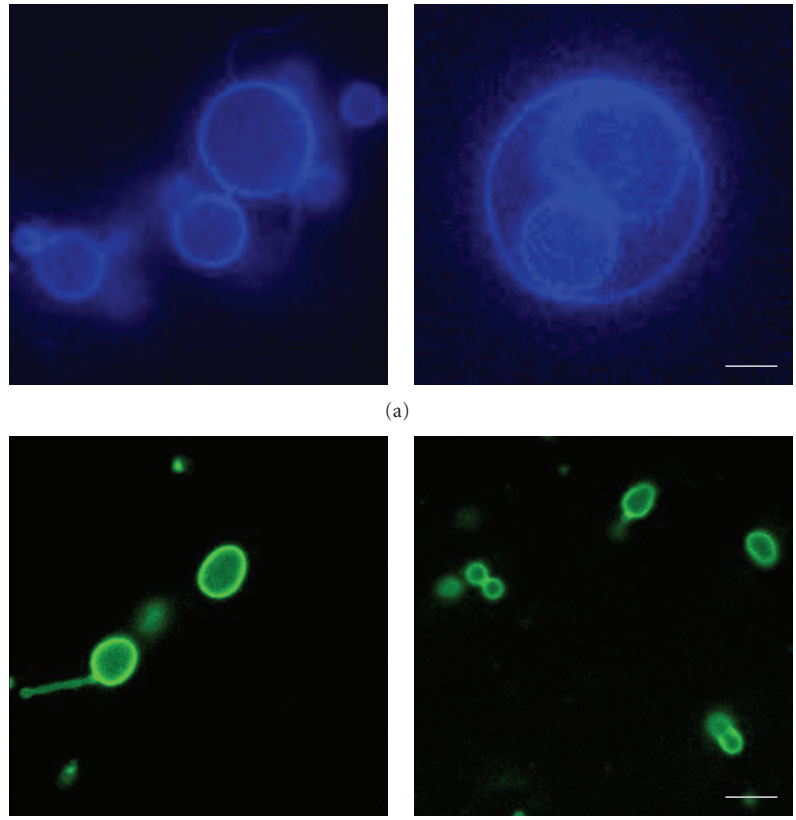

(a)

(b)

Figure 1: Morphologies from fluorescence microscopy. (a) Vesicles prepared from cascade blue conjugated to PAA-b-PBD. (b) Vesicles prepared from fluorescein conjugated to PBD-b-PEO. Scale bar is 5 μm.

polycaprolactone (PCL-Rh). Since PEO-b-PCL was synthesized by the ring-opening polymerization of ε-caprolactone, using PEO as the macroinitiator the resulting diblock copolymer does not have a reactive functional group on the PEO terminus for dye conjugation. Covalent attachment of dye to the hydroxyl terminus on the PCL side was not preferred, as it is likely to alter the geometry of the unimer, which might be perturbing to the morphology. In order to visualize these assemblies, a thiol-terminated polycaprolactone was conjugated to a maleimide bearing rhodamine and blended with PCL-b-PEO in small proportions. The reaction of thiols to maleimide is one of the common methods for labeling and attaching functional groups to proteins. The addition of a thiol to maleimide (Michael addition) results in the formation of a stable thioether bond and this reaction can be performed in aqueous phase at pH 7.0. However, since PCL is insoluble in water, the conjugation of maleimide rhodamine was performed using anhydrous DCM.

When chloroform solutions of PCL conjugated rhodamine and PCL-b-PEO were mixed, they co-self-assemble upon hydration and the resulting morphologies are presented in Figure 2(a). When 5% of PCL-rhodamine is mixed with PCL-b-PEO, self-assembly results in the formation of a mixture of worm-like micelles and vesicles (Figure 2(b)). However, at 50% PCL-rhodamine the dominant morphology is shifted to that of vesicles (Figure 2(c)). One of the major driving forces for self-assembly of amphiphilic diblock copolymers is the cohesive intermolecular hydrophobic interaction between PCL blocks. It is therefore not surprising to note that PCL-Rh is easily integrated within the hydrophobic cores of PCL-b-PEO assemblies.

3.4. Real Time Dynamics of Worm Micelles. Due to their "Brownian" interactions with water, worm micelles exhibit persistent thermal fluctuations along their contour lengths. The dynamics of worm micelles is clearly reflective of the physical state of the hydrophobic core—a rubbery or fluidic core gives rise to a flexible worm micelle. In this context, fluorescence microscopy is particularly attractive for assessing the fluctuation dynamics of polymer assemblies: the flexibilities of worm micelles can be readily quantified using time-lapse epifluorescence microscopy. This is shown in Figure 3(a) for a flexible PCL-b-PEO worm micelle incorporating 5% PCL-rhodamine. At long-time intervals, the conformation of the worm micelle is fully decorrelated. However, within the same sample there is a small proportion of worm micelles that are completely inflexible and exhibit rigid body motion in solution, as shown in Figure 3(b). The rigidity of worm micelles is perhaps due to crystallization of polycaprolactone and is currently an active area of investigation. Although the melting temperature of PCL

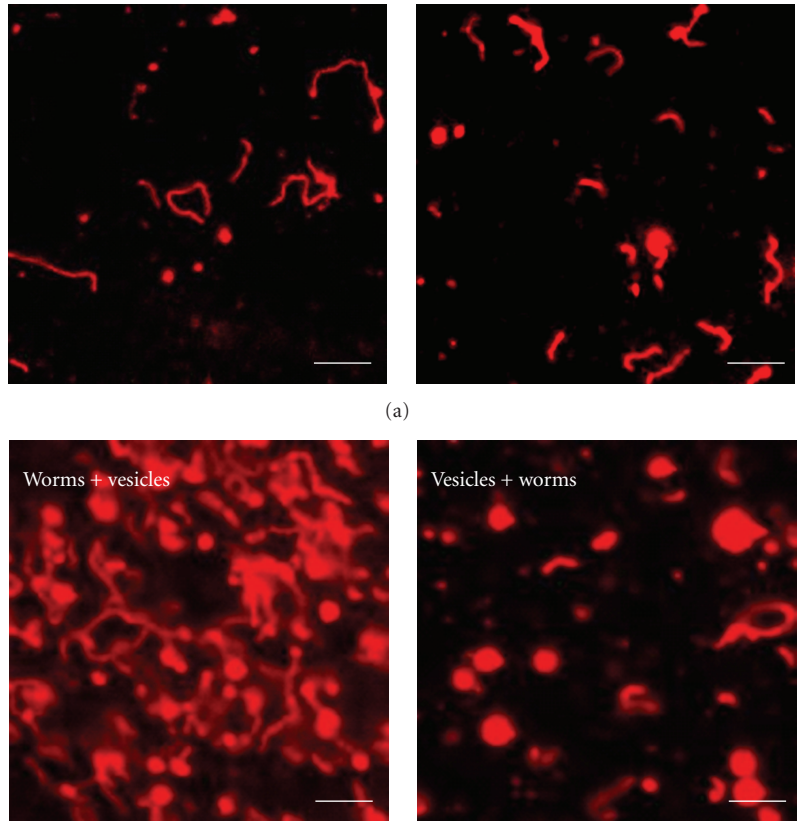

Figure 2: Blending PCL-Rhodamine in PCL-b-PEO assemblies. (a) Worm micelles and vesicles prepared from PEO-b-PCL diblock copolymer blended with 5% PCL-rhodamine. (b) At 5% PCL-rhodamine blending PCL-b-PEO worm micelles are obtained as the dominant morphology. (c) At 50% PCL-rhodamine, the dominant morphology shifts to vesicles. Scale bar is 10 μm.

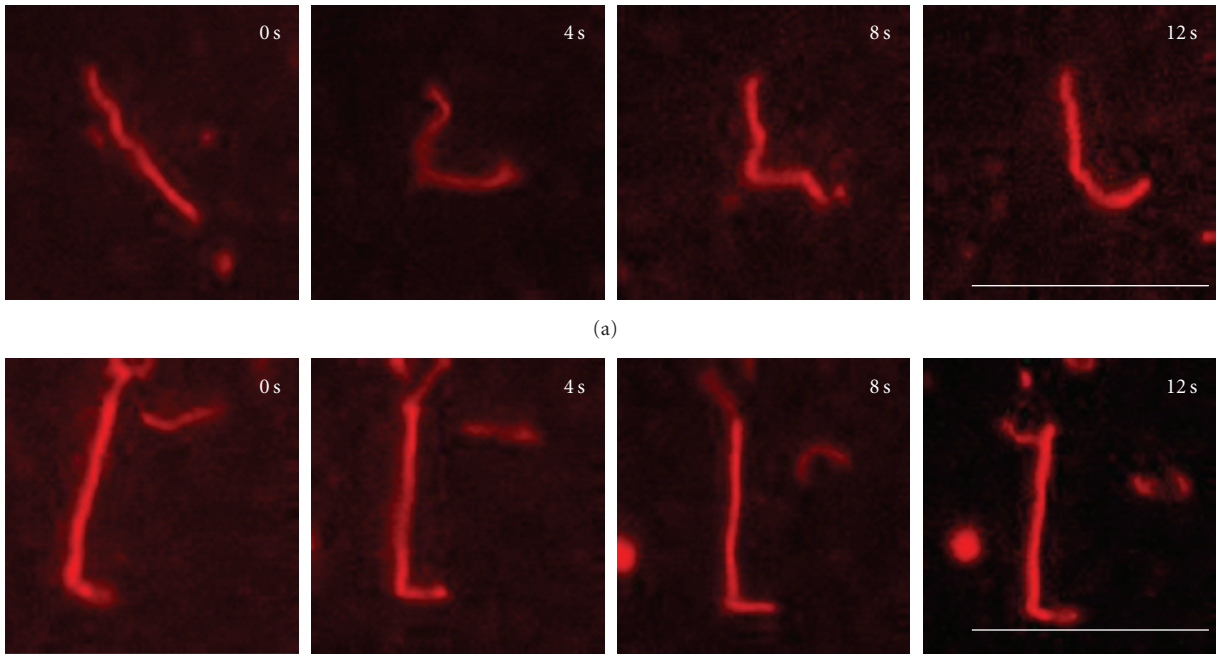

Figure 3: Dynamics of worm micelles from time-lapse fluorescence microscopy. Time-lapse fluorescence microscopy images of a flexible (a) and rigid (b) PCL-b-PEO worm micelle incorporating 5% PCL-rhodamine is shown. Scale bar is 10 μm.

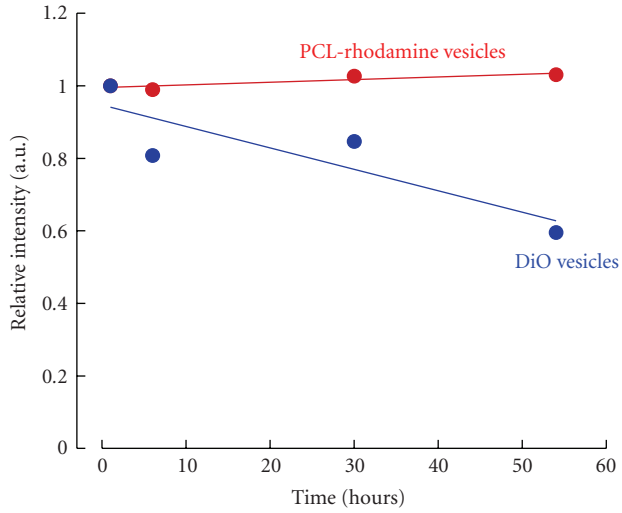

(a)

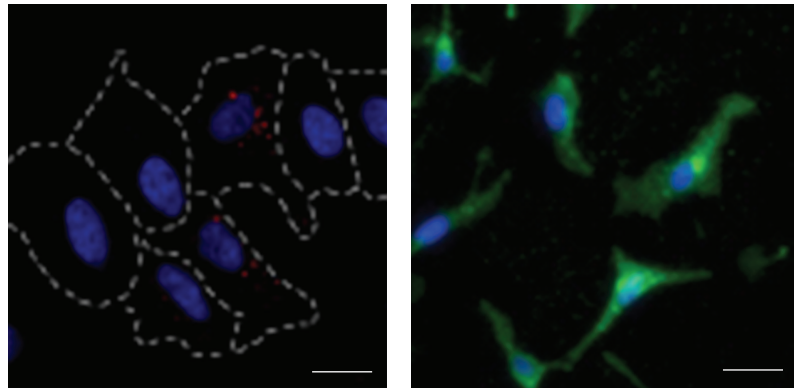

(b) (c)

Figure 4: Dye retention and intracellular tracking of polymer assemblies. (a) The plot shows the retention and release of fluorophores from PCL-b-PEO assemblies as a function of time. While PCL-rhodamine shows no release, DiI is gradually released with time. (b) Covalent conjugation of dyes to polymers enables their in vivo tracking via fluoroscence microscopy. The image shows cell internalization of PCL-b-PEO vesicles incorporating 5% PCL-rhodamine. The cell membrane is indicated with broken white lines and the vesicles are shown in red. (c) When the lipophilic dye, DiI, is used for labeling PCL-b-PEO vesicles, it is transferred to the cell membranes (green). Scale bar is 10 μm.

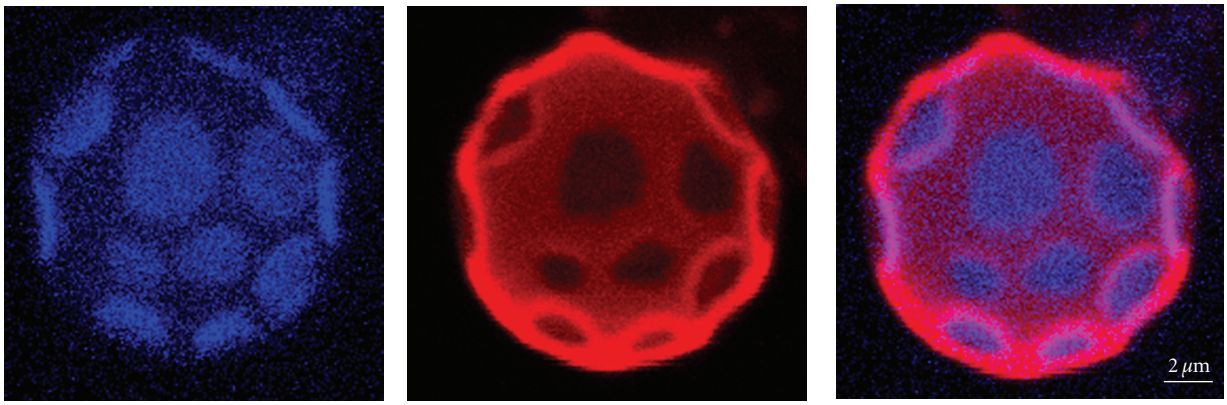

(a) (b) (c)

Figure 5: Visualization of phase separation in polymer assemblies. Vesicles prepared from cascade blue conjugated PBD-b-PAA (blue) and TMRCA-conjugated PBD-b-PEO (red) show phase separation in the presence of calcium at high pH conditions. Scale bar is 2 μm.

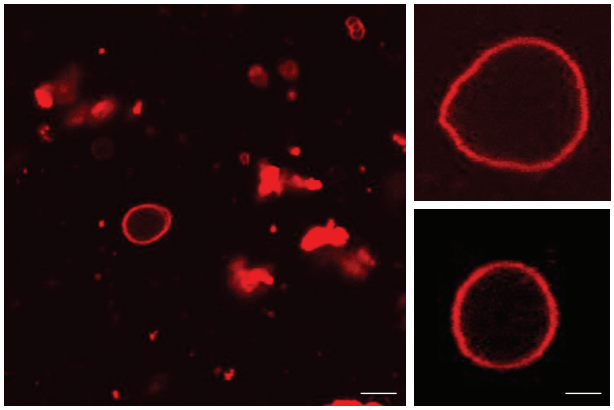

(a)

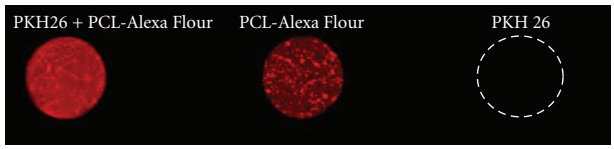

(b)

Figure 6: Near IR polymersomes. (a) Conjugation of AlexaFlour-750 to PCL enables visualization in the near IR region (748 nm excitation). The figure shows fluorescence microscopy images of PCL-b-PEO vesicles incorporating 5% PCL-Alexa Flour. (b) The vesicles can also be imaged using Licor Odyssey near-IR imager where the dye was excited using a 800 nm laser. As a control, when PKH26-labeled vesicles was excited at 800 nm and no fluorescence was observed. Scale bar is 10 μm.

depends on the molecular weight, it is likely to be above the ambient conditions under which the worm micelles were imaged. However, flexibility to rigidity transitions in polymeric assemblies can be identified and characterized using time-lapse fluorescence microscopy.

3.5. Dye Retention and Intracellular Tracking of Polymer Assemblies. Covalent conjugation of dyes to amphiphilic polymers is useful for investigating the intra-cellular transport of polymer assemblies. This is particularly important when the externally added dye has a tendency to preferentially transfer to the cell membranes [24]. To investigate this, PCL-b-PEO vesicles incorporating 5% PCL-rhodamine and labeled with DiO were prepared separately and the release of the dye was monitored as a function of time. The plot in Figure 4(a) shows that PCL-rhodamine is retained within the vesicles whereas DiO is released gradually with time. The labeled vesicles were then added to A549 human lung carcinoma cells and incubated for at least 12 hours. Figure 4(b) shows the images of cells incubated with PCL-rhodamine vesicles after 24 hours and 4B shows DiO-labeled vesicles after incubation for 12 hours. While PCL-rhodamine labeled vesicles (shown in red) do not show any labeling of the membranes and fluorescence is confined within the vesicles, the DiO dye transfers and labels the cell membranes. This clearly suggests that covalent conjugation of dye is important for intracellular tracking of polymer vesicles and worm micelles.

3.6. Visualization of Phase Separation in Polymer Assemblies. Phase separation between immiscible polymers in polymer assemblies like vesicles and wormlike micelles has been shown to occur from the nanoscale to the micron-scale. Most work has focused on immiscibility of the hydrophobic blocks as a driving force for phase separation. In these studies, phase separation occurs on the nano-scale, which requires the use of cryo-TEM and differences in the electron density of the two polymers to be visualized. More recently, ligand-induced phase separation has been observed between amphiphilic diblocks with similar hydrophobic blocks and dissimilar hydrophilic blocks (PBD-b-PEO and PBD-b-PAA) in the presence of a hydrophilic ligand (here, divalent calcium) [27]. In images taken by cryo-TEM, the hydrophilic blocks of these assemblies is difficult to image. To determine the distribution of each diblock species within these assemblies, fluorescence microscopy was used and a different fluorescent label was conjugated to each type of diblock. Phase separation in two-color polymersomes formed by film rehydration in the presence of calcium was imaged by laser scanning confocal microscopy (LSCM) (Figure 5). Distribution of PBD-b-PAA labeled with Cascade Blue was imaged using a 405 nm excitation laser source and seen Figure 5(a) as a confocal z-stack of one hemisphere of the polymersome. The distribution of PBD-b-PEO labeled with tetramethylrhodamine was imaged using a 543 nm laser excitation source as seen in Figure 5(b). A two-color overlay of the z-stacks (Figure 5(c)) clearly shows the lateral segregation of the two polymers within the polymersome assembly.

3.7. Near-IR Emissive Polymersomes. Polymersomes (polymer vesicles) encapsulate an aqueous lumen and typically range in size from a few hundred nanometers to a few tens of microns in diameter. The utility of these assemblies for drug delivery applications can be enhanced by tracking their biodistribution in vivo in live mice. Towards this goal, polymersomes labeled with near infrared emissive multiporphyrins [28], or lipophilic dyes as fluorophores can be used to track drug carriers or cells in live mice over time. Alternatively, Alexa flour C5 750 maleimide can be directly conjugated to thiol-terminated polycaprolactone and integrated within PCL-b-PEO vesicles. Figure 6(a) shows PCL-b-PEO vesicles incorporating 5% PCL-Alexa Fluor imaged using an LSCM with a 748 nm laser excitation source. As a proof of principle, solutions containing these PCL-Alexa Fluor 750 labeled vesicles were imaged in a 96 well plate on the Licor Odyssey using the 800 nm laser excitation source. Prior to imaging on the Odyssey, a red lipophilic dye PKH26 was added to the solution to confirm the presence of vesicles by epifluorescence microscopy. Solutions containing PCL-Alexa Fluor 750 labeled vesicles provided measurable fluorescence intensity when excited by the 800 nm laser on the Odyssey, which has been used in previous studies to image and quantify biodistribution in live animals and in freshly excised organs [29].

4. Conclusions

We have shown that polymeric wormlike micelles and polymersomes can be made fluorescent by covalently conjugating specific fluorophores. Commercially available fluorescent dyes are readily attached to diblock copolymers using simple conjugation chemistries. In addition to assessing the morphologies, covalent conjugation of dyes to diblock copolymers enables visualization of phase separation within assemblies and allows assessment of the fluctuation dynamics of worm micelles in real time. Covalent conjugation is particularly useful for the intracellular tracking of polymersomes. Finally, labeling with a near-infrared emissive dye (e.g., Alexa flour 750) provides new opportunity for tracking these assemblies in live rodents to better understand the in vivo behavior of these novel drug delivery and imaging vehicles.

References

[1] D. E. Discher and A. Eisenberg, "Polymer vesicles," *Science*, vol. 297, no. 5583, pp. 967–973, 2002.

[2] E. B. Zhulina, M. Adam, I. LaRue, S. S. Sheiko, and M. Rubinstein, "Diblock copolymer micelles in a dilute solution," *Macromolecules*, vol. 38, no. 12, pp. 5330–5351, 2005.

[3] P. Alexandridis and B. Lindman, Eds., *Editors Amphiphilic Block Copolymers: Self-Assembly and Applications*, Elsevier, New York, NY, USA, 2000.

[4] Y. Geng, P. Dalhaimer, S. Cai, et al., "Shape effects of filaments versus spherical particles in flow and drug delivery," *Nature Nanotechnology*, vol. 2, no. 4, pp. 249–255, 2007.

[5] Y. Geng and D. E. Discher, "Visualization of degradable worm micelle breakdown in relation to drug release," *Polymer*, vol. 47, no. 7, pp. 2519–2525, 2006.

[6] D. A. Christian, S. Cai, D. M. Bowen, Y. Kim, J. D. Pajerowski, and D. E. Discher, "Polymersome carriers: from self-assembly to siRNA and protein therapeutics," *European Journal of Pharmaceutics and Biopharmaceutics*, vol. 71, no. 3, pp. 463–474, 2009.

[7] Y. Kim, M. Tewari, J. D. Pajerowski, et al., "Polymersome delivery of siRNA and antisense oligonucleotides," *Journal of Controlled Release*, vol. 134, no. 2, pp. 132–140, 2009.

[8] K. Yu and A. Eisenberg, "Multiple morphologies in aqueous solutions of aggregates of polystyrene-block-poly(ethylene oxide) diblock copolymers," *Macromolecules*, vol. 29, no. 19, pp. 6359–6361, 1996.

[9] S. Jain and F. S. Bates, "On the origins of morphological complexity in block copolymer surfactants," *Science*, vol. 300, no. 5618, pp. 460–464, 2003.

[10] E. J. G. Peterman, H. Sosa, and W. E. Moerner, "Single-molecule fluorescence spectroscopy and microscopy of biomolecular motors," *Annual Review of Physical Chemistry*, vol. 55, pp. 79–96, 2004.

[11] J. W. Lichtman and J.-A. Conchello, "Fluorescence microscopy," *Nature Methods*, vol. 2, no. 12, pp. 910–919, 2005.

[12] J. Rao, A. Dragulescu-Andrasi, and H. Yao, "Fluorescence imaging in vivo: recent advances," *Current Opinion in Biotechnology*, vol. 18, no. 1, pp. 17–25, 2007.

[13] G. T. Hermanson, Ed., *Bioconjugate Techniques*, Academic Press, San Diego, Calif, USA, 1995.

[14] H. Shen and A. Eisenberg, "Morphological phase diagram for a ternary system of block copolymer PPS_{310}-*b*-PAA_{52}/Dioxane/H_2O," *Journal of Physical Chemistry B*, vol. 103, no. 44, pp. 9473–9487, 1999.

[15] S. Jain and F. S. Bates, "Consequences of nonergodicity in aqueous binary PEO-PB micellar dispersions," *Macromolecules*, vol. 37, no. 4, pp. 1511–1523, 2004.

[16] Y.-Y. Won, A. K. Brannan, H. T. Davis, and F. S. Bates, "Cryogenic transmission electron microscopy (cryo-TEM) of micelles and vesicles formed in water by poly(ethylene oxide)-based block copolymers," *Journal of Physical Chemistry B*, vol. 106, no. 13, pp. 3354–3364, 2002.

[17] H. Cui, Z. Chen, S. Zhong, K. L. Wooley, and D. J. Pochan, "Block copolymer assembly via kinetic control," *Science*, vol. 317, no. 5838, pp. 647–650, 2007.

[18] Y. Geng and D. E. Discher, "Hydrolytic degradation of poly(ethylene oxide)-block-polycaprolactone worm micelles," *Journal of the American Chemical Society*, vol. 127, no. 37, pp. 12780–12781, 2005.

[19] P. Dalhaimer, H. Bermudez, and D. E. Discher, "Biopolymer mimicry with polymeric wormlike micelles: molecular weight scaled flexibility, locked-in curvature, and coexisting microphases," *Journal of Polymer Science, Part B*, vol. 42, no. 1, pp. 168–176, 2003.

[20] Y. Geng, F. Ahmed, N. Bhasin, and D. E. Discher, "Visualizing worm micelle dynamics and phase transitions of a charged diblock copolymer in water," *Journal of Physical Chemistry B*, vol. 109, no. 9, pp. 3772–3779, 2005.

[21] P. Dalhaimer, F. S. Bates, and D. E. Discher, "Single molecule visualization of stable, stiffness-tunable, flow-conforming worm micelles," *Macromolecules*, vol. 36, no. 18, pp. 6873–6877, 2003.

[22] S. Cai, K. Vijayan, D. Cheng, E. M. Lima, and D. E. Discher, "Micelles of different morphologies advantages of worm-like filomicelles of PEO-PCL in paclitaxel delivery," *Pharmaceutical Research*, vol. 24, no. 11, pp. 2099–2109, 2007.

[23] P. L. Soo, L. Luo, D. Maysinger, and A. Eisenberg, "Incorporation and release of hydrophobic probes in biocompatible polycaprolactone-block-poly(ethylene oxide) micelles: implications for drug delivery," *Langmuir*, vol. 18, no. 25, pp. 9996–10004, 2002.

[24] H. Chen, S. Kim, L. Li, S. Wang, K. Park, and J.-X. Cheng, "Release of hydrophobic molecules from polymer micelles into cell membranes revealed by Förster resonance energy transfer imaging," *Proceedings of the National Academy of Sciences of the United States of America*, vol. 105, no. 18, pp. 6596–6601, 2008.

[25] L. Luo, J. Tam, D. Maysinger, and A. Eisenberg, "Cellular internalization of poly(ethylene oxide)-b-poly(ε-caprolactone) diblock copolymer micelles," *Bioconjugate Chemistry*, vol. 13, no. 6, pp. 1259–1265, 2002.

[26] S. Muthian, K. Nithipatikom, W. B. Campbell, and C. J. Hillard, "Synthesis and characterization of a fluorescent substrate for the N- arachidonoylethanolamine (anandamide) transmembrane carrier," *Journal of Pharmacology and Experimental Therapeutics*, vol. 293, no. 1, pp. 289–295, 2000.

[27] D. A. Christian, A. Tian, W. G. Ellenbroek, et al., "Spotted vesicles, striped micelles and Janus assemblies induced by ligand binding," *Nature Materials*, vol. 8, no. 10, pp. 843–849, 2009.

[28] P. P. Ghoroghchian, P. R. Frail, K. Susumu, et al., "Near-infrared-emissive polymersomes: self-assembled soft matter

for in vivo optical imaging," *Proceedings of the National Academy of Sciences of the United States of America*, vol. 102, no. 8, pp. 2922–2927, 2005.

[29] D. A. Christian, S. Cai, O. B. Garbuzenko, et al., "Flexible filaments for in vivo imaging and delivery: persistent circulation of filomicelles opens the dosage window for sustained tumor shrinkage," *Molecular Pharmaceutics*, vol. 6, no. 5, pp. 1343–1352, 2009.